



**Calhoun: The NPS Institutional Archive**

---

Theses and Dissertations

Thesis Collection

---

1998-06

# Construction and measurement of an actively mode-locked sigma laser

Butler, James M.

Monterey, California. Naval Postgraduate School

---

<http://hdl.handle.net/10945/8146>



Calhoun is a project of the Dudley Knox Library at NPS, furthering the precepts and goals of open government and government transparency. All information contained herein has been approved for release by the NPS Public Affairs Officer.

**Dudley Knox Library / Naval Postgraduate School  
411 Dyer Road / 1 University Circle  
Monterey, California USA 93943**

<http://www.nps.edu/library>



NPS ARCHIVE  
1998.06  
BUTLER, J.



DUDLEY  
NAVAL POSTGRADUATE SCHOOL  
MONTEREY, CA 93943-5101







NPS-EC-98-011

# NAVAL POSTGRADUATE SCHOOL MONTEREY, CALIFORNIA



## THESIS

### CONSTRUCTION AND MEASUREMENT OF AN ACTIVELY MODE-LOCKED SIGMA LASER

by

James M. Butler

June, 1998

Thesis Co-Advisors:

Phillip E. Pace  
John P. Powers

Approved for public release; distribution is unlimited.

Prepared for:  
Center for Reconnaissance Research  
Naval Postgraduate School  
Monterey, CA

**NAVAL POSTGRADUATE SCHOOL**  
**Monterey, California 93943**

Rear Admiral Chaplain  
Superintendent

This thesis was prepared in conjunction with research sponsored in part by the Center for Reconnaissance Research at the Naval Postgraduate School.

Reproduction of all or part of this report is authorized.



REPORT DOCUMENTATION PAGE			Form Approved OMB No 0704-0188	
Public reporting burden for this collection of information is estimated to average 1 hour per response, including the time for reviewing instruction, searching existing data sources, gathering and maintaining the data needed, and completing and reviewing the collection of information. Send comments regarding this burden estimate or any other aspect of this collection of information, including suggestions for reducing this burden, to Washington Headquarters Services, Directorate for Information Operations and Reports, 1215 Jefferson Davis Highway, Suite 1204, Arlington, VA 22202-4302, and to the Office of Management and Budget, Paperwork Reduction Project (0704-0188) Washington DC 20503.				
1. AGENCY USE ONLY (Leave blank)	2. REPORT DATE June 1998	3. REPORT TYPE AND DATES COVERED Master's Thesis		
4. TITLE AND SUBTITLE CONSTRUCTION AND MEASUREMENT OF AN ACTIVELY MODE-LOCKED SIGMA LASER		FUNDING NUMBERS MIPR 97110-T		
6. AUTHOR(S) Butler, James M.				
7. PERFORMING ORGANIZATION NAME(S) AND ADDRESS(ES) Naval Postgraduate School Monterey CA 93943-5000		8. PERFORMING ORGANIZATION REPORT NUMBER NPS-EC-98-011		
9. SPONSORING/MONITORING AGENCY NAME(S) AND ADDRESS(ES) Naval Postgraduate School Center for Reconnaissance		10. SPONSORING/MONITORING AGENCY REPORT NUMBER		
11. SUPPLEMENTARY NOTES The views expressed in this thesis are those of the author and do not reflect the official policy or position of the Department of Defense or the U.S. Government.				
12a. DISTRIBUTION/AVAILABILITY STATEMENT Approved for public release; distribution is unlimited.			12b. DISTRIBUTION CODE	
13. ABSTRACT (maximum 200 words) <p>The direct digitization of microwave signals of interest would allow rapid computer processing and analysis. Current analog-to-digital converters (ADCs) are bandwidth limited and electronic warfare systems must down-convert the signal before digitization causing a loss of information. Optical ADCs can directly digitize frequencies greater than 10 GHz using wideband integrated optical interferometers (folding ADCs). A critical component of the optical folding ADC is the pulsed laser used for sampling the wideband signal. The amplitude-modulated pulses become the discrete samples of the analog signal. Limiting factors in an optical ADC are the pulsewidth, the pulse rate, and the jitter noise of the optical pulse train. Mode-locked lasers provide pulse rates and pulsewidths suitable for high bandwidth applications.</p> <p>In this thesis a mode-locked sigma laser was constructed using fiber-optic, electro-optic, and microwave components. The theory of mode-locking, laser construction, output measurements, and sampling applications are discussed in detail. The mode-locked sigma laser demonstrated a pulse repetition frequency of 16 GHz, pulsewidth of 7.2 picoseconds, amplitude noise less than 1%, temporal jitter of 386 femtoseconds, and the ability to be harmonically mode-locked at twice the modulation frequency using only 200 mW of diode pump power in the optical amplifier. The analysis shows that this laser can be used in an optical ADC to sample a 6.44 GHz signal at 7 bits, 3.22 GHz at 8 bits, or 1.61 GHz at 9 bits of resolution.</p>				
14. SUBJECT TERMS Mode-Locked Laser, Sigma Laser, Erbium-Doped Fiber Amplifier, Optical Sampling, Analog-to-Digital Conversion, Amplitude Noise, Phase Noise, Temporal Jitter Noise, Timing Uncertainty			15. NUMBER OF PAGES 164	
			16. PRICE CODE	
17. SECURITY CLASSIFICATION OF REPORT Unclassified	18. SECURITY CLASSIFICATION OF THIS PAGE Unclassified	19. SECURITY CLASSIFICATION OF ABSTRACT Unclassified	20. LIMITATION OF ABSTRACT UL	



Approved for public release; distribution is unlimited.

**CONSTRUCTION AND MEASUREMENT OF AN ACTIVELY MODE-LOCKED  
SIGMA LASER**

James M. Butler  
Lieutenant, United States Navy  
B.S., United States Naval Academy, 1988

Submitted in partial fulfillment  
of the requirements for the degrees of

**MASTER OF SCIENCE IN ELECTRICAL ENGINEERING**

from the

**NAVAL POSTGRADUATE SCHOOL  
June 1998**

Author:

Approved by

Department of Electrical and Computer Engineering



ARCHIVE

98.06

UTLER, J.

~~09444~~  
C.1

MONTEREY, CA 94038  
NAVAL POSTGRADUATE SCHOOL  
LUDLEY KNOX LIBRARY

## ABSTRACT

The direct digitization of microwave signals of interest would allow rapid computer processing and analysis. Current analog-to-digital converters (ADCs) are bandwidth limited and electronic warfare systems must down-convert the signal before digitization causing a loss of information. Optical ADCs can directly digitize frequencies greater than 10 GHz using wideband integrated optical interferometers (folding ADCs). A critical component of the optical folding ADC is the pulsed laser used for sampling the wideband signal. The amplitude-modulated pulses become the discrete samples of the analog signal. Limiting factors in an optical ADC are the pulsewidth, the pulse rate, and the jitter noise of the optical pulse train. Mode-locked lasers provide pulse rates and pulsewidths suitable for high bandwidth applications.

In this thesis a mode-locked sigma laser was constructed using fiber-optic, electro-optic, and microwave components. The theory of mode-locking, laser construction, output measurements, and sampling applications are discussed in detail. The mode-locked sigma laser demonstrated a pulse repetition frequency of 16 GHz, pulsewidth of 7.2 picoseconds, amplitude noise less than 1%, temporal jitter of 386 femtoseconds, and the ability to be harmonically mode-locked at twice the modulation frequency using only 200 mW of diode pump power in the optical amplifier. The analysis shows that this laser can be used in an optical ADC to sample a 6.44 GHz signal at 7 bits, 3.22 GHz at 8 bits, or 1.61 GHz at 9 bits of resolution.





## TABLE OF CONTENTS

I. INTRODUCTION.....	1
A. OPTICAL SAMPLING OF WIDEBAND ANTENNA SIGNALS USING MODE-LOCKED LASERS.....	1
1. Sampling.....	1
2. Mode-Locked Lasers.....	3
3. Optical Modulators.....	4
4. Pulse Modulation Experiment.....	4
5. Optical Analog-to-Digital Converters.....	5
B. PRINCIPAL CONTRIBUTIONS.....	8
C. THESIS ORGANIZATION.....	9
II. OVERVIEW OF MODE-LOCKED LASERS.....	11
A. LASERS.....	11
B. MODE-LOCKING.....	15
C. MODE-LOCKING TECHNIQUES.....	21
1. Active Mode-Locking.....	21
2. Passive Mode-Locking.....	22
3. Active-Passive Mode-Locking.....	24
D. TYPES OF MODE-LOCKED LASERS.....	26
1. Solid State Lasers.....	27
2. Diode Lasers.....	28
3. Fiber Lasers.....	29
III. CONSTRUCTION OF THE SIGMA LASER.....	33
A. CAVITY DESIGN.....	33
1. Fiber Types.....	33
2. Polarization Maintaining Fiber.....	36
3. Singlemode Fiber.....	37

4. Dispersion-Shifted Fiber.....	37
5. Dispersion-Compensating Fiber.....	38
6. Erbium-Doped Fiber.....	38
7. Flexcor Fiber.....	39
8. Fiber Splicing.....	40
9. Birefringence Compensation.....	42
10. Polarization Maintaining Loop.....	43
11. Round Trip of a Pulse.....	45
B. ACTIVE MODE-LOCKING.....	46
C. ERBIUM-DOPED FIBER AMPLIFIER.....	51
D. FEEDBACK LENGTH STABILIZATION CIRCUIT.....	55
1. Microwave Phase Detector.....	56
2. Integrator Circuit Design and Construction.....	57
3. Piezoelectric Cylinder.....	61
E. CONCLUSION.....	64
IV. MEASUREMENTS OF THE SIGMA LASER.....	67
A. LASER MEASUREMENTS.....	67
B. COMPUTER CONNECTIONS.....	68
C. POWER MEASUREMENTS.....	72
D. OPTICAL SPECTRUM MEASUREMENTS.....	72
E. PULSEWIDTH MEASUREMENTS.....	75
F. THEORY OF JITTER MEASUREMENT.....	81
G. RADIO-FREQUENCY SPECTRUM ANALYZER NOISE JITTER MEASUREMENTS.....	84
H. SUMMARY OF MEASUREMENTS.....	88
I. OPTICAL POWER EXPERIMENT.....	91
J. SHORTEST PULSEWIDTHS.....	95
K. DISPERSION MANAGEMENT AND PULSEWIDTH.....	97

V. SAMPLING LIMITATIONS OF THE SIGMA LASER.....	99
A. AMPLITUDE JITTER NOISE.....	99
B. MAXIMUM TEMPORAL JITTER.....	100
C. OPTICAL TRANSIT TIME.....	102
D. MAXIMUM PULSEWIDTH.....	103
E. CONCLUSION.....	105
VI. CONCLUSIONS AND RECOMMENDATIONS.....	107
A. DISPERSION OPTIMIZATION.....	107
B. OPTICAL MODULATOR.....	107
C. NOISE REDUCTION.....	108
D. OPTICAL AMPLIFIER.....	109
E. SYSTEM MODIFICATION.....	109
F. MINOR MODIFICATIONS.....	110
G. SUMMARY REMARKS.....	111
APPENDIX A. PARTS AND EQUIPMENT.....	113
A. POLARIZATION MAINTAINING LOOP.....	113
B. ERBIUM-DOPED FIBER AMPLIFIER.....	114
C. PROPAGATION AND BIREFRINGENCE COMPENSATION BRANCH...	115
D. FEEDBACK LENGTH STABILIZATION CIRCUIT.....	115
E. TEST EQUIPMENT.....	116
F. OTHER EQUIPMENT.....	117
APPENDIX B. CONFIGURATION AND OPERATION OF THE SIGMA LASER..	119
A. SIGMA LASER CONNECTIONS AND CONFIGURATION.....	119
1. Feedback Length Stabilization Configuration.....	119
2. Mach-Zehnder Modulator Configuration.....	123
3. Pump Diode Configuration.....	125
4. Measurement Equipment Setup.....	126



B. SIGMA LASER OPERATION.....	132
1. Pump Diode Temperature Controller Operation.....	132
2. Pump Diode Laser Controller Operation.....	133
3. Polarization Controller Operation.....	134
4. Modulation.....	135
5. Autocorrelator Operation.....	136
6. Integrating Amplifier Pre-Operational Setup.....	137
7. Mode-Locking.....	138
8. Autocorrelator Software.....	140
9. Turning Off the Sigma Laser.....	141
LIST OF REFERENCES.....	143
INITIAL DISTRIBUTION LIST.....	149

## ACKNOWLEDGEMENTS

The author wishes to thank Dr. Phillip Pace and Dr. John Powers of the Naval Postgraduate School and Dr. Thomas Carruthers, Dr. Michael Dennis, and Dr. Irl Duling III of the Optical Sciences Division of the Naval Research Laboratory for their fruitful discussions and use of their laboratory equipment. In addition, thanks are due Jim Harden of Hewlett Packard for the equipment demonstration, Gene Kaiser of Alcatel Telecom and Timothy Espinoza of Lucent Technologies for the samples of dispersion-shifted fiber, Eric Mies of Vytran Corporation for the erbium-doped fiber splicing, and NPS Laboratory Engineer Jeffrey Knight for his assistance with LABVIEW programming. Finally, a special thanks to Tambria, James, and Brian, the author's wife and family, for their never-ending support in the production of this Thesis.



## I. INTRODUCTION

### A. OPTICAL SAMPLING OF WIDEBAND ANTENNA SIGNALS USING MODE-LOCKED LASERS

#### 1. Sampling

A key component in most modern electronic warfare or microwave receiver systems is the analog-to-digital converter (ADC). The radio frequency (RF) energy is sampled periodically, measured, and converted to digital data bits representing the signal sample. The number of bits representing the signal sample is the “resolution” of the ADC [Ref. 1]. A small number of bits per sample may be enough to accurately extract the information required from a signal. A high number of bits per sample are required for electronic warfare or signals analysis purposes. In either case, a computer can be used to convert the digitized signal into useful information.

The bandwidth of a signal can be the spectral width of a band-limited, baseband signal that spans the frequency spectrum from DC (0 Hz) to the maximum frequency  $f_{max}$  within the signal. More commonly, the bandwidth is the spectral width of a band-pass signal spanning from a minimum frequency  $f_{min}$  to  $f_{max}$  and centered about a frequency  $f_c$ . The Nyquist rate is a sampling frequency  $f_s$  that is twice the bandwidth  $BW$  of a signal of interest. This signal can be represented digitally if it is sampled at a rate higher than the Nyquist rate,  $f_s > 2BW$  [Ref. 2].

The digital representation will be unambiguous if the signal is sampled at twice the maximum frequency,  $f_s > 2f_{max}$ . However, the signal can be under-sampled at the less than twice maximum frequency,  $f_s < 2f_{max}$  as long as it exceeds the Nyquist sampling rate  $f_s > 2BW$ . This will produce an alias signal that can still be correctly represented digitally by using a symmetrical-numbering-system (SNS). The alias signal produces a symmetrical “folded” signal in the complex plane about the folding frequency  $f_o$ . The folding frequency is exactly half the sampling frequency,  $f_o = f_s / 2$  and sampled folding series produces a set of pair-wise relatively prime numbers. These numbers can be mathematically resolved to produce the correct digital representation of the signal of interest [Ref. 3].



The digitization of RF signals (including microwave) directly from an antenna is an application pursued by a variety of defense related organizations. Communications reception, electronic warfare, and signals intelligence are obvious applications in which high-speed ADC technology can replace numerous types of receivers. If the ADC can operate directly on the RF signal, then down-conversion to an intermediate or base-band frequency can be eliminated.

Current ADC integrated chips are limited to a maximum frequency ( $f_{max}$ ) of 150 MHz (8 bits) commercially [Ref. 4] and 2 GHz (6 bits) experimentally [Ref. 5]. Signals with a higher center frequency ( $f_c$ ) are usually down converted before digitization causing some loss of information and a slow information rate [Ref. 1].

The flash converter in Figure 1.1 is the fastest integrated chip ADC [Ref. 5]. This circuit converts the waveform signal to parallel bits. A "sample and hold" circuit reduces the waveform into discrete periodic samples of analog voltages. During each sample period,  $2^N - 1$  parallel comparators quantize the signal into the discrete samples. Logic circuits convert the comparator states into digital data of N bits.

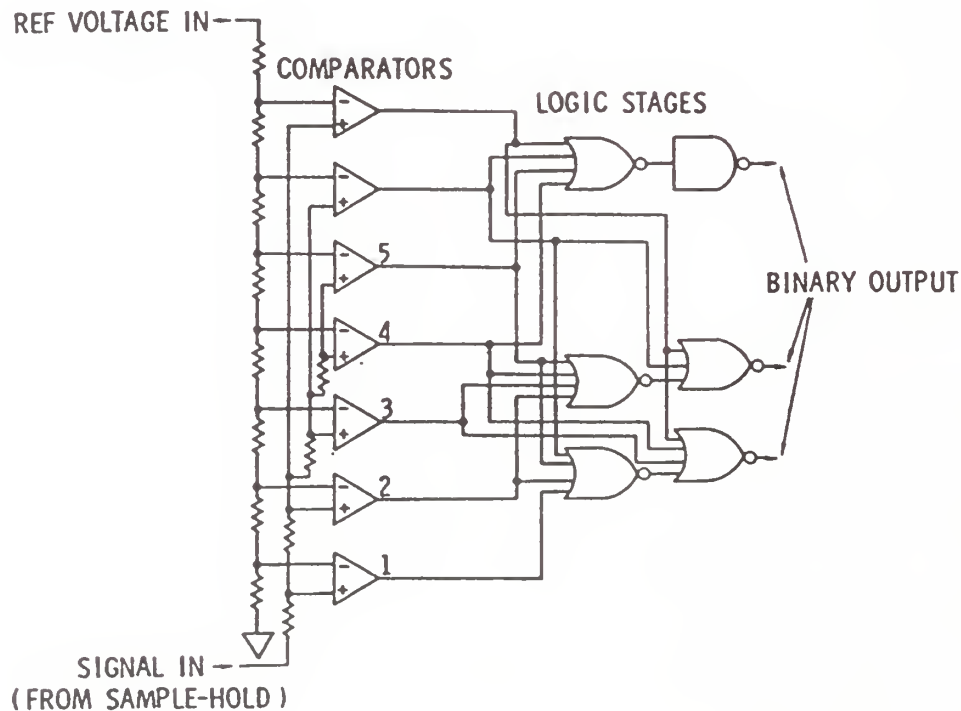


Figure 1.1. Flash ADC. (From [Ref. 6].)

Given the technological trend toward wide-bandwidth communications and radar signals with center frequencies in the tens of Gigahertz, sampling rates will have to increase. To meet current and future ADC requirements, much research has been conducted in the area of optical sampling. An optical ADC can offer 100 times the maximum center frequency and bandwidth of integrated chip ADCs currently available. High-speed data transmission already occurs through optical fiber; the same high frequency, wide-bandwidth components can be used to optically sample RF signals. The two critical components of an optical ADC are the mode-locked laser and the Mach-Zehnder optical modulator.

## **2. Mode-Locked Lasers**

The mode-locked laser produces very short duration pulses in the picosecond range at high pulse repetition frequencies (PRFs) in the Gigahertz regime. An optical modulator then amplitude modulates the traveling laser pulses with the received signal of interest. Each amplitude modulated pulse is a discrete sample of the received signal. The mode-locked laser and modulator replace the sample and hold circuit that is used in the integrated chip ADC and the pulse rate of the laser is the sampling frequency of the optical ADC [Ref. 6].

Mode-locked lasers are produced from any typical laser configuration including solid state lasers, semiconductor diode lasers, and fiber lasers. The fiber lasers use glass fibers common to the telecommunications industry and other fiber optic components to form a laser cavity. These fiber mode-locked lasers have demonstrated pulse repetition frequencies (PRFs) of 20 GHz at pulsewidths of one picosecond [Ref. 7] and are ideal sources laser pulses for an optical ADC. The critical performance concerns of mode-locked laser used for optical sampling are pulse repetition frequency, pulsewidth, amplitude jitter noise, and temporal jitter noise [Ref. 6]. These items will be discussed in detail and measured later in this Thesis.

### 3. Optical Modulators

In the Mach-Zehnder optical modulator, the pulsed laser light is split between two arms of the modulator and at least one arm has a set of electrodes. The electrodes change the phase of the light wave based on the voltage on the electrodes and the electrode length. When the laser light is recombined within the modulator, the phase change between the two arms becomes amplitude modulation of the re-combined light [Ref. 8]. Since the modulator transfers the RF signal to the laser pulses, its bandwidth capability is critical. Commercially available Mach-Zehnder modulators are capable of up to 20 GHz bandwidth [Ref. 9]. Current research seeks to significantly increase the modulation bandwidth of these devices to 100 GHz and beyond [Ref. 10].

### 4. Pulse Modulation Experiment

An experiment was conducted to investigate laser pulses modulated by an analog signal. The layout of the experiment is shown in Figure 1.2 where a diode laser is pulsed by a 2 MHz signal. The resulting laser pulses are modulated in an optical modulator by a 100 kHz sine wave. The resulting signal is detected and displayed on an oscilloscope.

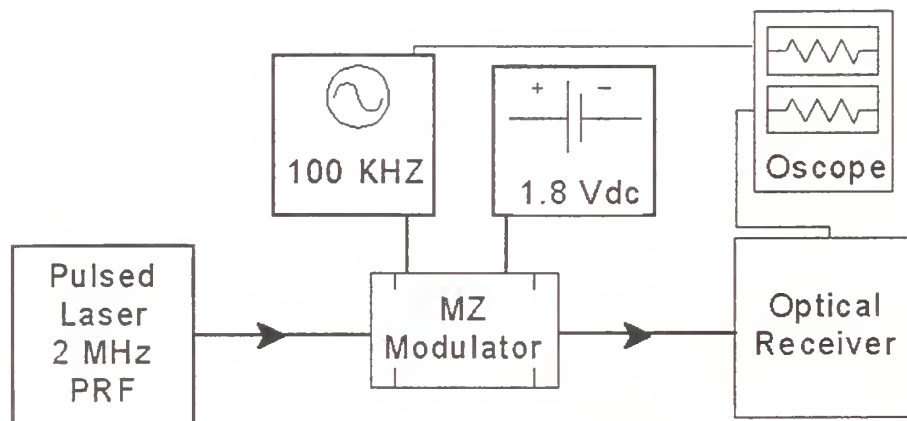


Figure 1.2. Layout of a pulsed laser modulation experiment.

The results of the experiment are shown in digital oscilloscope display of Figure 1.3. The experiment was conducted at low frequencies to observe the modulation in the

time domain. The train of 2 MHz pulses that modulated a 1300 nm laser diode is shown in the bottom trace. The modulating 100 kHz sine wave is shown in the top trace. The center trace is the modulated output where the sine wave can be seen in the envelope of the laser pulses. These discrete samples of the sine wave are representative of what would be quantized in an optical ADC system. Each discrete sample can be converted to digital data representing the sampled sine wave.

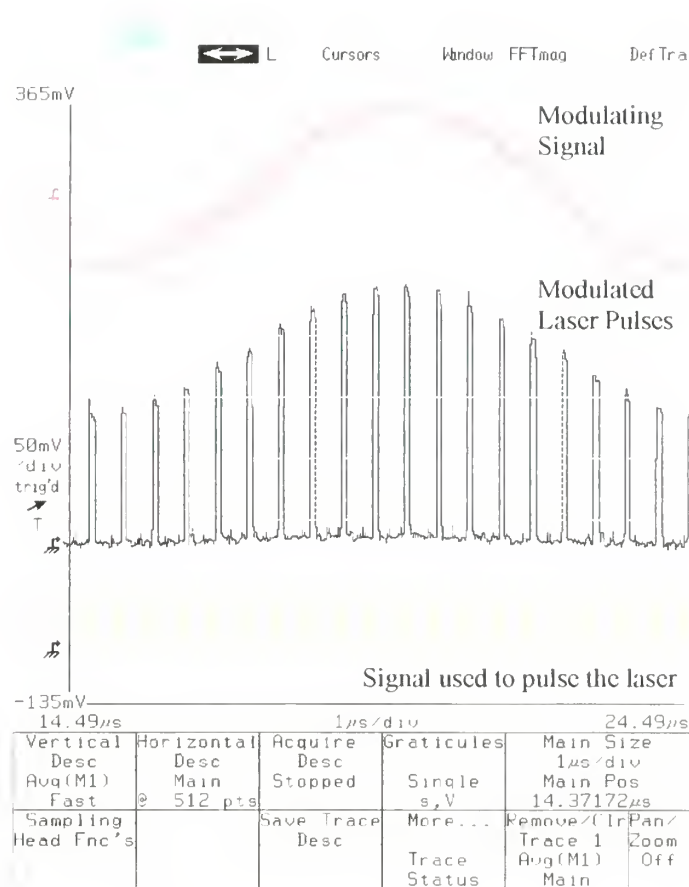


Figure 1.3. Laser pulses modulated by an analog signal

### 5. Optical Analog-to-Digital Converters

There are two types of amplitude-analyzing optical ADCs, the original Taylor scheme and the SNS ADC. In the Taylor scheme shown in Figure 1.4, the mode-locked laser pulses and RF signal of interest are split between several modulators. The pulse is



converted to a voltage in a detector and a comparator determines if the quantization threshold level has been exceeded. If the detector voltage is high enough, the detected signal becomes a bit [Ref. 6].

A single modulator is used for every bit of resolution in digitization of the signal. Each modulator has a set of electrodes of a different length. The RF signal will amplitude modulate the light differently within each modulator based on the electrode lengths and the signal amplitude. The different levels of amplitude modulation enable the detectors and comparators to quantize the level of energy in the signal sample. The more modulators in parallel with increasingly longer electrode lengths, the more finely the system can quantize a signal. The binary output is usually digital Gray code [Ref. 6]. Figure 1.4 is an example of an optical ADC that can replace the flash ADC in Figure 1.1 [Ref. 6].

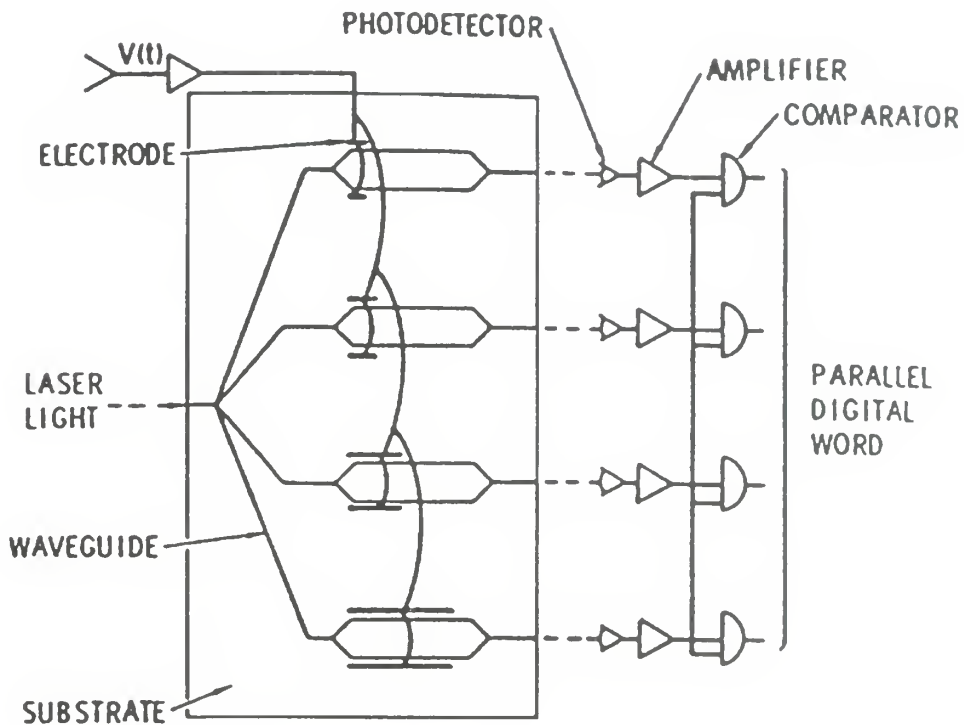


Figure 1.4. Taylor scheme optical ADC. (From [Ref. 6].)

An advanced optical ADC is shown in Figure 1.5. Instead of one comparator per interferometer, several comparators can be used to quantize the detected output of a modulator (greater than one – bit per interferometer). This preprocessing scheme





produces a “folding waveform” which is quantized and decoded using the symmetrical-numbering-system (SNS). The SNS residues are then translated to binary digital data. Based on the number of comparators, the SNS ADC dramatically improves the digital resolution with fewer modulators. In the Taylor scheme, three modulators will produce 3 bits of resolution. In the SNS system, the same three modulators can produce 10 bits of resolution [Ref. 3].

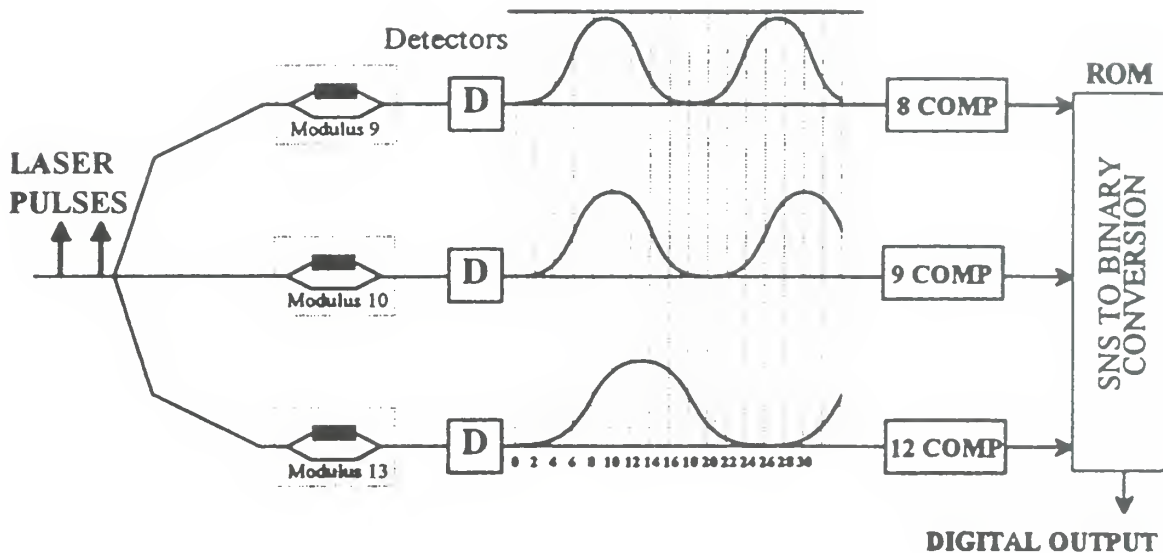


Figure 1.5. Symmetrical-numbering-system ADC. (From [Ref. 3].)

Both the Taylor and SNS schemes are amplitude-analyzing converters and are subject to the same quantization noise problems as their integrated-chip counterparts. The amplitude and temporal jitter noise in the ADC are a significant factor and can directly affect the resolution and maximum frequency that can be sampled. In the optical ADC, amplitude and temporal jitter noise comes from the train of mode-locked laser pulses used to sample the signal of interest [Ref. 6].

The Taylor and SNS ADCs have been in existence for some time and their performance is well understood. However, there are techniques in analog-to-digital conversion that reduce the effects of quantization noise. The sigma-delta modulator is one example where the system uses a feedback loop and an analog filter to significantly reduce the effects of quantization noise [Ref. 11].

As a starting point, this Thesis will use these amplitude-analyzing schemes in the analysis of application of a mode-locked laser to an optical ADC. It is expected that the results will be improved upon by use of a sigma-delta modulator and other available techniques to reduce the effects of quantization noise.

## **B. PRINCIPAL CONTRIBUTIONS**

There were three principal goals of this Thesis. The first was to construct a mode-locked laser with a 10 GHz pulse repetition rate. The second goal was to accurately measure the temporal jitter noise and pulsewidth in the laser output. The final goal was to analyze its output for use in an optical sampling system with an expected maximum sampled frequency of 5 GHz signal at 10 bits of resolution.

A 16 GHz PRF actively mode-locked erbium fiber laser was successfully constructed in the Naval Postgraduate School Optical Electronics Laboratory. The parts procurement for this laser required approximately ten months and actual construction time is estimated at 180 hours in the laboratory. A significant amount of test equipment was assembled in the laboratory and about 30 hours were expended in programming a computer for data collection using General Purpose Interface Bus (GPIB) and serial data ports. This improved the accuracy of the data collected, eased jitter analysis, and amounted to more data collection.

The laser pulsewidth, pulse repetition frequency, output noise, wavelength, and spectral linewidth were measured. Finally the noise was analyzed for temporal and amplitude jitter content and the results applied to a theoretical amplitude-analyzing optical sampling system. The details of laser construction, measurement, and sampling applications are presented in the chapters to follow.

This laser is modeled after the original “sigma” mode-locked laser invented at the Naval Research Laboratory (NRL) in Washington D.C. The NRL laser is selected for construction for a number of reasons. It is capable of high pulse rates of 10 to 20 GHz and is one of the few high PRF lasers that had published jitter measurements [Ref. 12]. Calculations using the published pulsewidth and jitter measurements indicated that it can Nyquist sample a 5 GHz signal at 7 bits of resolution. In addition, the school enjoys an

excellent working relationship with the Naval Research Laboratory. The available expertise of the NRL Optical Sciences Division and use of their laboratory equipment was instrumental in the success of this Thesis.

## **C. THESIS ORGANIZATION**

Chapter II gives an overview of the mode-locked laser and includes the theory of mode-locking as well as some common mode-locked lasers. The construction of the actively mode-locked sigma laser is detailed in Chapter III. This Chapter will discuss the details of the amplifier and the feedback system as well as the cavity design and types of fiber uses. Chapter IV extensively details the measurements of the laser output and presents the final results. The management of dispersion is also discussed in this Chapter and is based on the laser measurements. An experiment relating optical power to temporal uncertainty and pulsewidth is also included. The results of Chapter IV are used in Chapter V to determine the sampling limitations of this laser. In Chapter VI, the Thesis conclusions and recommendations are given. They include recommendations for possible sources of noise as well as improvements in the present configuration. Finally, the Appendices will contain a detailed parts list and instructions for laser set up and operation.



## II. OVERVIEW OF MODE-LOCKED LASERS

### A. LASERS

A basic laser can be created from any medium that can be used to generate or amplify light and a cavity that will feed the light through the amplifying process. It can be built from a crystal, saturable dye solution, doped glass, or even semiconductor material. The addition of power into the laser medium raises the energy state of the individual atoms. The atoms cannot maintain this high energy state so they drop down to a lower energy state. When the energy drop occurs, a spontaneous emission may be emitted from the atom as a photon of light energy. The direction of the emission is initially random. If the medium is continually pumped with enough power, the number of atoms in a higher state will exceed the number of atoms in a lower or ground state. This is known as a population inversion. The pump energy can be light from a flash lamp, a laser beam from a pump laser, or electric current. Figure 2.1 is a typical graph of a population inversion created by continually pumping a laser medium with energy [Refs. 13, 14].

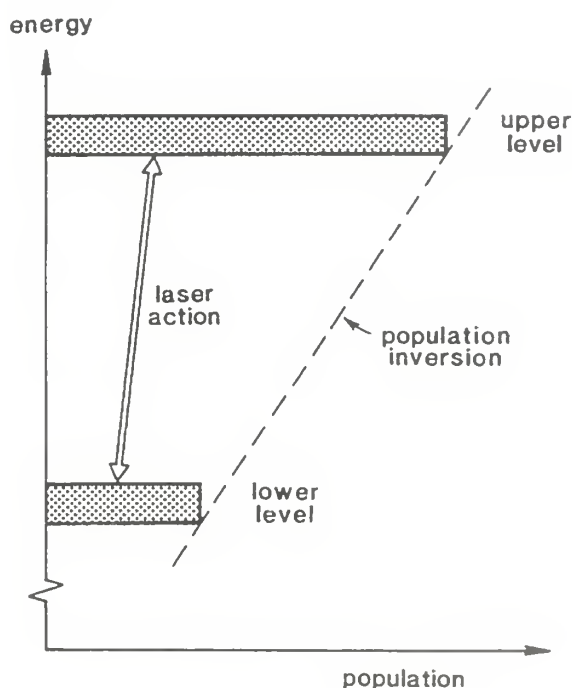


Figure 2.1. Population inversion of atoms in a laser cavity. (From [Ref. 14].)



As the atoms drop to a lower state and emit light, other atoms are pumped to the higher energy state to maintain the relative population inversion. As a photon passes by other atoms, it causes a stimulated emission and the atom is reduced to a lower energy state. The stimulated emissions are additive and are a source of gain since they coherently amplify the passing light energy. This device can produce a weak but coherent beam and is known as a “laser”, an acronym for light amplification by the stimulated emission of radiation [Ref. 15].

If the ends of the laser cavity are reflective, a photon of light striking the mirror will reflect back into the cavity to be amplified even further. The amplified light may oscillate at certain frequencies between the reflective ends of the laser cavity to create a laser action. A single frequency of laser light oscillating in the cavity is known as longitudinal mode. The laser cavity actually becomes a laser oscillator and produces a laser beam with much more power due to the repeated amplification. The laser may be built into the oscillator or may be a separate, external component. When separate, laser light is pumped into the oscillator cavity to resonate, become amplified, and/or be converted to another wavelength of light [Ref. 14]. Most devices use oscillation for greater gain and higher power. For purposes of this Thesis, the laser and laser oscillator will be referred to as a laser.

In many lasers, more than one mode will be operating within the laser cavity. A singlemode or adjacent group of modes will dominate in the amplification process and will become the laser beam emitted from the cavity. There are still spontaneous emissions that are produced and amplified in the laser cavity but do not coherently combine with the laser beam. These amplified spontaneous emissions (ASE) are significant and are a source of noise in the laser output. A certain percentage of the laser light is removed from the laser cavity by a mirror that has a reflectivity of less than 100% or by other means. The laser beam contains one or more frequencies that are generated by oscillation within the cavity. Figure 2.2 is a typical laser oscillator that is pumped by an external source of energy [Ref. 13].

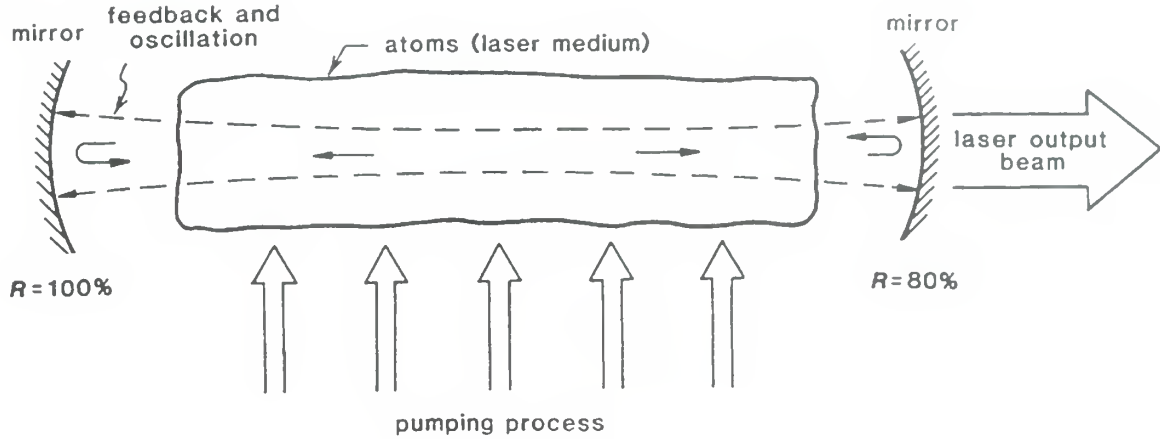


Figure 2.2. Typical laser oscillator. (From [Ref. 13].)

Two conditions are required to create frequency oscillation of light within a resonant laser cavity. First, the round trip gain must equal the round trip losses as a light wave oscillates between the ends of the cavity. This is usually accomplished by pumping the cavity with enough energy to maintain a population inversion and provide coherent amplification of laser light [Ref. 13]. The range of frequencies that can be amplified is limited by the gain bandwidth of the laser medium. The atoms in the material used to create the amplifying medium dictate this gain bandwidth. Since the frequency of light is very large number (THz), it is often expressed as a wavelength. The conversion of optical frequency  $\nu$  to wavelength  $\lambda$  is

$$\lambda = c / n \nu \quad 2.1$$

where  $n$  is the material index of refraction and  $c$  is the speed of light [Ref. 14].

The second condition requires that the light wave only oscillate at a resonant frequency if its phase change per cavity round trip is equal to an integer multiple of  $2\pi$  radians. The phase change is primarily due to the time for light to travel one round trip between the ends of the cavity. The round trip time is based on the length of the cavity and speed of light within the cavity material. The phase change  $\Delta\phi$  for one round trip is

$$\Delta\phi = (2\pi)(2L) / \lambda_q = 2\pi q \quad 2.2$$

where  $L$  is the length of the cavity and  $q$  is the integer, and  $\lambda_q$  is the wavelength at that integer multiple. Using Equation 2.2, the mode wavelength is found to be

$$\lambda_q = 2L / q . \quad 2.3$$

The  $\lambda_q$  can be converted to  $\nu_q$ , the frequency of the oscillating mode. Manipulating Equations 2.1 and 2.2,  $\nu_q$  becomes

$$\nu_q = qc / 2nL . \quad 2.4$$

The oscillating frequencies can be expressed as angular frequencies in radians/s. For purposes of this Thesis, optical frequency  $\nu$  and other frequencies  $f$ , to be used later, are expressed in Hertz [Ref. 14].

The integer value of  $q$  in Equations 2.2 to 2.4 might lead one to believe that there can be an infinite number of modes resonating in a laser. In reality, lasers are built to oscillate within certain wavelengths of the optical spectrum thus limiting the number of modes actually operating. Limiting the bandwidth of the gain of the laser is one method of limiting the number of modes. If  $\nu_q$  falls within the bandwidth gain  $\Delta\nu$  of the laser medium, then it can become an oscillating mode [Ref. 14]. In another method, the length of the cavity can be adjusted for singlemode operation, as in the case of some laser diodes. Other lasers, such as an erbium-doped fiber laser, may have a very broad gain bandwidth of 30 to 40 nm.

A group of modes oscillating within the bandwidth gain of the laser will eventually become dominant and will absorb most of the available gain. The frequency spacing between the dominant modes is periodic. Using Equation 2.4, the frequency spacing between two operating modes  $d\nu_q$  is [Ref. 14]

$$d\nu_q = \nu_{q+1} - \nu_q = c / 2nL . \quad 2.5$$

The group of modes can be seen as a signal within the optical frequency domain. The full-width half-maximum of this signal is known as the frequency linewidth  $\Delta\nu$  and can be calculated using [Ref. 14]

$$\Delta\nu = c\Delta\lambda / \lambda^2. \quad 2.6$$

The frequency linewidth can be used to find the number of modes actually operating in the laser. The number of modes  $N$  becomes [Ref. 14]

$$N = 2nL\Delta\nu / c. \quad 2.7$$

The spectral linewidth  $\Delta\lambda$  of a laser can be measured on an optical spectrum analyzer. From this measurement the frequency line width can be calculated using Equation 2.6. This measurement is demonstrated in Chapter IV [Ref. 14].

## B. MODE-LOCKING

When there are multiple modes operating within a laser cavity, the relative phase between the modes in the frequency domain is often random and incoherent. In the time domain, the amplitude of light coming from the laser will fluctuate as the modes interact constructively and destructively in a random fashion. Techniques exist to force the modes to oscillate coherently and lock them together in phase. The peak amplitudes of these modes oscillating together in phase periodically combine constructively to form a mode-locked pulse [Ref. 16].

The evolution of mode-locked pulses can mathematically be shown in the frequency domain. In the time domain, a mode can be thought of as a cosine function. A Fourier transform is used to transform a function in the time domain to a function in the frequency domain. Using the Fourier transform, the cosine function in the time domain is converted into an impulse function in the frequency domain. Each oscillating mode will have a corresponding impulse function at its frequency in the frequency domain. The

laser linewidth can be thought of a band-pass step function in the frequency domain. The impulses multiplied by the band-pass step function produces a band of impulses. The inverse-Fourier transform of the band of impulses is a periodic sinc function in the time domain. The periodic sinc functions are the pulses produced from the mode-locked laser. Figure 2.3 is a graphic illustration of the mathematics in the frequency domain.

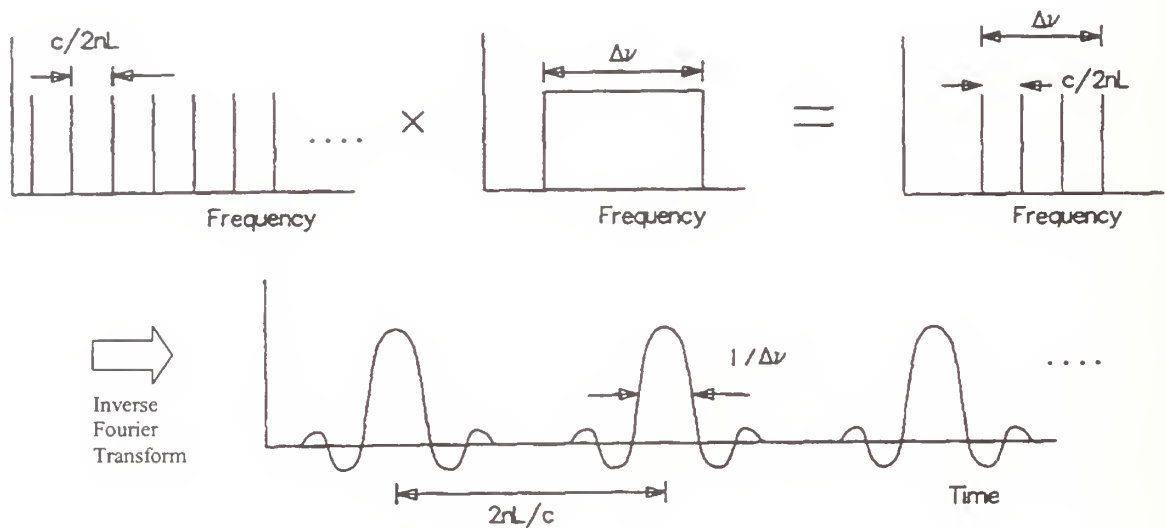


Figure 2.3. Frequency domain illustration of mode-locking, conversion to the time domain shows the mode-locked pulses. (After [Ref. 14].)

The pulse formation can also be shown in the time-domain. A simulation was created using MATLAB to study mode-locking. The six cosine waves (modes) shown in Figure 2.4a are generated using frequencies that are multiples of  $2\pi$ . Figure 2.4b shows the six frequencies on the same graph. As shown, the waves are in phase at the 400 and 800 marks on the time axis. The modes are added together and the absolute value of the sum is squared to show the intensity of the pulse in Figure 2.4c [Ref. 13].

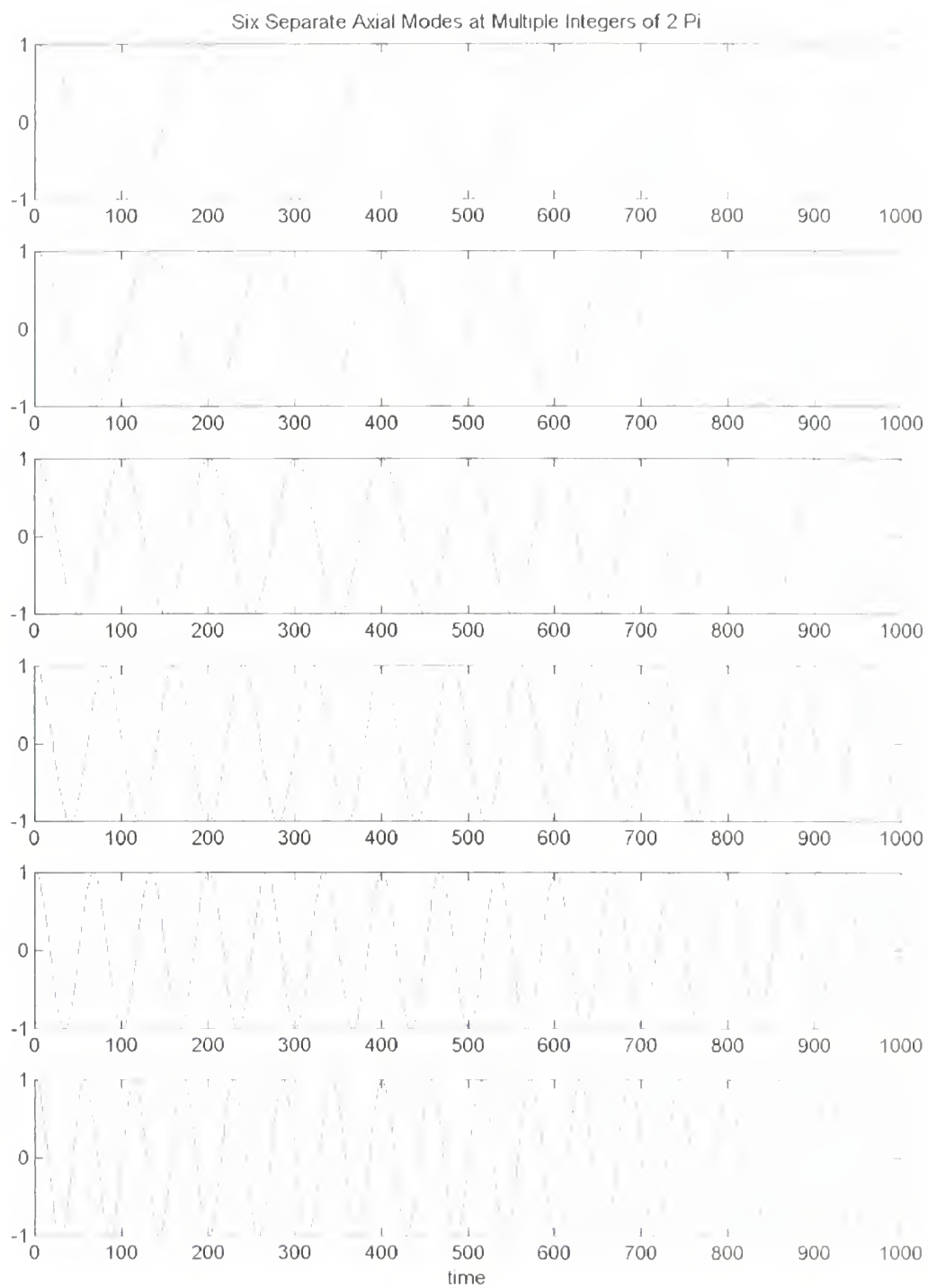


Figure 2.4a. Six separate modes at integer multiples of  $2\pi$ .





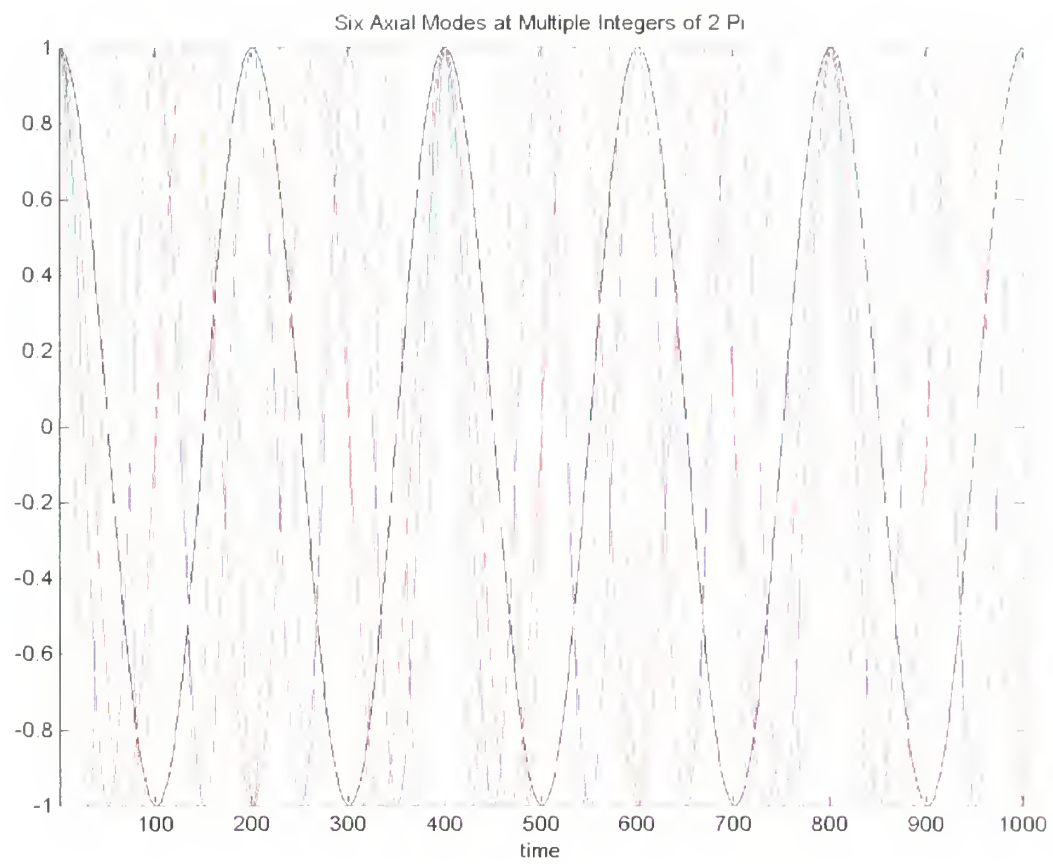


Figure 2.4b. Modes plotted together, note matching phase at time 400 and 800.



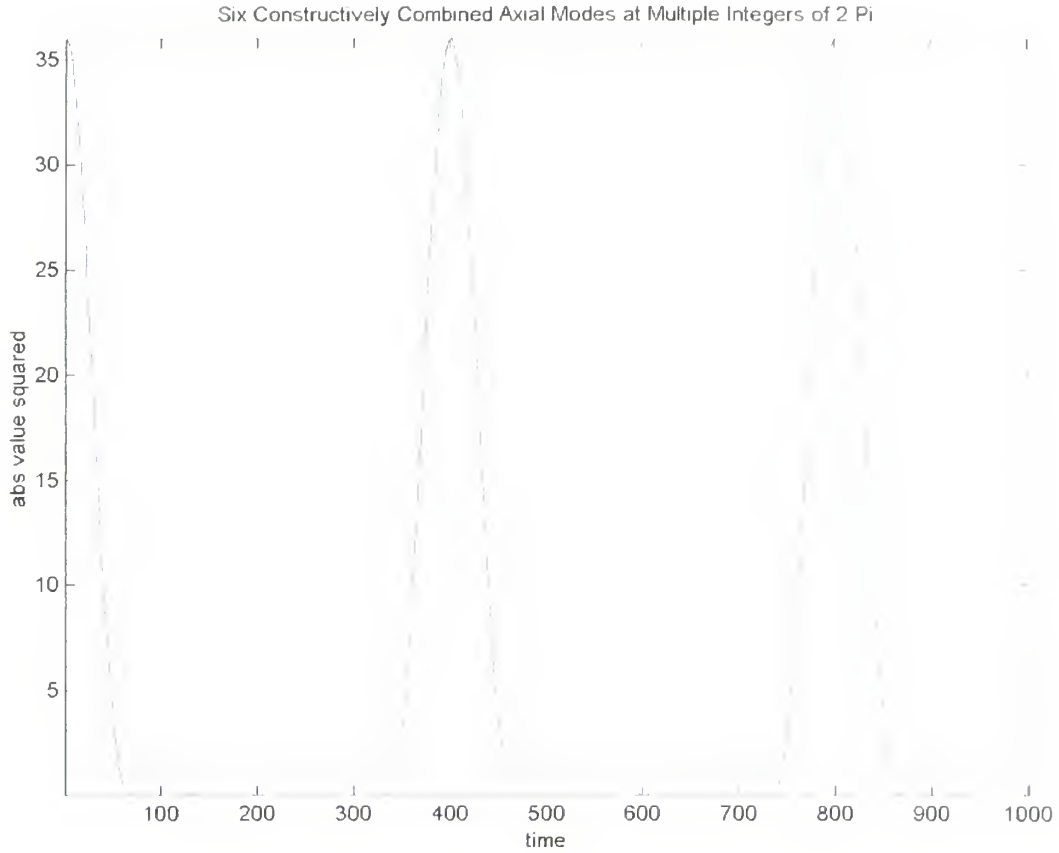


Figure 2.4c. Intensities of the modes constructively combine to produce mode-locked laser pulses.

In the basic mode-locked laser, the mechanism above will produce a period between pulses based on the round trip time of the laser cavity [Ref. 13]. The pulse period  $T$  is function of cavity length and the speed of light within the laser cavity. The period is also related to the frequency spacing between modes  $\Delta\nu_q$  [Ref. 16]. The period  $T$  is

$$T = 2nL/c = 1/\Delta\nu_q. \quad 2.8$$

The pulse repetition frequency (PRF) is simply the inverse of  $T$ . Equation 2.8 shows that cavity length  $L$  plays an important role in the pulse period. Higher PRFs will require



shorter cavity lengths. If the laser cavity is constructed of a ring or a loop instead of a standing wave cavity of length  $L$ , then the perimeter  $p$  of the loop will replace  $2L$  in Equation 2.8 [Ref. 13].

Pulsewidth is another important factor and is a function of the linewidth. The pulsewidth  $\Delta t$  is

$$\Delta t \approx 1 / \Delta \nu = 2 n L / N c = T / N . \quad 2.9$$

The second equality of the equation is found by manipulating Equation 2.6. The last equality is found by substituting  $T$  from Equation 2.8. One important observation is the impact of  $N$  on pulsewidth. A higher number of modes locked together in phase will produce a shorter pulse [Ref. 13].

The shape of a pulse is important and is a function of a number of factors within the laser cavity such as gain and dispersion. The mode-locked pulse can be Gaussian in shape but can be shortened to a squared hyperbolic secant ( $\text{sech}^2$ ), Lorentzian, or exponential shape using a nonlinear medium in the laser cavity. Typically, the pulses are either Gaussian or  $\text{sech}^2$ . The cavity effects on pulse shaping will be discussed later in this chapter with further discussion and measurement in Chapter IV [Ref. 16]. Using Equation 2.9, the number of  $N$  modes in a pulse can be approximated by [Ref. 13]

$$N \cong T / \Delta t . \quad 2.10$$

The calculations for PRF and pulsewidth are applicable when the laser light circulates within the laser cavity without any change per pass other than the mode-locking [Ref. 13]. The techniques used to promote mode-locking often place linear and nonlinear materials or active devices within the cavity. These changes may alter the equations above.





## C. MODE-LOCKING TECHNIQUES

The general categories of mode-locking techniques can be broken down into active mode-locking, passive mode-locking, or active-passive (hybrid) mode-locking, a combination of the two [Ref. 16]. The common techniques and combinations will be covered in the following sections. Some examples of these lasers along with some performance data will be covered later in the Chapter. It is important to recognize that like other lasers, mode-locked lasers can be constructed in a wide variety of ways and by using different materials. The laser can be constructed using “bulk devices” in which the pulses transmit through free air until they strike a mirror, lens or other device used to direct or modify them. The mode-locked laser can also be constructed using fiberoptic or semiconductor materials and the output transmitted through optical fiber. The latter devices are self-contained and are more useful in the application of an optical ADC and to telecommunications in general.

### 1. Active Mode-Locking

In active mode-locking, a modulating mechanism is introduced into the laser cavity to actively couple or force the oscillating frequencies to lock together in phase. The modulation can be amplitude modulation (AM), frequency modulation (FM), or phase modulation (PM) [Ref. 13]. The modulation of light is generally accomplished in one of four ways including electro-optic, acousto-optic, moving-mirror, or synchronously pumping the gain medium of the laser [Ref. 14].

In AM modulation, the of laser light is typically intensity modulated by an electro-optic or acousto-optic modulator. The electro-optic amplitude modulator uses phase modulation in an interferometric configuration to amplitude modulate the light. The acousto-optic modulator can amplitude modulate light by diffracting most or all of the laser beam away from the output port [Ref. 14].

Frequency modulation can be accomplished using an acousto-optic modulator. The diffracted beam undergoes a frequency shift and is used in place of the original laser light. An axially moving mirror at the end of a laser cavity can also be used for FM. The

mirror changes the light frequency by changing the length of the cavity. The synchronous pumping of the laser gain medium is another form of AM and is accomplished by amplitude modulating the laser pump source. One example of synchronous modulation is modulating the drive current of a pump laser diode that is then used to pump an erbium-doped fiber laser [Ref. 14].

The active modulation frequency  $f_m$  must be an integer multiple  $m$  of the mode frequency spacing interval  $\Delta\nu_q$  and is given by

$$f_m = m\Delta\nu_q = mc / 2nL . \quad 2.11$$

The PRF will be the modulation frequency  $f_m$  or an integer multiple of  $f_m$  [Ref. 13]. In the actively mode-locked laser, the pulsewidth becomes [Ref. 13]

$$\Delta t \approx (0.5) / (f_m \Delta\nu)^{1/2} = (0.5) / (f_m N^{1/2}) . \quad 2.12$$

This equation is known as the Kuizenga-Seigman equation and is often used as a minimum pulsewidth for purely, actively mode-locked lasers [Ref. 17]. Later we will find that the pulsewidth can be reduced, incorporating passive mode-locking techniques into an actively mode-locked laser.

## 2. Passive Mode-Locking

In passive mode-locking, a loss mechanism such as a saturable-absorber is introduced into the cavity to create a periodic loss of intensity. As light passes through this material, it loses energy to the absorber. The absorber eventually becomes saturated, alters the index of refraction of the material, and the light is then allowed to pass with much less loss. The absorber loses its saturation over time (relaxes) and the process repeats. This repetition forces the modes into phase to begin the mode-locking. The mode-locked pulse passes through the absorber more efficiently since it has a higher peak power and immediately saturates the material allowing its passage. The required saturation energy of the material may be so high that constant-wave (CW) laser light may

be fully attenuated but a high intensity pulse will easily pass through the energy absorbing material [Ref. 13].

The pulses produced in a passively mode-locked laser tend to be much shorter in duration and have been measured at less than 13 femtoseconds [Ref. 18]. There are many nonlinear mechanisms that contribute to the pulsewidth in these lasers making it difficult to predict pulsewidth either theoretically or experimentally [Ref. 13], so equations for passively mode-locked pulsewidths are not offered here. The designer will probably have to derive them based on the materials and techniques particular to the cavity being constructed.

Depending on the design of the laser, the pulse compression (in time) mechanism can be a function of gain saturation in the laser amplifier section and saturation of an absorber section. In gain saturation, the leading edge is absorbed and saturates the amplifier. This amplifies the pulse amplitude and will fractionally reduce the pulsewidth due to the leading edge being lost to the amplifier [Ref. 16]. However, high gain amplifiers often have a positive dispersion factor that still broadens the pulse beyond the shortening effect of gain saturation [Ref. 17]. The saturable absorber reduces the pulsewidth similarly. Here the leading edge is “clipped” in the absorber’s saturation process so that the rest of the pulse is allowed to pass through. The clipping of the leading edge serves to shorten the pulse duration [Ref. 16].

The overall dispersion in the laser cavity can have a broadening or narrowing effect depending on design. As a pulse travels through the laser cavity or any other medium, material dispersion will cause the pulse to broaden in time. Depending on the length of the cavity, waveguide dispersion will cause a narrowing or broadening of the pulse due to fact that the different modes at different optical frequencies travel at different velocities. This waveguide dispersion is also called group velocity dispersion (GVD) and is a function of the average material dispersion in the cavity [Refs. 16, 17]. The average material dispersion  $D_{avg}$  in the laser cavity is a function of the lengths of different fibers used and the overall length of the cavity [Ref. 19]. The GVD is given by [Ref. 17]

$$\beta = \lambda^2 D_{avg} / 2 \pi c . \quad 2.13$$

At certain wavelengths for the material, waveguide dispersion will be negative thus shortening a pulse rather than broadening it. In combination the total dispersion of a cavity can be adjusted so that it is negative and will induce pulse compression [Ref. 20].

### 3. Active-Passive Mode-Locking

The actively mode-locked laser tends to be much more stable in maintaining a steady stream of pulses because it is essentially driven by an externally clocked modulation frequency  $f_m$ . Passively mode-locked lasers produce the shortest pulses but provide a less stable output [Ref. 17]. Since the overall goal is to produce narrow pulsewidths at high PRFs, mode-locking is often accomplished by using a combination of the techniques. The laser maintains a stable PRF driven by an external clock but the pulses are narrower than the results of Equation 2.12 above because of the passive techniques.

One method of pulse shortening is through the formation of solitons. A soliton is a nonlinear pulse created from the frequency chirp at the leading and trailing edges of a traveling pulse. The chirp is created from the rapid interaction of the pulse edges with the saturable absorber material and forces the pulse to undergo a self phase modulation (SPM) [Ref. 21]. The self phase modulation is a nonlinear effect that counteracts the pulse spreading from dispersion and allows the pulse to travel through the transmitting medium more efficiently. The chirp and accompanying SPM is often accomplished by using a large negative dispersion throughout the total length of the laser cavity [Ref. 16]. Overall, solitons require more power to maintain their nonlinearity and must be amplified more often in any transmission system [Ref. 20].

The minimum requirements for soliton formation can be found through analysis of the laser cavity dispersion. In a fiberoptic cavity, the total fiber dispersion  $D_f$  is given by

$$D_f = \beta L, \tag{2.14}$$

where  $L$  is the length of the cavity in kilometers and  $\beta$  is the GVD from Equation 2.13. The dispersion attributed to gain  $D_g$  also contributes to soliton formation and is given by

$$D_g = G / B^2 \quad 2.15$$

in which  $G$  is the gain of the amplifier and  $B$  is the gain bandwidth of the amplifier in Hertz. The soliton formation can occur if [Ref. 17]

$$D_f / D_g \geq 0.652 . \quad 2.16$$

The mode-locked laser pulse can evolve into a soliton if it meets the criteria of Equation 2.16. The soliton is a  $\text{sech}^2$ -shaped pulse that is shorter in duration for the same pulse amplitude than a Gaussian-shaped pulse. The soliton is used in an active-passive mode-locked laser to reduce overall pulsewidth. The maximum amount of reduction  $R_{\max}$  due to soliton formation is

$$R_{\max} \approx 1.37(D_f / D_g)^{1/4} . \quad 2.17$$

When  $D_f/D_g = 0.652$ , the factor  $R_{\max}$  is its minimum value of 1.23. Larger values of  $D_f/D_g$  increase  $R_{\max}$  to values of 4.4 or more [Ref. 12].

This reduction is important because active mode-locking tends to give broad pulses as shown in Equation 2.12. In addition to Equation 2.16, soliton formation requires an average cavity dispersion of less than or near zero as well as more power. The higher the power in the laser cavity, the greater the nonlinearity and shorter pulses will result. If soliton formation is possible, then Equations 2.12 and 2.17 can be combined as

$$\Delta t \approx (0.5) / (f_m \Delta \nu)^{1/2} / R_{\max} = (0.5) / (f_m N^{1/2}) / R_{\max} \quad 2.18$$



and the minimum pulsewidth for an active-passive mode-locked laser can be calculated [Ref. 17].

#### **D. TYPES OF MODE-LOCKED LASERS**

There are a variety of mode-locked lasers that exist experimentally or are available commercially. For purposes of this Thesis, only mode-locked lasers that fit the requirements of an optical sampling system are considered. The performance criteria expected from a mode-locked laser are pulsewidth, pulse rate, temporal jitter, wavelength, and stability. An optical ADC used for military applications such as communications or Electronic Warfare would be expected to operate continuously without human interaction. The experimental lasers that are inherently unstable, only produced bursts of mode-locked pulses, or do not operate continuously were excluded from this study because they cannot be used in an optical ADC.

The wavelength of the laser is also considered. Given the reduction in defense procurement dollars, the laser must be built from commercial off the shelf (COTS) products. This helps to ensure parts availability for experimentation and component replacement in an existing laser system. There are three "Transmission Windows" at 850, 1300, and 1550 nm that favor low loss light transmission through optical fiber. The telecommunications industry had used equipment operating at 1300 nm and has transitioned to 1550 nm equipment due to improved transmission efficiency [Ref. 22]. The lasers that operate at non-industry wavelengths without the capability or promise of moving to these standards were also discarded from consideration.

This leaves pulsewidth, PRF, and noise performance for consideration. The pulse amplitude is not considered a limiting factor because a pulse can always be externally amplified. Although many types and examples of these lasers exist, they can be grouped into three major categories: solid state, fiber, and diode mode-locked lasers.

## 1. Solid State Lasers

There are a number of crystalline materials used for solid state mode-locked solid state lasers. Neodymium yttrium lithium fluoride (Nd:YLF), neodymium yttrium aluminum garnet (Nd:YAG), and titanium sapphire (Ti:Al<sub>2</sub>O<sub>3</sub>) lasers are three common commercially available lasers. These lasers are usually bulk devices with the crystals externally pumped by pump diodes, flash lamps, or even other high powered lasers such as an argon ion laser [Refs. 18, 23]. Figure 2.5 shows a typical solid state mode-locked laser. In this Ti:Al<sub>2</sub>O<sub>3</sub> laser, the cavity is actively mode-locked using an acousto-optic modulator (AOM) [Ref. 23].

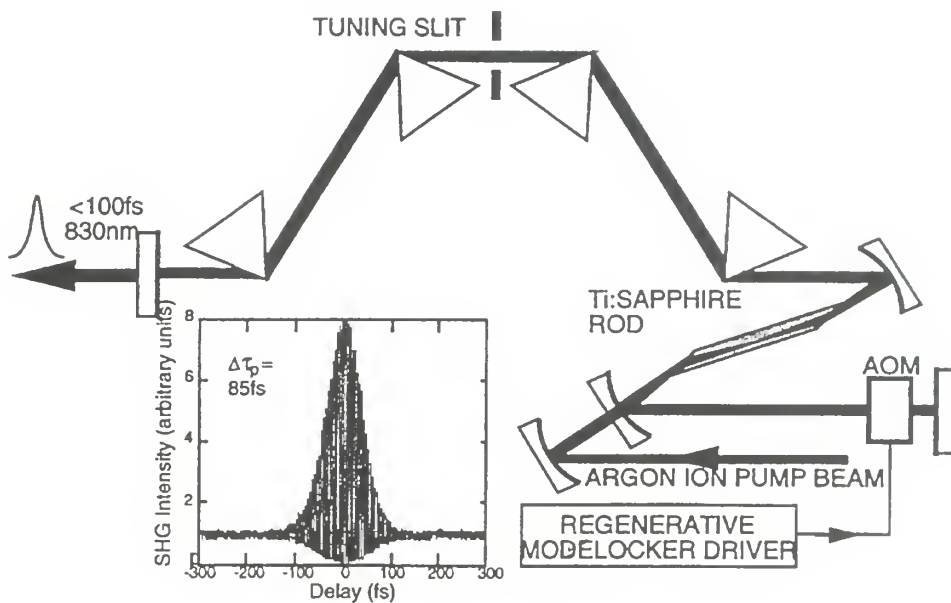


Figure 2.5. Solid state titanium sapphire mode-locked laser. (From [Ref. 23].)

The Nd:YAG lasers can be passively or actively mode-locked to operate up to 100 MHz PRF with pulsewidths as low as 7 ps at wavelengths around 800 nm. The noise jitter measurements were not available but the lasers are typically low noise [Ref. 24].

The Ti:Al<sub>2</sub>O<sub>3</sub> lasers have produced some of the shortest pulsewidths ( $\Delta t < 13$  fs). These lasers also operate in the 800 nm range and can be passively or actively mode-locked to a PRF of 100 MHz [Ref. 18]. In one Ti:Al<sub>2</sub>O<sub>3</sub> laser locked at 84 MHz, timing jitter was measured at 84 fs [Ref. 23]. The Nd:YLF lasers have demonstrated mode-





locking PRFs of up to 250 MHz at a 1300 nm wavelength and pulsewidths as low as 400 fs. Noise measurements were not available for the Nd:YLF laser [Ref. 18]

Solid state lasers can provide stable mode-locking at useful wavelengths with very short pulsewidths. However, PRFs in the GHz range are required for an optical sampling system and solid state lasers have only demonstrated themselves in the MHz region of the spectrum.

## 2. Diode Lasers

The laser diode can also be mode-locked by active, passive, or active-passive means. The passively mode-locked laser uses a saturable absorber in the cavity while the actively mode-locked laser is driven by modulation of the current of the laser diode [Ref. 25]. These lasers can produce soliton pulse shapes at pulsewidths as low as 200 fs. One published paper lists an actively mode-locked diode laser with a PRF of 18 GHz and demonstrates a passively mode-locked laser with a 64 GHz PRF. The lowest amplitude and timing jitter measured in the passively mode-locked laser was 0.005% and 65 fs [Ref. 26]. More recently, the Oki R&D Group in Japan claims to have constructed an actively mode-locked laser with a 40 GHz PRF with pulsewidths as low as 240 fs. The company also claims passive mode-locking at 350 GHz PRF. The noise measurements for the Oki lasers are not available [Ref. 27]. Figure 2.6 is an example of a passively mode-locked semiconductor laser.

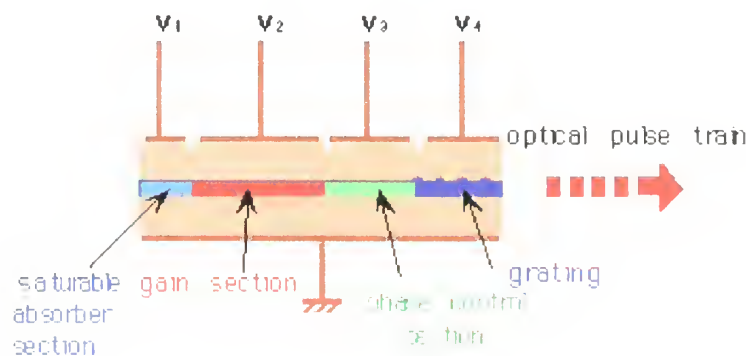


Figure 2.6. Passively mode-locked semiconductor laser. (From [Ref. 27].)



Although mode-locked diode lasers show promising performance for use in an optical sampling system, they cannot be purchased commercially. They appear to exist in only in laboratories that are capable of production of semiconductor devices. There is ongoing research in semiconductor mode-locked lasers at corporations and at a number of universities so they may eventually be commercially available.

### 3. Fiber Lasers

The rapid advances in the telecommunications industry have brought with it a variety of fiberoptic components as well as different types of fiber. Instead of using the bulk devices as in solid state lasers, the modulators, amplifiers, and other optical components have been incorporated into fiberoptic packages for insertion in a fiber system. The fiber becomes a waveguide and eliminates the need for exact alignment as in the bulk configurations. The three common designs that have emerged in fiber lasers are the fiber ring laser (Figure 2.7a), the figure-eight laser (Figure 2.7b), and the sigma laser (Figure 2.7c) [Ref. 11].

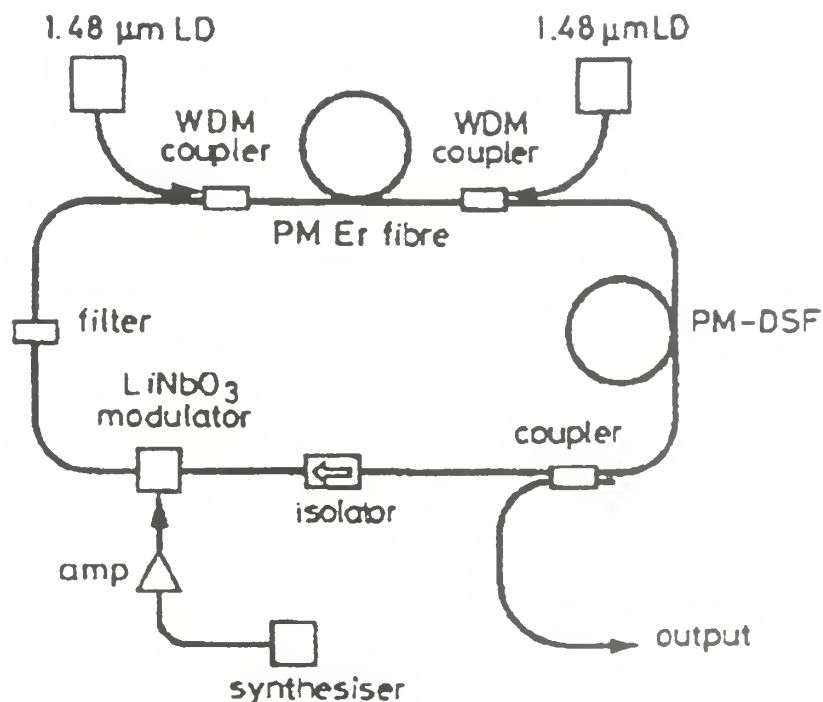


Figure 2.7a. Actively mode-locked fiber ring laser. (From [Ref. 28].)

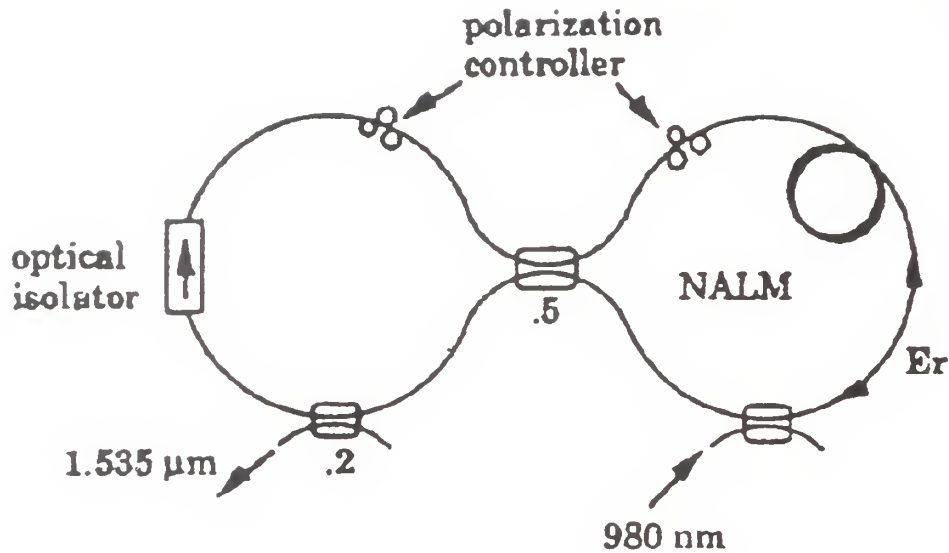


Figure 2.7b. Passively mode-locked figure-eight nonlinear-loop-mirror fiber laser. (From [Ref. 29].)

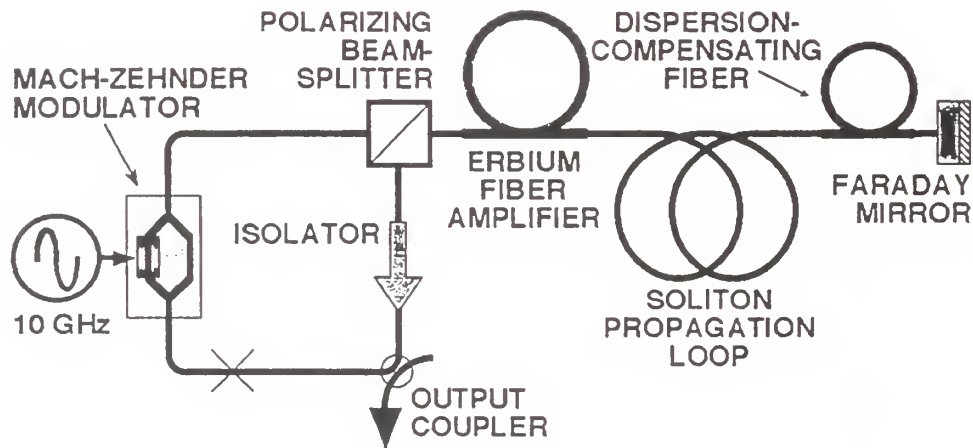


Figure 2.7c. NRL actively mode-locked sigma laser. (From [Ref. 30].)

These lasers can be mode-locked by active, passive, or active-passive means. The amplifying medium is usually a rare earth doped fiber such as erbium (ER) or erbium-ytterbium that is pumped using laser diodes or high power solid state constant-wave lasers mated to optical fiber. The laser wavelengths are usually 1300 or 1550 nm. The

components and types of fiber in each laser are typical of all fiber lasers and a more detailed discussion of these parts is presented in the next chapter.

The fiber ring laser is a simple cavity in which the light resonates around a loop instead of between the two mirrors of a more typical laser such as in Figure 2.2 on page 13. The ring laser has produced pulsewidths as short as 75 fs [Ref. 31] and has been mode-locked at PRFs of 20 GHz [Ref. 32]. The ring laser has also been harmonically mode-locked at PRFs of 300 GHz [Ref. 33]. Harmonic mode-locking is where the laser produces a pulse rates at an integer multiple of the modulation frequency. One fiber ring laser was measured to have 2 ps of timing jitter at a PRF of 100 MHz [Ref. 34].

The figure-eight laser is essentially a ring laser with a coupler in the center. One side of the figure eight has an isolator to force the light in one direction. The other side is referred to as a mirror loop. The light traveling in both directions of the mirror loop causes a nonlinear phase change that promotes mode-locking at high powers in the entire cavity. The passively mode-locked figure-eight laser has produced pulses as short as 100 fs duration pulses [Ref. 29] and PRFs of up to 2 GHz [Ref. 35]. Noise measurements were not available for these lasers.

The sigma laser was originally invented and patented at the Naval Research Laboratory (NRL) in Washington D.C. and was designed for a 100 GHz time domain multiplexed fiberoptic communication system [Ref. 30]. The laser has a published performance of 1.3 ps pulsewidths, 1 to 20 GHz PRF, 160 fs of temporal jitter, and 1.1% amplitude jitter [Refs. 7, 12]. With further optimization of dispersion in the cavity, NRL has recently reduced the laser pulsewidth to 740 fs [Ref. 19].

The sigma laser was selected by NPS for construction because its published performance parameters look promising for application in an optical ADC. An NPS optical ADC is likely to be used in a mobile platform that is limited in power consumption. Since the mode-locked laser is a critical component of the ADC, a lower power optical amplifier is incorporated into the design.

NRL uses an erbium/ytterbium (Er/Yb) co-doped fiber amplifier pumped by a neodymium (Nd) solid state laser. The Nd laser is pumped with one watt of optical power from two 800 nm pump laser diodes. Saturated output power from this amplifier

is 200 mW [Ref. 12]. The NRL version is commercially available from PriTel, Inc. in Naperville, Illinois [Ref. 7].

The NPS laser differs in design from the NRL sigma laser in optical power and type of amplifier built into the cavity. The NPS sigma laser uses an erbium-doped fiber pumped by 200 mW of optical power from two 980 nm pump laser diodes. Saturated output power from this erbium-doped fiber amplifier power was measured at 51 mW. The details of the ER amplifier will be discussed in the next chapter.

The theory of mode-locked lasers is an important factor in design of any mode-locked laser. The next chapter is a description of the construction of the NPS sigma laser, its components, stabilization system, and operation.



### III. CONSTRUCTION OF THE SIGMA LASER

The NPS sigma laser is an actively mode-locked laser that uses some of the passive laser techniques described in Chapter II to promote pulse shortening [Ref. 12]. The laser can be thought of as four major sections: 1) a polarization maintaining loop for modulation, 2) an erbium-doped amplifier for generating 1560 nm laser light and pulse amplification, 3) a propagation section for dispersion management, and 4) a feedback length stabilization system used to maintain the laser in a mode-locked state. Figure 3.1 on the next page is a detailed drawing of the sigma laser in its present form and will be referred to throughout the Chapter.

#### A. CAVITY DESIGN

The actively mode-locked erbium fiber laser is shaped in the form of a  $\sigma$ , thus earning the title “sigma” laser. In broad terms, the laser operates similar to the oscillator shown in Figure 2.2 where the light waves oscillate between the two ends of the cavity. At one end, the laser has a mirror to reflect the light. The mirror at the other end is replaced with a loop of fiber that redirects the light back through the cavity for another round trip. The shape of the cavity performs three functions: polarization maintenance for modulation purposes, birefringence compensation, and dispersion management. Different types of glass fibers used to construct this laser perform these various functions.

##### 1. Fiber Types

The laser cavity primarily consists of six types of glass fibers that include polarization maintaining (PM) fiber, erbium-doped (ER) fiber, dispersion-shifted (DS) fiber, dispersion-compensating (DK) fiber, singlemode (SM) fiber, and “Flexcor” fiber. The total cavity length, consisting of these fibers and different components, is approximately 127 meters. In general, glass fiber is made up of an inner core and an

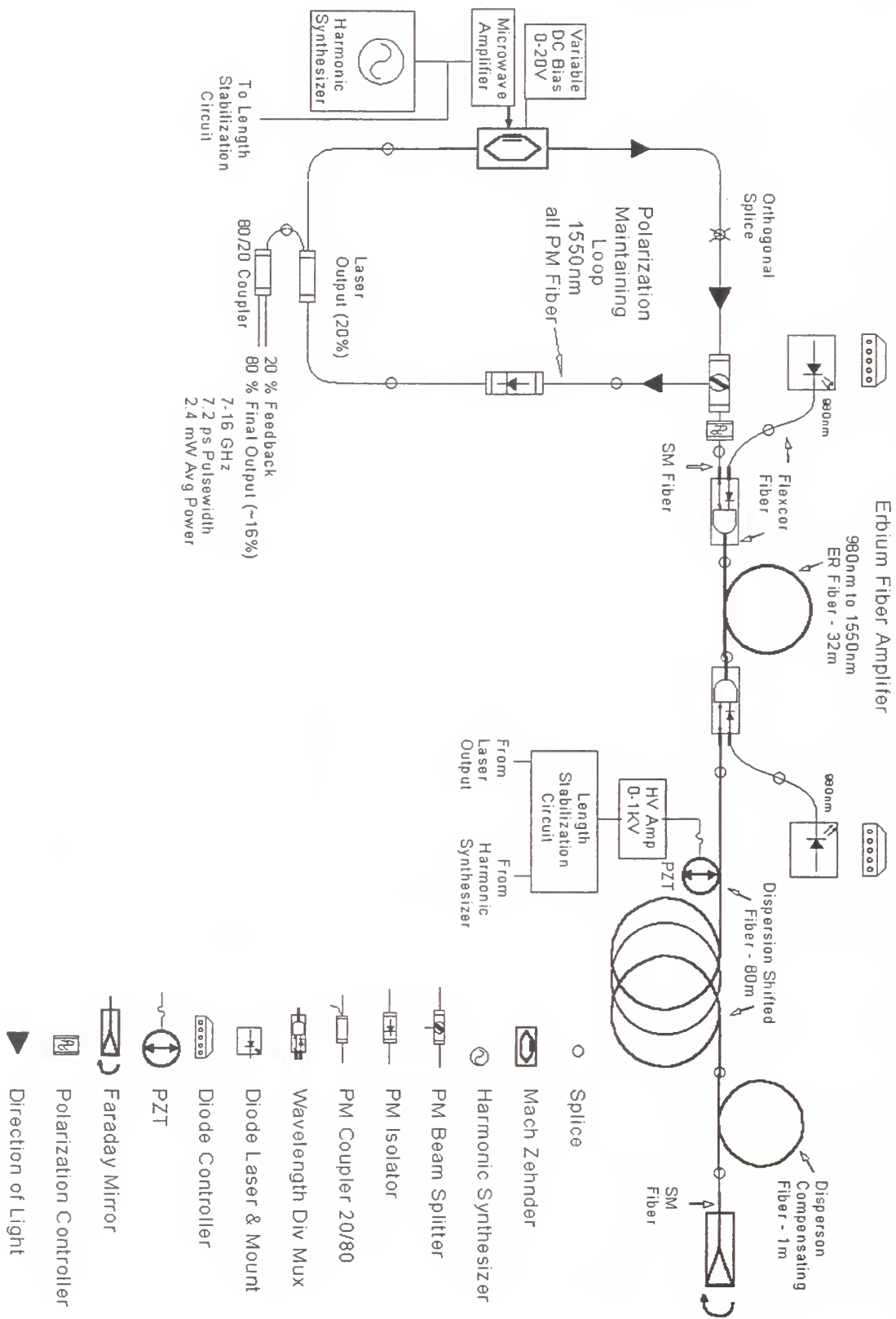


Figure 3.1. NPS actively mode-locked sigma laser.

outer cladding as seen in Figure 3.2. The inner core has a slightly higher index of refraction than the cladding. Because of the different indices, the boundary between the two induces a total internal reflection relative to the core producing a waveguide for light [Ref. 36].

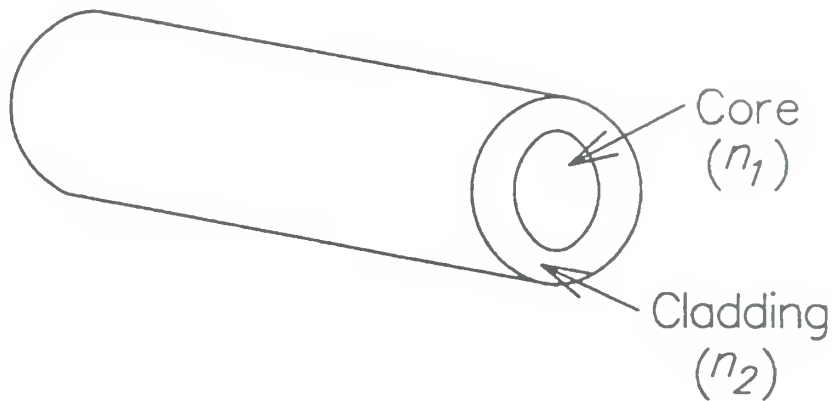


Figure 3.2. Fiber showing the inner core and outer cladding. (From [Ref. 20].)

The core diameters of the fiber in this laser range from 3.5 to 10.5  $\mu\text{m}$ . The cladding is typically 125  $\mu\text{m}$  in diameter. The cladding of the fiber usually has a protective acrylic coating that increases the overall diameter to about 250  $\mu\text{m}$ . The term “bare fiber” refers to fiber that only has the acrylic coating for protection. Often the fiber is sheathed in a plastic cable for industrial and commercial purposes. Most fibers in the sigma cavity are bare fiber. The main exception is the two output fibers (pigtails) that are cabled for handling purposes.

To enhance the waveguide effect, most of the fibers in this laser are designed for singlemode (SM) operation. Singlemode fiber has a small core radius to promote propagation of light directly down the center of the fiber instead of continuously reflecting off of the core-cladding boundary as a means of propagating through the fiber [Ref. 37]. In singlemode fiber, the area in and around the inner core is often called the mode field because it contains most of the propagating light. The mode field diameter rather than inner core diameter specifies the guiding action of singlemode fibers.

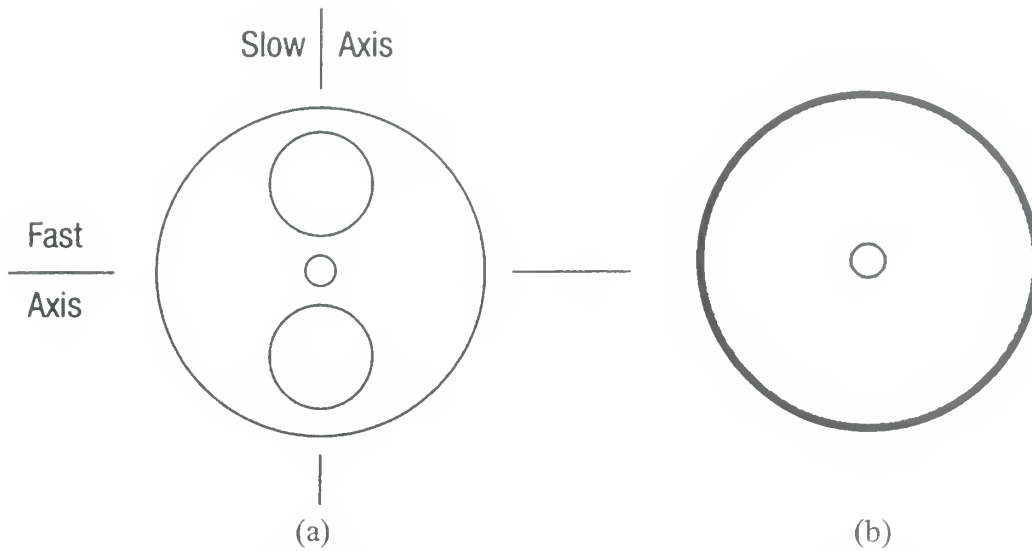
The laser light in the sigma laser can be described as a linearly polarized electromagnetic field of energy [Ref. 14]. The linearly polarized light will travel through the fiber on a single axis relative to the core center. Without any polarization control in long lengths of fiber, the axis of polarization will become random. This occurs when mechanical and environmental effects acting on the fiber rotate the polarization unintentionally.

## **2. Polarization Maintaining Fiber**

The polarization maintaining (PM) fiber maintains the linearly polarized light on a specific axis required for active modulation. This fiber is made with two birefringent stress fibers (rods) along either side of the mode field [Ref. 37]. Birefringence is a formation of orthogonal fast and slow axes by structural variations within the fiber [Ref. 14] and can be induced by fiber structure, lattice structure in the material, or even random stresses due to imperfections in the glass. The structural variations present different indices of refraction to the passing light depending on the axis of polarization relative to the internal structure. The birefringent stress rods in PM fiber are designed to cause the formation of the fast and slow axes for the light to travel on. When linearly polarized light is guided down a fast or slow axis in the PM fiber, it stays on that axis and maintains polarization [Ref. 37].

Figures 3.3a and 3.3b are cross sections of PM and SM fibers for comparison. The tiny circle in the center is the inner core. The birefringent stress rods can be seen in the PM “Panda” type fiber above and below the core. The SM fiber has nothing to purposely induce birefringence.

All of the PM components are produced with Fujikura brand UV-400 Panda fiber. This fiber has a mode field diameter of 8  $\mu\text{m}$  [Ref. 38] and a dispersion factor of approximately 20 ps/nm/km. Approximately 8 meters of PM fiber are used in the sigma laser cavity.



Figures 3.3 (a) PM and (b) SM fiber cross sections. (From [Ref. 37].)

### 3. Singlemode Fiber

Three of the components in the branch of the cavity are made with SM fiber pigtails for splicing. This fiber is Corning brand SMF-28 fiber that has a mode field diameter of  $8.3\ \mu\text{m}$  and a dispersion of  $20\ \text{ps/nm/km}$  [Refs. 20, 39]. The wavelength division multiplexers (WDMs) and Faraday mirror are also made with this fiber; these devices will be explained later. Approximately 3 meters of SMF-28 are used in the cavity.

### 4. Dispersion-Shifted Fiber

Dispersion-shifted fiber is a singlemode fiber typically used for long haul telecommunications [Ref. 40]. As previously mentioned, dispersion will cause a broadening of the pulse, or any other signal in the time domain. In singlemode fiber, dispersion can be a product of the material index of refraction and is called material dispersion. Material dispersion also increases with wavelength but is approximately zero  $\text{ps/nm/km}$  at  $1300\ \text{nm}$  for typical step index fiber. Step index fiber has an index of refraction that is constant throughout the core diameter. In dispersion-shifted fiber, the core is doped with a material such as germanium dioxide to shift the minimum dispersion point closer to  $1550\ \text{nm}$  [Ref. 20].

The Corning SMF/DS CPC6 dispersion-shifted (DS) fiber has a nominal dispersion of 2.7 ps/nm/km for the third transmission window [Ref. 40]. This is about an 85% dispersion reduction over typical SM fiber at 1550 nm [Ref. 20]. The DS fiber has an attenuation factor of 0.05 dB/km and a mode field diameter of 8.1  $\mu\text{m}$ . Approximately 80 meters of DS fiber were used in the construction of the laser. About 40 meters were wrapped on a ceramic piezoelectric cylinder for length stabilization purposes.

## **5. Dispersion-Compensating Fiber**

Dispersion-compensating (DK) fiber was originally designed for singlemode telecommunications links that originally used 1300 nm light but now use 1550 nm light at a large dispersion penalty. The dispersion-compensating fiber is doped to have a large negative dispersion of around  $-100$  ps/nm/km to reverse the effects of positive dispersion found in most non-DS fibers at 1550 nm. The negative dispersion comes with a higher penalty of attenuation [Ref. 20].

The Lucent Technologies brand DK-SM dispersion-compensating fiber has a dispersion factor of  $-104.2$  ps/nm/km, a mode field diameter of 5.2  $\mu\text{m}$ , and an attenuation factor of 0.52 dB/km [Ref. 41]. This attenuation is ten times that of the DS fiber. Originally the laser was built with 10 meters of DK fiber in the cavity but the length was reduced to 1 meter when the laser appeared unstable in terms of mode-locking.

## **6. Erbium-Doped Fiber**

Erbium-doped fiber is a specialty fiber used for fiber amplifiers (EDFAs). This fiber is structured like the singlemode fiber in Figure 3.3b. This fiber is produced by FIBERCORE in the UK and is made primarily for use with 980 nm pump diodes for producing and amplifying laser light in the third transmission window [Ref. 42]. Approximately 32 meters of ER fiber were used in the EDFA. This fiber has a mode field diameter of 3.5  $\mu\text{m}$  and an attenuation factor of 3.1 dB/km. The material dispersion for the fiber is not available from the manufacturer but a similarly doped fiber is found to



have dispersion of  $-0.09$  ps/nm/km [Ref. 43]. The design and construction of the EDFA will be discussed in detail later in the chapter.

## 7. Flexcor Fiber

Corning Flexcor 1060 brand fiber is used to connect the laser light from the pump diodes to the ER fiber. This fiber is made for use with pump lasers and is optimized for 980 nm laser light. The fiber has a mode field diameter of  $5\text{ }\mu\text{m}$  and a maximum attenuation of 5 dB/km [Ref. 39]. Approximately seven meters of Flexcor 1060 fiber were used in this laser. Three of the seven meters contribute to the length of the cavity.

The entire cavity could have been constructed from PM fiber to form a fiber ring laser or another configuration but some of the fiber types are not typically available in PM form. The erbium-doped PM fiber has recently become available; however, DS and DK fiber are not typically produced in PM form but are instead mass produced for the telecommunications and cable TV industries. In addition, the DK fiber is both difficult to make and splice properly. As a result it is not generally sold unless prepackaged in telecommunications type modules [Ref. 44]. In general PM fiber and PM fiber components are much more expensive than SM fiber and non-PM components. In this fiber laser design, PM fiber and components were only used where necessary and SM fiber and components were used for the rest of the laser cavity. This partly accounts for the shape of the cavity for the sigma laser. Table 3.1 is a summary of the types of fibers used in the laser cavity; the locations of these fibers are identified in Figure 3.1.

Fiber Type	Brand	Attenuation @ 1550 nm dB/km	Mode Field Diameter $\mu\text{m}$	Dispersion ps/nm/km	Length Uses meters
PM	Fujikura UV-400	0.5	8.0	20	8
SM	Corning SMF-28	0.3	8.3	20	3
DS	Corning SMF/DS CPC6	0.05	8.1	2.7	80
DK	Lucent DK-SM	0.52	5.2	-104.2	1
Flexcor	Corning Flexcor 1060	5 (@980 nm)	5.0	not avail.	3
ER	Fibercore 1500A	3.1	3.5	-0.09	<u>32</u>
Total					127

Table 3.1. Summary of fibers used in the sigma laser.



## 8. Fiber Splicing

The fibers listed above were fusion spliced together to form the sigma laser cavity. In fusion splicing, the acrylic coating is stripped from the bare fiber, the glass is cleaved at a 90 degree angle, and the two ends to be fused were cleaned and placed in the splicing machine. The ends of the fiber are aligned on each axis and separated laterally by approximately 5  $\mu\text{m}$ . The DS, DK, and Flexcor fibers are spliced together using a manual Sumitomo 11X Splicer. A 1550 nm or 980 nm laser source was connected at one end and an optical multimeter read the power at the other end. The X and Y axes were continually adjusted until the maximum power was attained on the multimeter indicating that the fibers were aligned. An electric arc of about one second in duration fused the two ends of glass together. The fused splice creates a continuous waveguide between the two fibers. The losses from a splice are usually less than 0.1 dB [Ref. 45].

As shown in Table 3.1, the fibers have different mode field diameters. When splicing these fibers together, the different diameters cause a loss of light when light propagates from the larger diameter to a smaller diameter. There is no loss when going from a smaller to larger diameter [Ref. 20]. The loss in power can be expressed as [Ref. 38]

$$L_{MFD} = -10 \log \left[ \frac{4}{(d_2 / d_1 + d_1 / d_2)^2} \right]. \quad 3.1$$

There are two significant mode field mismatches within the laser at the DK and ER fibers. The length of DK fiber (5.2  $\mu\text{m}$ ) has DS fiber (8.1  $\mu\text{m}$ ) fiber on one side and SM fiber (8.3  $\mu\text{m}$ ) on the other. These lengths are directly spliced together in the manual Sumitomo splicer and have  $L_{MFD}$  of 0.83 dB and 0.92 dB, respectively.

A mismatch of mode field diameters occurs between the Flexcor (5  $\mu\text{m}$ ) and erbium-doped fibers (3.5  $\mu\text{m}$ ). If directly spliced together, they would cause a 0.54 dB loss. This is a critical junction in the cavity since about 6% of the power from the pump diodes would be lost. The newer, automatic splicing machines are capable of preheating

the smaller diameter fiber of a mismatched splice. The preheating expands the smaller diameter to the appropriate size so that the fibers can be fused together with no mismatch losses. The Vytran Corporation, a splicing machine vendor exhibiting a new machine at the 1998 Photonics Systems for Antenna Applications Symposium in Monterey, demonstrated this technique on the erbium-doped fiber amplifier. The Vytran machine is programmed to perfectly preheat the ER fiber to match the Flexcor fiber mode field diameter. Both ends of the ER fiber were spliced to the Flexcor fibers from the wavelength division multiplexers (WDMs) resulting in negligible splice losses from the mismatched mode-field diameters. The end result is that all of the power from the pump diodes is transmitted into the ER fiber.

The splicing of the PM fiber required a PM splicer that would automatically line up the stress rods in this type of fiber. All PM fiber was spliced using a Fujikura FSM-20PM splicing machine at the Naval Research Laboratory in Washington DC. This machine can also produce an orthogonal splice by aligning the rods in each cleaved end at a 90 degree angle from each other.

After a splice is made, the point where the glass is fused together is fragile and can break under minimal handling conditions. At NRL, splice protectors were applied after fusing the PM fibers together. Before each splice, a splice protector was slid over one of the ends of fiber and then down the fiber and out of the way. The splice protector is a 1" plastic tube with a length of metal rod inside. After a splice was made, the splice protector slides over the splice and both are inserted in a small oven mounted on the splicing machine. The oven evenly melts the plastic and holds the fused fibers and metal rod together permanently. This makes the fiber safe to handle without breaking.

The Vytran splicing machine that spliced the ER and Flexcor fibers has a device that re-coats the spliced fiber with acrylic. The acrylic coating replaces the splice protectors and makes the spliced fiber safe for handling. This process appears to be as durable as a splice protector.

The NPS machine does not have a method for splice protection. To make the splices safe for handling, splice protectors were created from 1/64" drill rod and electrical shrink tubing available at the local hardware store. The shrink tubing was placed over the splice and the cut-to-length rod inserted. A heat gun was used to shrink the tubing over

the rod and fiber to make the splice permanent and safe to handle. This method worked fine for laboratory applications where the fiber was placed in a system and did not require further handling. If the splice requires further handling or is used in a system that will become mobile, then a commercial splice protection system is necessary.

## **9. Birefringence Compensation**

Birefringence is a desired quality in the PM fiber and is used to maintain proper polarization for modulation. The PM fiber maintains polarization of the laser light within the PM loop and transmits the light into the branch that makes up the rest of the cavity [Ref. 12]. This branch, as seen in Figure 3.1, is made up of the erbium, dispersion-shifted, and dispersion-compensating fibers. These fibers satisfy other functions within the laser cavity, but together in tandem with the Faraday rotator mirror compensate for the negative effects of birefringence in the singlemode fiber. These fibers are constructed like the singlemode fiber in Figure 3.3b and are not structured to maintain the polarization on a particular axis. As a result, light passing through the fiber can form birefringent fast and slow axes due to thermal effects, mechanical stresses, and imperfections in the fiber [Ref. 38]. This is an undesired effect and can cause instability in the laser pulses and noise due to random variations in polarization [Ref. 30].

To eliminate the birefringence a Faraday rotator mirror was used at the end of the branch. The Faraday rotator mirror is a combination of a Faraday rotator and a mirror in one package. The mirror is simply used to reflect the light back through the laser for another round trip such as in Figure 2.2. The Faraday rotator uses the Faraday Effect to rotate light polarization in a non-reciprocal fashion by  $45^\circ$ . This is accomplished by passing the light through a bismuth iron garnet crystal. Permanent magnets on either side of the crystal in combination with the magnetic iron ions in the crystal rotate the polarization in the same direction regardless of the direction the light originally came from. A collimating lens expands the light to pass through the crystal and then focuses it back into the fiber on the return trip. The double pass through the crystal causes a total rotation of  $90^\circ$  [Ref. 38]. Figure 3.4 depicts the internal components of a Faraday rotator mirror.

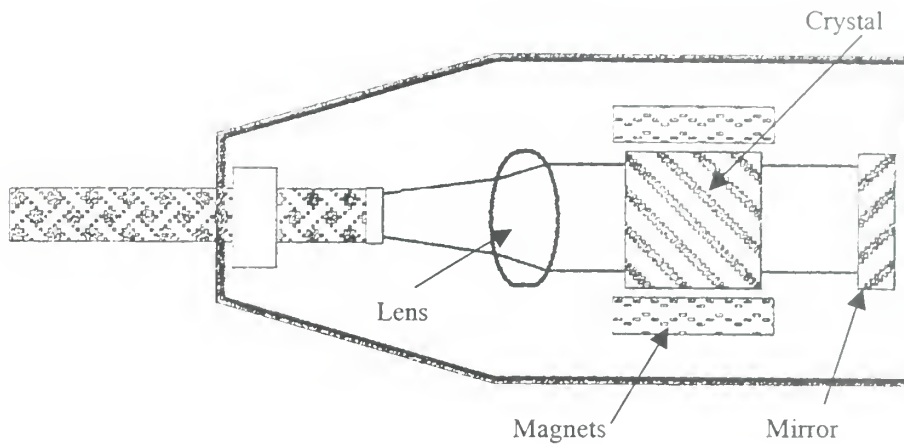


Figure 3.4. Faraday rotator mirror. (After [Ref. 38].)

When the rotated light passes through the dispersion-compensating, dispersion-shifted, and erbium fiber, it passes by the light traveling in the other direction on the orthogonal axis. The pulses of light passing by each other in opposite directions and on orthogonal axis eliminate any formation of the orthogonal fast and slow axes and compensate for any birefringence that might otherwise occur [Ref. 30].

## 10. Polarization Maintaining Loop

The PM loop consists of a polarization beam splitter, a PM isolator, a PM output coupler, and a modulator. The polarization beam splitter consists of three sections of PM fiber connected to a polarized optical filter. Light can enter the beam splitter on either axis of the PM fiber. The filter splits the light based on its polarization. Light entering the filter on the fast axis passes directly through the filter to one output port. Light entering the splitter on the slow axis is reflected to the other output port (see Figure 3.5). The light can pass both directions through the device [Ref. 46].

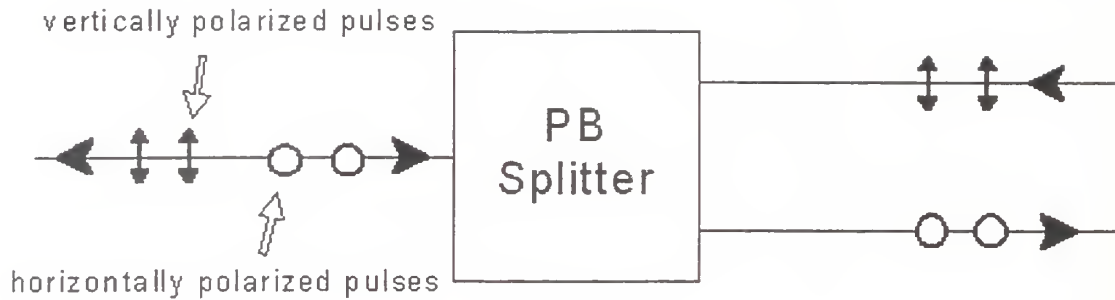


Figure 3.5. Schematic of a polarization beam splitter. (After [Ref. 46].)

The laser pulses coming from the ER amplifier are guided into the slow axis of the PM fiber of the beam splitter by a polarization controller. The polarization controller is a rotating mechanical device that simply twists a section of fiber until the light comes out at the desired application angle. The PM beam splitter passes the light to the correct output port in the direction of the PM fiber isolator. The fiber isolator uses PM fiber for both input and output ports to maintain the polarization. This device also uses a polarized filter to allow light to pass only in one direction and only on the slow axis. The isolator is used to force the laser light to transmit in one direction around the PM loop [Ref. 47].

The term “filter” is used loosely here to describe the optical wave plates used in these devices to isolate or reflect the polarized light. There are a variety of common optical plates that can be combined to perform these functions. However details of which plates are used in these devices are regarded as proprietary and are not released by the manufacturers.

The isolator passes the light to a coupler also created from PM fiber. The light passes through a partially reflective mirror inside the device. Since this is an 80/20 coupler, 80% of the light passes through and continues in the laser cavity. The mirror reflects 20% of the light into a singlemode fiber that exits the laser cavity and is used for the laser output [Ref. 48].

The remaining 80% of the laser light continues in the PM loop to the Mach-Zehnder modulator. This electro-optic modulator is used for active modulation of the cavity as described in Chapter II and requires that the polarized laser light pass through



the device on a slow axis of the PM fiber to maintain correct orientation with the modulator electrodes.

The PM loop rotates the light by  $90^\circ$  at the splice between the output fiber of the modulator and the PM fiber of the fast axis port of the beam splitter. The slow axis of the modulator PM fiber is spliced in line with the fast of the PM fiber of the beam splitter. The light enters the beam splitter on the fast axis, travels through the filter, and exits toward the ER amplifier on the fast axis of the PM fiber that it originally came in on.

## **11. Round Trip of a Pulse**

In the sigma mode-locked laser, 1560 nm constant-wave laser light forms from the spontaneous emissions in the EDFA, which is then amplified by stimulated emissions. The active modulation from the Mach-Zehnder modulator promotes mode-locking at the fundamental modulation frequency or a harmonic. The round trip path of a single pulse traveling through the cavity is as follows. Leaving the output coupler, the pulse is reduced by the light removed from the cavity to serve as laser output. The pulse passes through the modulator on the slow axis of the PM fiber. In the orthogonal splice between the modulator and PM beam splitter, the pulse is passed to the fast axis of the PM fiber. The pulse travels directly through the beam splitter and into the EDFA while maintaining a polarization axis relative to the fast axis of the PM fiber that it just left.

The pulse is amplified in the EDFA and continues on through the DS and DK fiber. The polarization of the pulse is rotated  $90^\circ$  as it returns from the Faraday rotator mirror. The polarization is approximately aligned with the slow axis of the PM fiber of the PM beam splitter. The pulse passes through the DK and DS fibers and is amplified again by the EDFA. A polarization controller corrects the polarization that may have rotated in the SM fiber to guide the pulse directly into the slow axis of the PM fiber of the beam splitter. The pulse is reflected toward the correct port of the splitter and passes through the isolator. The output coupler removes some of the pulse power for output and the round trip starts over [Ref. 30].

## B. ACTIVE MODE-LOCKING

The active mode-locking was accomplished using a Mach-Zehnder modulator. The E-TEK microwave wideband electro-optic modulator has two electrode sections, one for DC bias and one for the RF signals. This modulator is of the traveling wave electrode type and uses both sections on one arm to electro-optically change the phase. The  $-3$  dB bandwidth of this modulator is rated at 10 GHz [Ref. 49]. The operation of the modulator is the same as described in Chapter I where the induced phase difference between the two arms serve to amplitude modulate the light when it recombines just prior to exiting the modulator [Ref. 50].

The half-wave voltage  $V_\pi$  is the amount of voltage required to change the phase of the laser light by  $\pi$  radians in the modulator. The  $\pi$  radians phase change is the difference between the adjacent minimum and maximum output intensity  $I_{out}$ . A bias voltage  $V_{bias}$  applied to the DC electrode in the modulator causes a constant phase change in the laser light wave. In the RF section, the signal is placed on one end of the electrodes and travels the same direction as the laser at approximately the same velocity. The RF voltage also affects the phase change and adds or subtracts from the phase change induced by the DC electrodes [Ref. 50].

The input voltage  $V(t)$  is the total voltage applied to the modulator electrodes and includes the changing RF voltage and the DC bias voltage. The relationship between the  $I_{out}$ ,  $V(t)$ , and  $V_\pi$  can be seen in the modulator transfer function given by

$$I_{out} = \alpha I_{in} \cos^2 \left[ (\phi_0 / 2) - (\pi * V(t) / 2 * V_\pi) \right]. \quad 3.2$$

The output intensity  $I_{out}$  is a function of the intensity of the light entering the device, the insertion loss  $\alpha$ , and the modulator fixed phase difference  $\phi_0$  when  $V(t)$  is zero volts [Refs. 8, 51]. The insertion loss of the device is listed as 4.5 dB [Ref. 49]. The above relationships were confirmed in the pulse modulation experiment described in Chapter I using constant-wave laser light.

The  $V_\pi$  and  $\phi_0$  for this modulator were measured as 13.55 V and  $-1.54$  radians experimentally by successively recording the values of the light intensity for different

bias voltages. The maximum  $I_{out}$  occurred at 15.9 V and the minimum was found at 2.35 V.

The voltage-intensity curve in Figure 3.6 graphically shows the relationship between  $V_\pi$ ,  $V_{bias}$ , and  $I_{out}$ . The normal modulation of laser light is accomplished by setting  $V_{bias}$  at the quadrature point of  $V_\pi$ , shown as the “normal operating bias” on the graph [Ref. 51]. The RF voltage is then applied to the separate electrode section and serves to modulate the light around the bias point. Experimentally, light is normally measured as power instead of intensity. Optical power is proportional to intensity and is used in Figure 3.6 [Ref. 14].

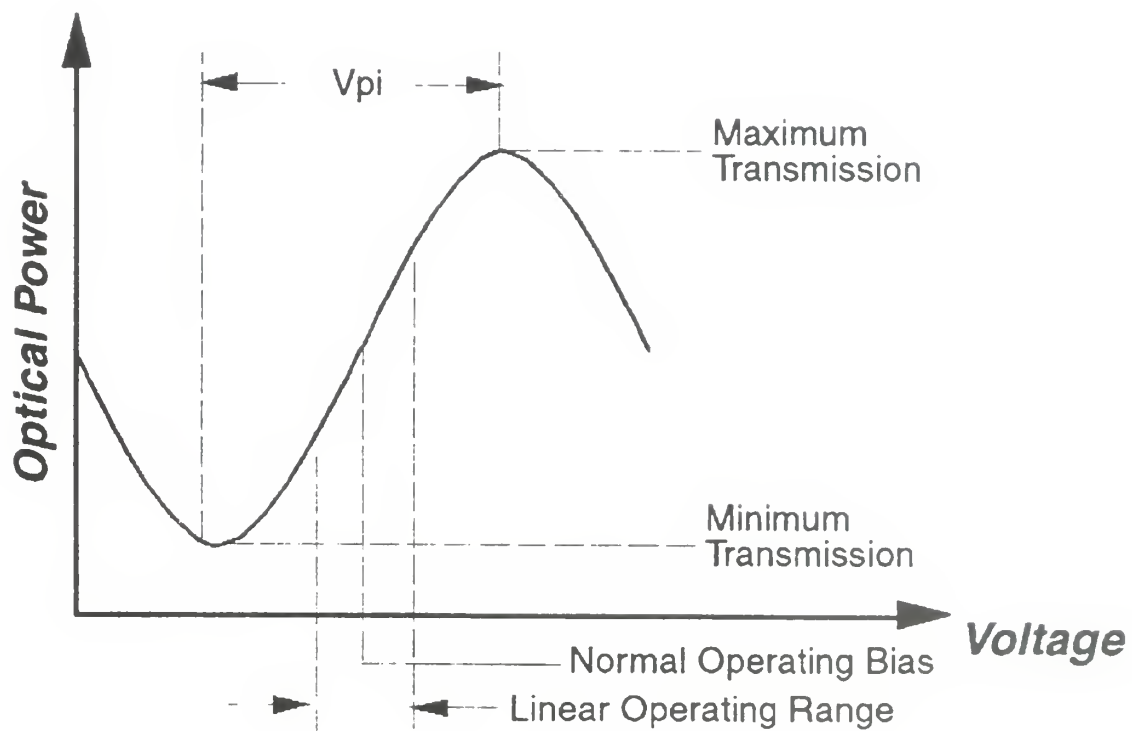


Figure 3.6. Transfer function of an electro-optic modulator. (From [Ref. 51].)

In the mode-locked laser the modulation serves to bring the different modes together in phase to produce a pulse as shown in Figure 3.7 [Ref. 13], the pulses tend to be centered under the peak modulator output  $I_{out}$  and are maintained there by the modulation. In this graph, the optical transmittance  $T(V)$  is simply  $I_{out}$  normalized by  $I_{in}$



[Ref. 8]. The modulation index  $2\Delta_m$  is simply the peak-to-peak transmittance of modulated light passing through the modulator [Ref. 13]. This index is measured using constant-wave light instead of mode-locked pulses. The modulation index is obviously related to the magnitude of the RF modulating voltage in Equation 3.2. The normalized  $2\Delta_m$  is found to be 19% of the overall light passing through the E-TEK modulator.

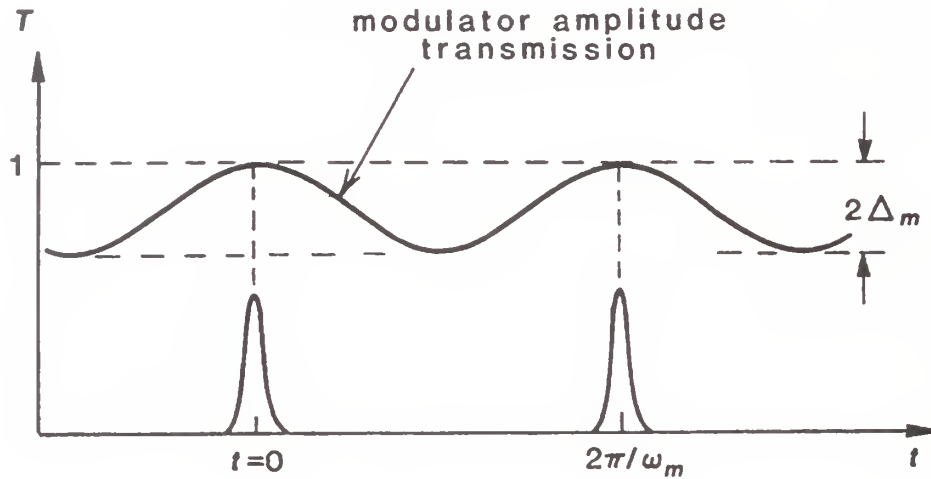


Figure 3.7. Pulses in an actively mode-locked laser. (From [Ref. 13].)

To allow most of the laser light to pass through the modulator, the bias voltage was placed near the top of the voltage-intensity curve. The modulating RF voltage is provided by a Hewlett Packard Synthesized Signal Generator (HP83731B) and is amplified by a MITEQ brand medium power microwave amplifier that provides 20 dB of gain and a minimum output power of 25 dBm for a bandwidth range of 8 to 18 GHz [Ref. 52]. The synthesizer provides a RF signal between 1 and 20 GHz at 10 dBm of power [Ref. 53]. A microwave power divider with a 5 dB insertion loss splits the signal. Half of the microwave signal is passed to the feedback stabilization system to maintain active mode-locking. The other half is amplified in the MITEQ amplifier and guided to the RF section of the modulator. The amplified signal ranges from 22 to 28 dBm and provides an average of 316 mV of modulation voltage over the input impedance of  $50\ \Omega$  [Ref. 52].

The frequency that the laser will mode-lock at must be an integer multiple of the mode frequency spacing interval as described in Chapter II. (The mode frequency

spacing is also called the fundamental cavity rate [Ref. 30].) Using Equation 2.5 and a cavity length of 127 meters, the mode spacing is calculated to be approximately 843 kHz. In theory this laser can be actively mode-locked at any integer multiple of 843 kHz within the operational bandwidth of the modulator and microwave amplifier.

The modulator has a  $-3$  dB bandwidth of 10 GHz but will probably operate much higher due to the slow roll-off of the modulator's frequency response curve provided by the manufacturer [Ref. 49]. The  $-6$ dB point is estimated to be approximately 20 GHz. The gain bandwidth curve provided by the manufacturer for the MITEQ amplifier drops off rather sharply after 18 GHz [Ref. 52]. The maximum frequency that this amplifier can be used for is estimated at 20 GHz also. Overall, the modulator limits the maximum active mode-locking pulse repetition frequency (PRF) to a range between 10 and 20 GHz. The PRF is limited to a minimum of approximately 7 GHz, just below the bandwidth of the MITEQ amplifier [Ref. 52].

The laser is actively mode-locked by fine tuning the synthesizer frequency until the mode frequency spacing is found and a pulse begins to form in the autocorrelator output. (The autocorrelator is a device that displays a time domain autocorrelation of a pulse assembled over numerous samples of the laser output and will be explained in detail in Chapter IV.) The mode-locked condition is fine-tuned by adjusting the length of fiber wound on the PZT. This changes the length of the cavity and thus the mode frequency spacing to more closely match the frequency of modulation. By maintaining the cavity length and mode spacing at the modulation frequency, the laser maintains a stable, actively mode-locked condition. The feedback stabilization circuitry, described later in this Chapter, is then adjusted to maintain the actively mode-locked condition.

In a recent paper, a sigma laser was harmonically mode-locked at twice the modulation frequency [Ref. 54]. This can be accomplished by biasing the DC voltage of the modulator at the peak of the voltage-intensity curve and modulating around that point. The result is an inverted, double modulation of the laser light resonating within the cavity.

The experiment described in Chapter I was extended to constant-wave modulation. A Mach-Zehnder modulator was biased very close to peak intensity and modulated around that point. The resulting inverted, double modulation can be seen in



Figure 3.8. The bottom sine wave is the modulating wave, the top sine wave is the modulated laser output that is detected and displayed on the same sampling oscilloscope. Note that there are twice as many signal peaks in the output as in the input modulating sine wave.

Using this technique, the laser can be actively mode-locked at a PRF of twice the modulating frequency and the pulses will form under each peak in the modulation just as they do in Figure 3.7. The only stipulation is that the inverted, double modulation frequency must be within the bandwidth of the modulator being used. The peak intensity for the E-TEK modulator is found to be around 15.9 V. This is where the modulator was DC biased for active harmonic mode-locking.

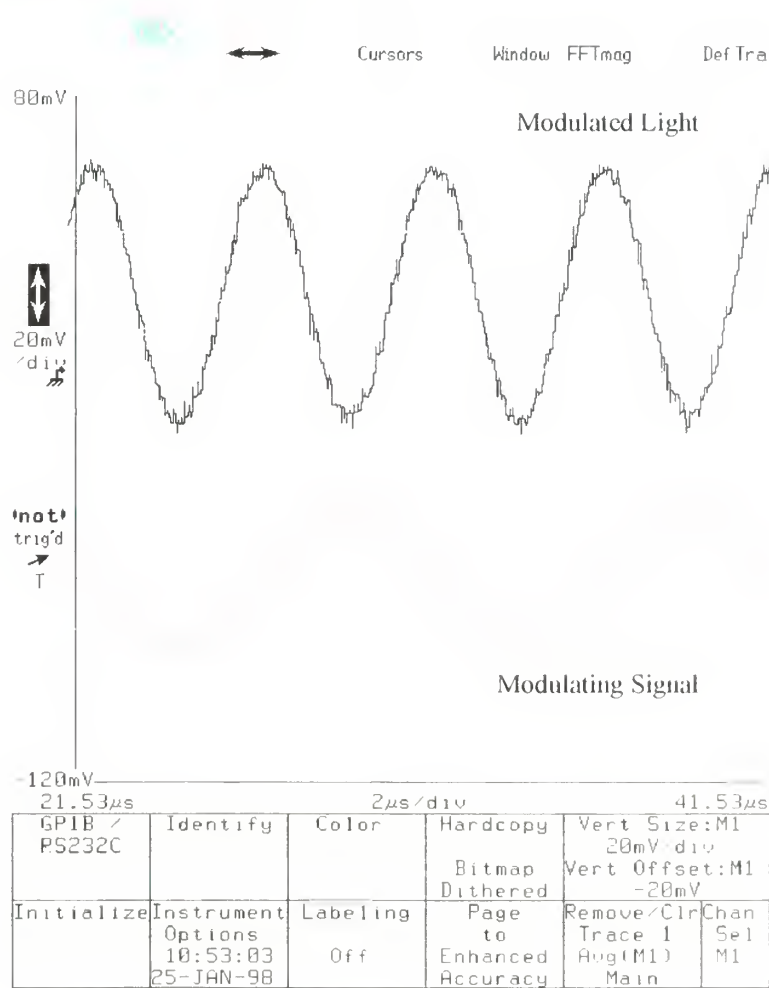


Figure 3.8. Inverted, double modulation of a modulator,  $I_{dc}$  set to peak intensity



### C. ERBIUM-DOPED FIBER AMPLIFIER

These fiber amplifiers are primarily used in fiber communications systems to amplify 1550-nm laser light. Since a laser beam can be initiated from the ASE noise and then amplified by the stimulated emissions, the EDFA has become a typical light source for fiber lasers.

An erbium-doped fiber amplifier (EDFA) is a combination of the ER fiber, wavelength division multiplexers (WDM), the pump diodes, and the associated electronic equipment. The EDFA acts as any other laser amplifier as described in Chapter II with the exception of an additional “relaxation” between upper energy levels. When pumped with enough laser energy from the 980 nm pump laser diodes, the erbium atoms rise to an excited energy state, undergo a fast decay to meta-stable state, and then drop to their ground energy state. During this drop, they release photons in the form of spontaneous and stimulated emissions centered on 1550 nm [Refs. 37, 55]. As a 1550 nm signal, such as a mode-locked pulse, passes through the amplifier, it stimulates the spontaneous emissions and is amplified.

The erbium fiber is connected to the rest of the branch via two wavelength division multiplexers (WDMs) [Ref. 56]. A WDM is essentially a coupler consisting of two types of fibers, Flexcor and SM. The SM fiber is fused to the Flexcor fiber by the “twist and pull” method where the fibers are twisted together, placed under tension, and then heated by an electric arc or torch. The result is a fused taper where the two fibers meet [Ref. 20]. The 1550 nm light passes through to the erbium-doped fiber via the singlemode fiber, the fused taper, and Flexcor fiber. The 980 nm light enters the erbium-doped fiber solely through the Flexcor fiber.

A number of papers have been written on the design of an EDFA. Unfortunately a large number of them optimized the design with fiber parameters not commonly available from commercial vendors. The specifications for a well-designed EDFA commonly become proprietary information. When discussing product application of the ER fiber with the vendor, the “cut back” method was always suggested [Ref. 37]. In this method, an excess amount of ER is spliced to a WDM. The fiber is pumped with a 980 nm pump diode laser and a 1550 nm transmission signal is passed through the amplifier

and evaluated at the output end for wavelength and signal gain. The ER fiber is continually cut back until the designer is satisfied with the output.

Typically the EDFAs are designed with pump powers of 100 mW or less. This is due to a relatively low gain saturation point of around 20 mW pump power and an increase in ASE noise after that point. The specification sheet for the ER fiber that was purchased showed an optimized level of gain for lengths between 10 m and 18 m with the highest gain achieved using 15 m of fiber and 100 mW of pump power [Ref. 42]. In the sigma laser, the ASE noise at 1550 nm is the initial source of light and the highest possible saturated output power is required.

Since 15 m appeared optimum at 100 mW, 33 meters were purchased in two lengths of 13 and 20 meters. The initial design was considered to be two amplifiers with each consisting of 15 m of fiber pumped with 100 mW of power. The extra fiber would account for fiber loss during splicing. These two amplifiers were spliced together at the center of the erbium fiber to form a long double amplifier. The initial design of the two amplifiers spliced together to make one high power amplifier is shown in Figure 3.9

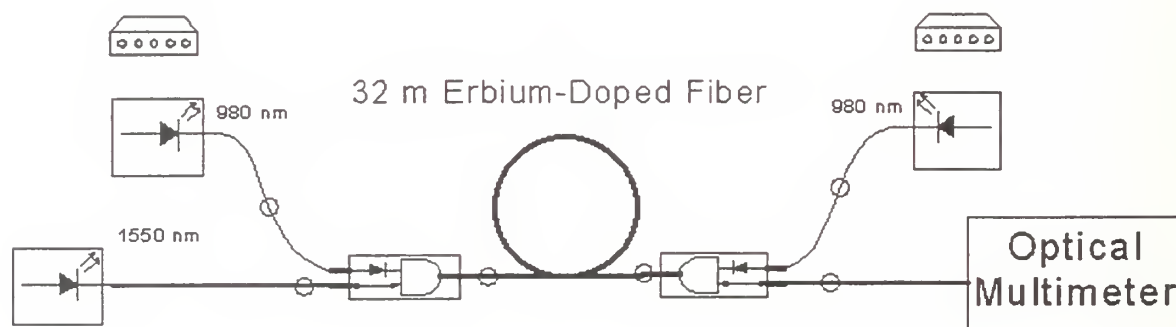


Figure 3.9. Combined EDFAs to form a high power amplifier. (After [Ref. 56].)

The WDMs were correctly spliced with a mode-field matching taper on each end of a length of ER fiber. This length was then cut so that different lengths could be evaluated for gain and wavelength performance. Instead of cutting back, different lengths were added together and evaluated by co-pumping, counter-pumping, and dual-pumping the fiber while transmitting a CW 1550 nm signal through fiber at different



power levels and measuring the wavelength and power using an optical multimeter as shown in Figure 3.9. The recorded values were calculated and plotted as gain and noise using MATLAB.

Lengths of 12, 20, 25, and 33 m were evaluated in different configurations. The plotted gain results are shown in Figure 3.10. In terms of gain, the dual-pumped 20 m length of fiber actual had 1 dB of gain more than the 33 meters of fiber at 200 mW of total power. In addition, the 20 m length produced a saturated signal wavelength of 1550 nm where the 33 m produced a 1560 nm signal. The signal-to-noise ratio for each was also calculated. For 200 mW pump power, the 20 m length had an SNR of about 1 dB higher for each level of the transmission signal.

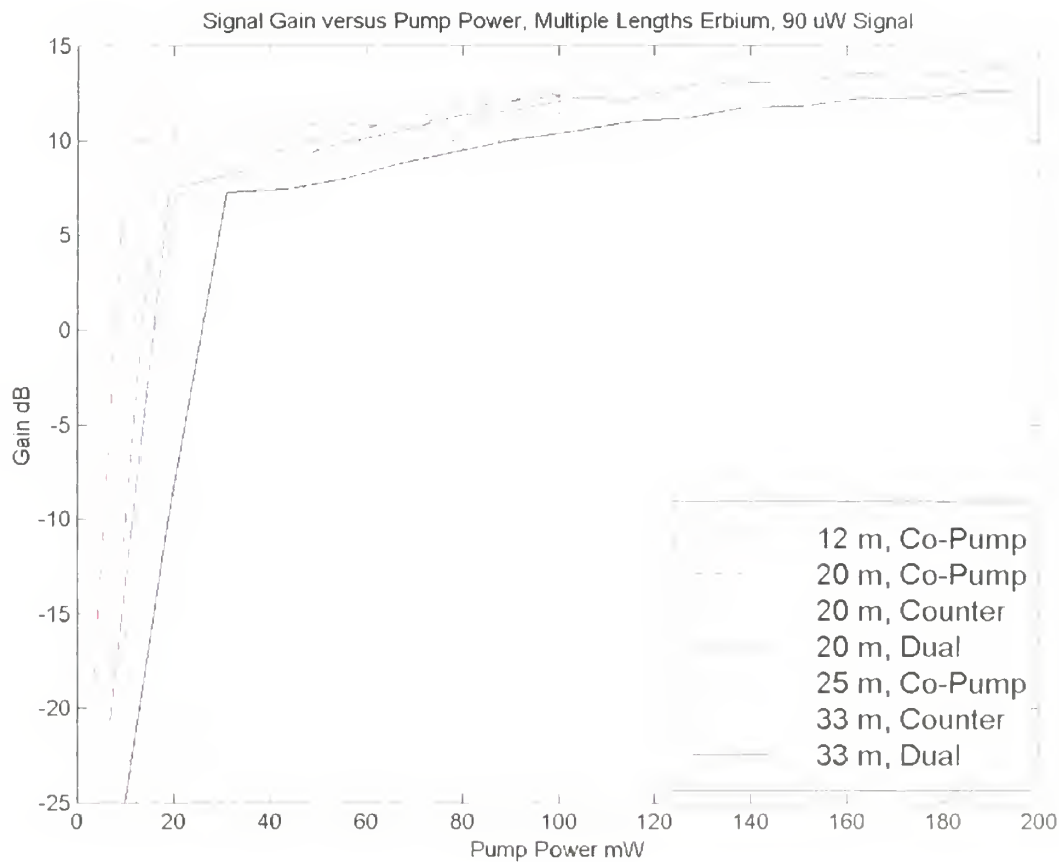


Figure 3.10. Amplifier gain for several pump configurations and lengths of erbium-doped fiber.



The 33 m length was selected for pump diode protection and additional conversion of 980 nm laser light to ASE. Since the two diodes are essentially pointed at each other, there is some concern that leftover 980 nm pump laser light from one diode might affect the diode at the other end. The additional ER fiber would convert the unused 980 nm light to 1560 nm ASE and buffer the other diode.

Each amplifier was measured for saturated ASE noise at full power but with no signal. The 20 m amplifier produced 42.8 mW of ASE noise at 200 mW of pump power while the 33 m produce 51.4 mW. The higher noise level would be useful in laser start up since the resonant longitudinal modes and pulses were initially formed from the ASE noise. The SNR was measured with a low power 1550 nm CW signal. It is expected that the high power pulses passing through the amplifier would reduce ASE noise by stimulating many more emissions than the low power CW laser diode.

The performance of the dual-pumped 33 m amplifier can be seen in Figure 3.11. This plot is for large signal gain and SNR. The highest power steady-state gain is measured as 5 dB at 200 mW of pump power. This is the gain that the high power mode-locked pulses would encounter in the amplifier. A small signal gain of 27 dB is measured using a 2.8  $\mu$ W signal. This larger gain would help in initial pulse formation and amplification.

The final EDFA configuration used 32 meters of erbium-doped fiber between two WDMs as shown previously in Figure 3.9. One meter was lost to fusion splicing. The two 100 mW diodes used in this design were mounted in “butterfly” package laser diode mounts. Each diode was then driven at 180 mA of current to produce a 100 mW of 980 nm light for a combined power of 200 mW power pumping the ER fiber. The efficiency of this conversion process was calculated at 25.7%.

The diodes are constructed with thermoelectric coolers to remove excess heat while pumping current through the device. The device is also built with a thermistor that changes resistance as temperature of the device rises. An external temperature controller, connected to the diode through the butterfly mount, maintains a constant temperature by reading the thermistor resistance and adjusting current flow through the thermoelectric cooler inside the diode [Ref. 39].



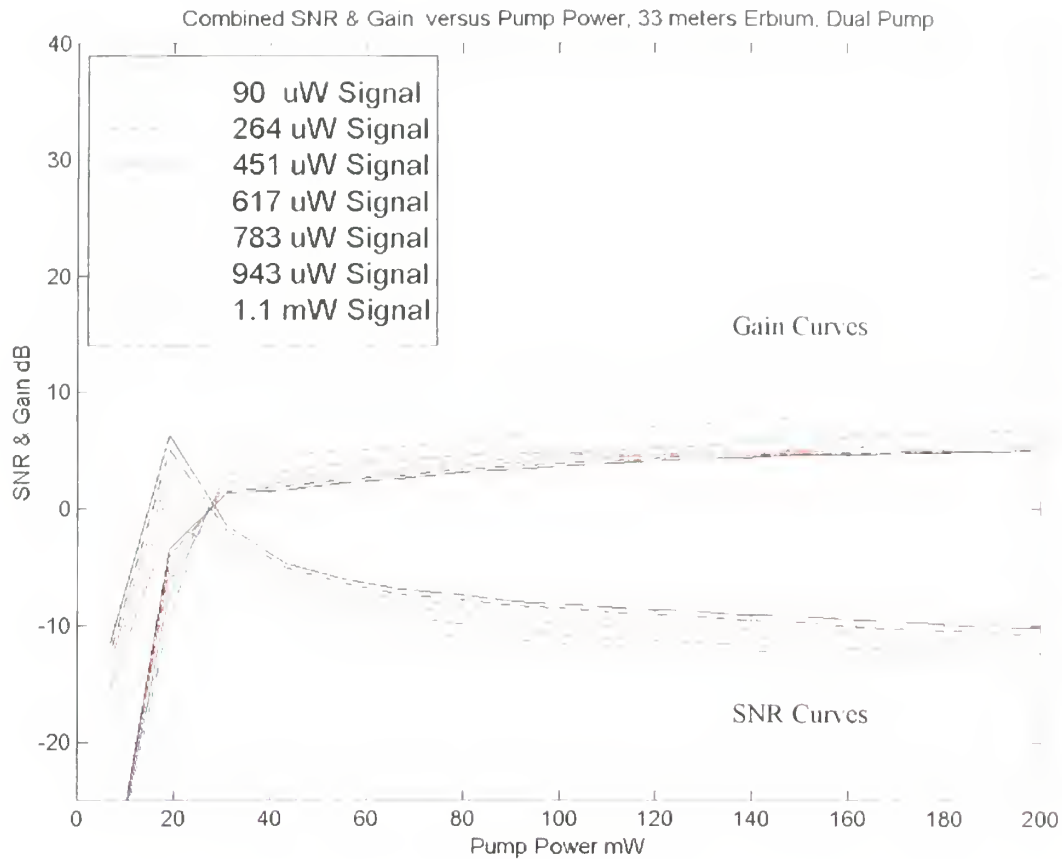


Figure 3.11. Amplifier gain and SNR results for 33 meters of erbium-doped fiber.

#### D. FEEDBACK LENGTH STABILIZATION CIRCUIT

During the course of hours, room temperature changes cause the 127 meters of fiber in the laser to change length at a rate of approximately  $72 \mu\text{m}/\text{C}^\circ$  [Ref. 44]. As discussed in Chapter II, the frequency of laser light in a cavity is based on the round trip phase change of an integer multiple of  $2\pi$  radians. When mode-locking is initialized, the modulation frequency is set based on this round trip phase change and the cavity length at the time. A change in cavity length due to temperature effects causes the resonant frequency to shift and the modes to lose phase synchronization with each other. This causes the mode-locked condition to destabilize and fail despite the active modulation of the laser cavity [Ref. 57].



To combat the problem of temperature effects, a feedback control circuit is designed [Ref. 57] and implemented in the sigma laser [Ref. 17] to compare the phase of the modulating signal to that of the laser pulses and to adjust the cavity length as necessary. Figure 3.12 is the feedback length stabilization circuit implemented in the NPS sigma laser. A microwave phase detector circuit mixes the two frequencies and produces an error signal based on the difference in phase. An operational amplifier circuit integrates the signal over a fixed time constant and produces an output ranging from 0 to 5 Vdc. The high voltage piezoelectric (HVPZT) amplifier converts this 0 to 5 Vdc to 0 to -1000 Vdc. The high voltage is applied to a ceramic PZT, which expands based on the applied voltage and stretches the 40 meters of fiber wrapped around its circumference.

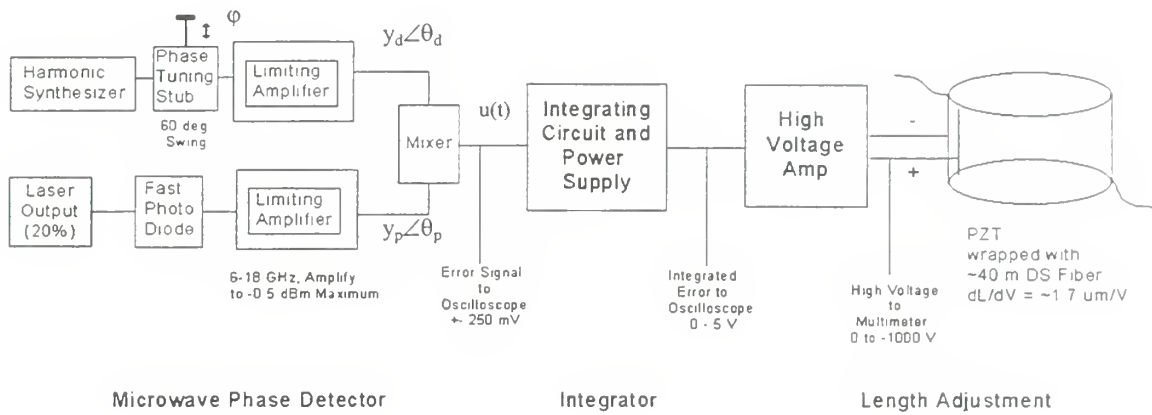


Figure 3.12. Feedback length stabilization circuit. (After [Ref. 17].)

### 1. Microwave Phase Detector

A microwave power divider splits the modulating signal from the signal generator. One half of the power is amplified and used to modulate and actively mode-lock the cavity laser light using the Mach-Zehnder modulator. The other half is amplified to approximately -0.5 dBm using a microwave limiting amplifier. Using a combination of fiberoptic output couplers, twenty percent of the total laser output is passed to a photo-detector using a fiber cable. The laser pulses are converted to electrical pulses that are then amplified to -0.5 dBm by an identical limiting amplifier. A microwave phase shifter





is used between the power divider and the limiting amplifier to adjust the phase to match the phase of the laser output during the start of mode-locking. The two signals are multiplied together in a microwave mixer that produces an error signal based on the phase difference in the signals. The output of the mixer is given by

$$u(t) = Ky_d y_p(t) \cos[\theta_d - \theta_p(t) + \varphi]. \quad 3.3$$

The value  $K$  is the conversion factor of the mixer,  $y_d$  and the  $\theta_d$  are the amplitude and phase of the signal generator and  $y_p(t)$  and  $\theta_p(t)$  are the amplitude and phase of the pulse signal from the detector [Ref. 57]. The value  $\varphi$  is the phase introduced by the phase shifter. When the sum of the different phases approaches  $90^\circ$ , the output of the mixer approaches 0 Vdc.

This phase detector circuit provides an error signal up to  $\pm 250$  mV. The mixer output includes a DC voltage as well as a small AC component generated by the multiplication of a narrow pulse and a sine wave. On start up, the initial phase difference is set to 0 Vdc using the phase shifter between the power divider and the limiting amplifier. The phase shifter has the potential to shift the modulating signal by  $60^\circ$ .

## 2. Integrator Circuit Design and Construction

The Naval Research Laboratory initially designed the integrator circuit with three operational amplifier circuits [Ref. 17]. A “True Integrator Amplifier” and an “AC Amplifier” operate in parallel to integrate the DC component and amplify the AC component of the phase detector signal. An “AC Integrator” sums the two signals and integrates amplified AC component for a final integrated and amplified output [Ref. 58].

The original NRL circuit provided an output of  $\pm 10$  Vdc to a rack mounted electronic high voltage amplifier to drive the PZT. This design was modified to provide an output of 0 to 5 Vdc to a small, high-voltage PZT (HVPZT) amplifier mounted on a circuit board. The original NRL design with modifications is shown in Figure 3.14 on page 59. The circuit was packaged in a commercial electronic box for handling, protection, and operation. The circuit controls, including the rotary variable resistors and

other switches, were mounted through the circuit box face plate and act as a user interface with the integrator amplifier. The integrator amplifier requires a significant amount of user control during the mode-locking feedback initialization process and is occasionally fine-tuned during system operation. For clarification of the discussion below, the printed face plate of the integrator amplifier electronic box is included as Figure 3.13

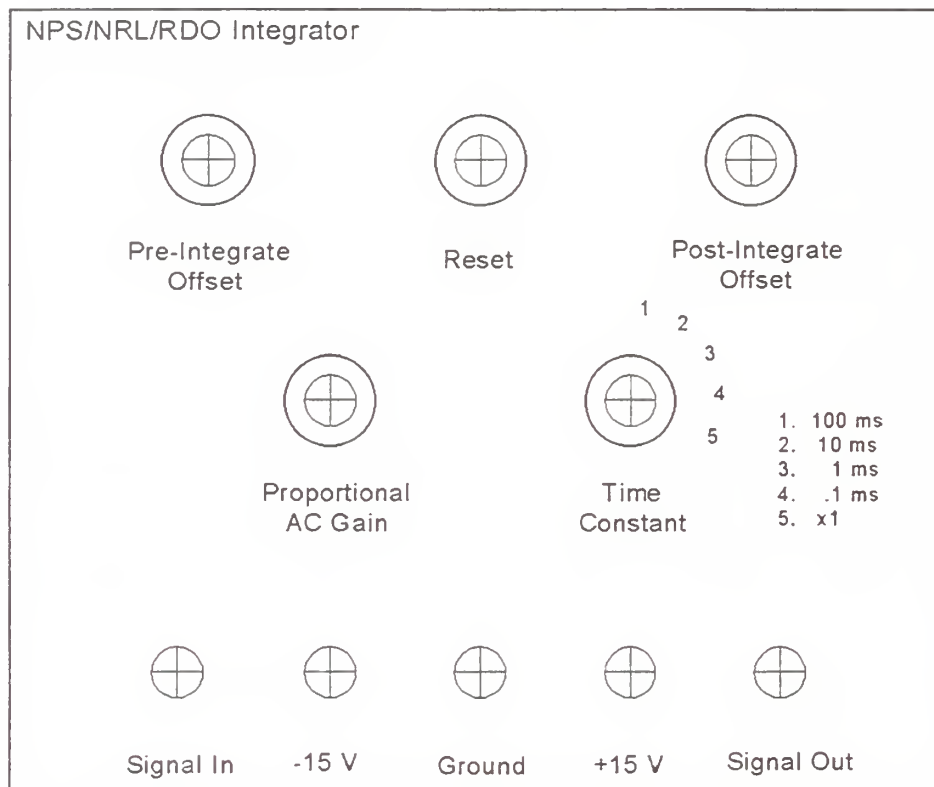


Figure 3.13. Integrating amplifier control face plate.



A “Pre-Integrate Offset” potentiometer knob provides control of a 0 to  $\pm 0.8$  Vdc input prior to the True Integrator to tune the circuit on start up. A “Post-Integrate Offset” potentiometer knob provides control of a 0 to  $-1000$  Vdc pre-load on the PZT. A momentary on/off (MOM) push-button reset switch resets the circuit to the pre-load by discharging the capacitors in the true integrator circuit. The PZT pre-load is usually set while in reset mode so that the pre-loaded voltage can be accurately read on a digital multimeter monitoring the voltage on the PZT.

A rotary switch selects different capacitors in the True Integrator circuit to change the integration time constant from 0.1 to 100 milliseconds. This selector switch also includes a resistor for a 1:1 gain that defeats the integration and can be used for system troubleshooting. The slowest time constant of 100 ms is most often used. A knob potentiometer also provides gain control of the AC Amplifier and is used as a fine phase control adjustment.

Some changes to the NRL circuit design were required to account for the different piezoelectric high voltage amplifier that accepts an input voltage of 0 to 5 Vdc. A zener diode was added to the AC Integrator to limit the signal swing from  $-0.6$  to 3.1 Vdc. A voltage divider of 0.6 Vdc was added to the signal through an “Inverting Summing Amplifier,” in series after the AC integrator, to prevent the final output from dropping below zero. An “Inverting Gain Amplifier” was added in series after the inverting summing amplifier to raise the maximum output to 5 Vdc.

The NRL circuit design originally used the Motorola MC34081 operational amplifier designed with external offset null pins to control the DC offset voltage inherent in all operational amplifiers. Control of the offset null proved critical because the true integrator circuit would integrate the DC offset along with the signal and the other amplifiers would amplify this offset in the final output. Unfortunately, Motorola no longer makes the MC34081, so the MC34082 chips were used. Offset bias was experimentally measured as 0.5 to 5 mV and a large voltage divider on the positive input terminals was used to finely counteract this voltage in the true integrator, AC amplifier, and AC integrator circuits [Ref. 59].

During the offset bias measurement, the noise from the power supply and other local electronics was measured to be approximately 40 mV. This noise is passed to

ground through a 10 pf capacitor on the positive input terminal. The offset bias was not as critical in the “Inverting Gain Amplifier” and the “Inverting Summing Amplifier” and is controlled by using standard bias compensating resistance techniques [Ref. 59].

### 3. Piezoelectric Cylinder

The HVPZT amplifier is a programmable amplifier that accepts a 0 to 5 Vdc input signal and transforms it to a 0 to –1000 Vdc output. This high voltage is applied to the PZT to cause the cylinder to expand in the radial direction, effectively changing its diameter. Since the amplifier provides negative voltage, the positive lead was soldered to the inside of the cylinder so that the electric field created by the voltage differential still flows outward for PZT expansion.

The PZT, as shown in Figure 3.15, is a Channel Industries lead zirconate titanate (C-5500) thin-walled cylinder [Ref. 60]. The device was wrapped with approximately 40 meters of Corning SMF/DS fiber that was fusion spliced into the laser cavity.

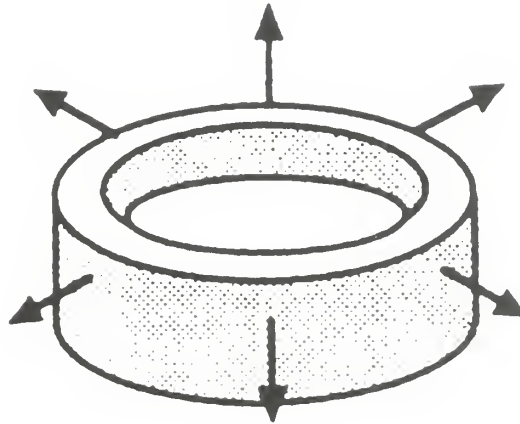


Figure 3.15. Lead zirconate titanate piezoelectric cylinder. (From [Ref. 60].)

As the voltage changes the diameter, the length of fiber wrapped around the cylinder changes length as the cylinder stretches. Excluding any countering force, the change in mean cylinder diameter  $\Delta d_m$  based on applied voltage was calculated using

$$\Delta d_m = d_{31} d_m V / t \quad 3.4$$

as 2.898  $\mu\text{m}$ . The piezoelectric constant  $d_{31}$  is  $-185 \times 10^{-12} \text{ m/V}$ ,  $d_m$  is the mean diameter of the cylinder (5.37 cm),  $t$  is the cylinder wall thickness (3.4 mm), and  $V$  is the applied voltage (1000 Vdc) [Ref. 60].

The wrapped fiber actually provides a countering block force to the cylinder expansion. The tensile strength  $S$  of the fiber wound on the cylinder was approximated experimentally in the laboratory and calculated using

$$S = E d C / d_{break} \quad 3.5$$

as  $1.339 \times 10^9 \text{ N/m}^2$ . Young's Modulus  $E$  is  $1.05 \times 10^7$  pounds per square inch (psi), and  $d$  is the measured fiber diameter of 111  $\mu\text{m}$  including the core and cladding,  $d_{break}$  is the breaking diameter of 6 mm for a loop of fiber. The conversion factor  $C$  is  $6.895 \times 10^3 \text{ N/m}^2/\text{psi}$  [Ref. 61].

The force of one fiber countering the expansion was calculated from the tensile strength and the area of the core and cladding. The number of wraps (*wraps*) of fiber on the PZT was estimated to be 192 and was calculated from the fiber coating diameter of 245  $\mu\text{m}$  and the width of 47 mm of all of the fiber wraps measured along the side of the PZT. The number of wraps multiplies the force of each fiber. This gives a total force  $F_{act}$  resisting the cylinder expansion and is calculated using

$$F_{act} = S (d\pi / 4) \text{wraps} \quad 3.6$$

as 2.49 kN.

The zero displacement force  $F_b$  is an internal block force created within a cylinder that is under placed voltage but not allowed to expand. This force was calculated using

$$F_b = d_{33} Y_{33} A V / t \quad 3.7$$



as 61 kN. The modulus of elasticity  $Y_{33}$  is  $5.2 \times 10^{10}$  N/m<sup>2</sup>, the piezoelectric constant  $d_{33}$  is  $4.0 \times 10^{-12}$  m/V, and  $A$  is the outside surface area of the cylinder,  $0.01$  m<sup>2</sup>. The two forces work against each other during expansion so the actual change in the mean diameter of the cylinder  $\Delta d_{act}$  is reduced by

$$\Delta d_{act} = \Delta d_m (F_b - F_{act}) / F_b \quad 3.8$$

to  $2.78 \mu\text{m}$  [Ref. 60].

A change in circumference  $\Delta c$  was calculated using  $\Delta d_{act}$  from

$$\Delta c = \Delta d_{act} \pi \quad 3.9$$

as  $8.73 \mu\text{m}$  [Ref. 62]. This change in circumference is also the change in length of each wrap of fiber around the cylinder. The number of wraps of fiber multiplied by the change in length per wrap is the total change in length  $\Delta l$  of the fiber on the cylinder. This is calculated using

$$\Delta l = \Delta c \text{ wraps} \quad 3.10$$

as  $1.68$  mm. Since the fiber wrapped on the piezoelectric cylinder is an integral part of the laser cavity, the change in fiber length is effectively a change in the laser cavity length. A change room temperature will cause the sigma laser to become unstable and lose the mode-locked condition due to changes in cavity length. The change in cavity length available from the PZT acting on the fiber will prevent the loss of mode-locking and accommodate a maximum room temperature change  $\Delta T$ . The maximum temperature change handled by this system is calculated using

$$\Delta T = \Delta l \varepsilon / l \quad 3.11$$

to be  $23^\circ\text{C}$  ( $42^\circ\text{F}$ ). The thermal expansion coefficient  $\varepsilon$  of glass fiber is  $5.7 \times 10^{-7}$  ( $^\circ\text{C}$ )<sup>-1</sup>



and  $l$  is the overall cavity length of 127 m [Ref. 44].

The temperature change accommodation is calculated using a full swing in PZT voltage. In reality, the PZT would be initially biased somewhere in the middle leaving half of the operational temperature range of 11.5 C° (21 F°).

## E. CONCLUSION

The construction of the NPS sigma laser was an extensive effort consisting of parts procurement, fiber splicing, assembly of test equipment, and circuit construction. The final product is shown in a series of pictures in Figures 3.16a-c. A wide-angle view shows the associated power supplies and equipment uses to operate the laser. A side view shows modulator, microwave amplifier and some of the cavity fiber. The top view clearly shows the microwave phase detector circuit on top of the laser. The results of these efforts are presented in the next chapter where pulsewidth, pulse rate, and noise are measured to quantize the usefulness of the laser output.

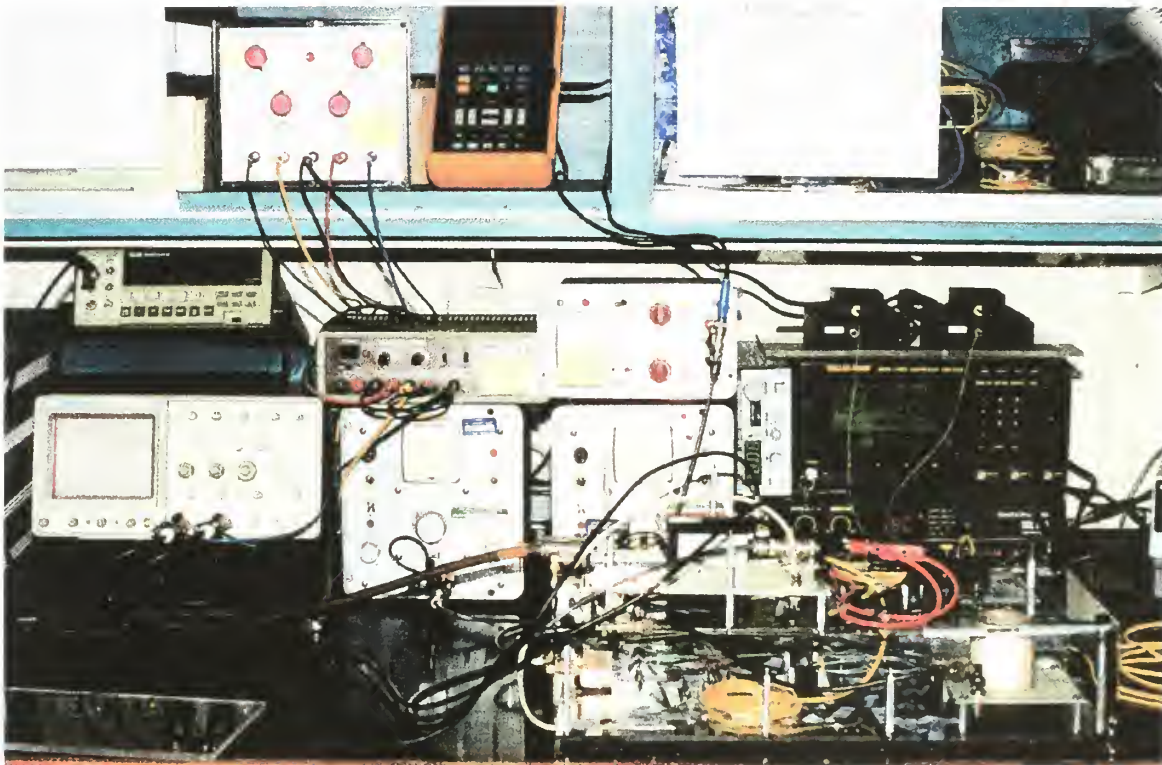


Figure 3.16a. Wide-angle view of the Naval Postgraduate School sigma laser.





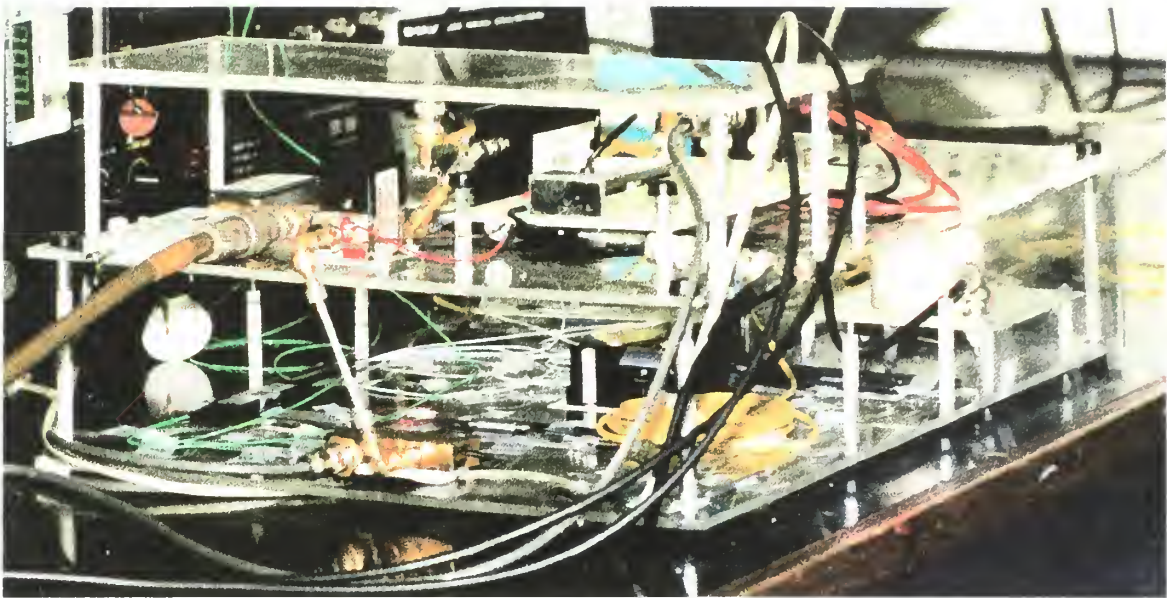


Figure 3.16b. Side view of the Naval Postgraduate School sigma laser.

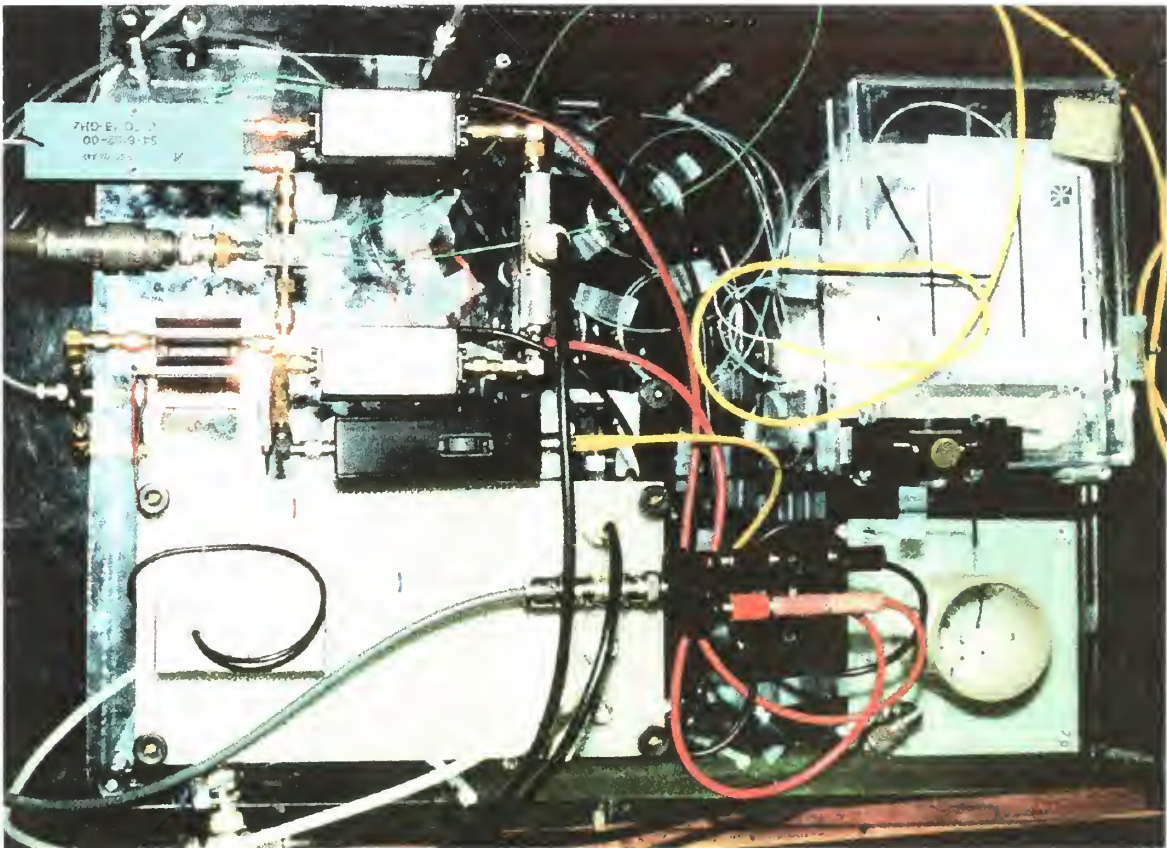


Figure 3.16c. Top view of the Naval Postgraduate School sigma laser









## IV. MEASUREMENTS OF SIGMA LASER

### A. LASER MEASUREMENTS

In the previous Chapter, the construction of the NPS sigma laser was discussed in detail. In its present form, the laser is operational and provides a range of pulse rates from 7 to 16 GHz. A number of techniques exist for measuring the laser output. This Chapter concentrates on measurements common to pulsed laser performance which include average power, peak pulse power, wavelength, spectral linewidth, and pulsewidth. Laser pulses are often used in measurement systems that can be degraded by the presence of amplitude jitter noise [Ref. 34]. Optical sampling systems have the additional concern of temporal uncertainty or timing jitter. If present in extensive amounts, it has an obvious effect in an optical ADC or fiber communications system where the pulse-to-pulse amplitude variations exceed system tolerances of the electronic receiving system. Amplitude jitter also plays an important role in the noise measurement process and is also included in the analysis.

To make these measurements, at least two laser outputs were required in the form of fiber cable pigtails with attached connectors. One cable was used to operate the feedback length stabilization system. The other pigtail was the final output of the laser, was used for measurement purposes, and would also be used to operate an optical sampling system. The final output of the laser is about 16% of the total laser light resonating in the cavity. An inline polarization controller was added to the final output fiber to satisfy polarization input requirements of the autocorrelator.

Optical equipment often comes with cable connections for ST or FC connectors. The output of the laser is a ST fiber connector. Whenever a FC connector is required, a fiber cable patch cord with a ST connector at one end and a FC connector at the other was used between the laser and the FC device. A ST-to-ST cable connector joins the laser output and patch cord. Losses through this connector and patch cord were measured at 0.5 dB. Table 4.1 is a list of all measurement equipment used and connector types.

<u>Device Nomenclature</u>	<u>Connector</u>
ILX Optical Multimeter (OMM-6810) with OMH-6706 Measurement Head	FC/ST
Femtochrome FR-103MN/IR Autocorrelator	FC
Hewlett Packard 71450B Optical Spectrum Analyzer	FC
Hewlett Packard 8563E RF Spectrum Analyzer using a DC Block and	
Newport/Picometrix D-15ir Photo-Detector	ST
Textronix Digital Sampling Oscilloscope using a	
Newport/Picometrix D-15ir Photo-Detector	ST

Table 4.1. List of test and measurement equipment.

Figure 4.1 shows a general layout of the test equipment and connections. The output pigtail was moved from machine to machine and the ST/FC patch cord inserted as necessary. The typical sequence of measurements taken after the laser was locked at the desired frequency is the pulsewidth on the autocorrelator, the average power on the optical multimeter, the wavelength and the spectral linewidth on the optical spectrum analyzer, and the noise measurements on the radio-frequency (RF) spectrum analyzer.

## B. COMPUTER CONNECTIONS

A computer was connected to the RF spectrum analyzer through a general-purpose interface bus (GPIB). LABVIEW 4.0 software was used to extract the frequency domain information in dBm directly from the analyzer's memory. An interface developed under a previous thesis [Ref. 63] plots the RF spectrum on the computer screen and saves the information as a numerical text string to a file on the hard drive for further analysis. Successive recording of the RF spectrum was convenient with this method. The RF spectral data was then imported into MATLAB and the noise analyzed using some of the software code and techniques from the previous Thesis.

The autocorrelator was acquired with a computer data acquisition card installed and was connected through an RS-232 serial port to the same computer. The computer interface allows real time pulse analysis and provides the option of saving data. Using the vendor's software, data was collected and saved to a file as both a graphics image and text string of data similar to LABVIEW [Ref. 64].

The digital sampling oscilloscope was used late in the laser development phase for data acquisition and troubleshooting in the time domain. Connected through an

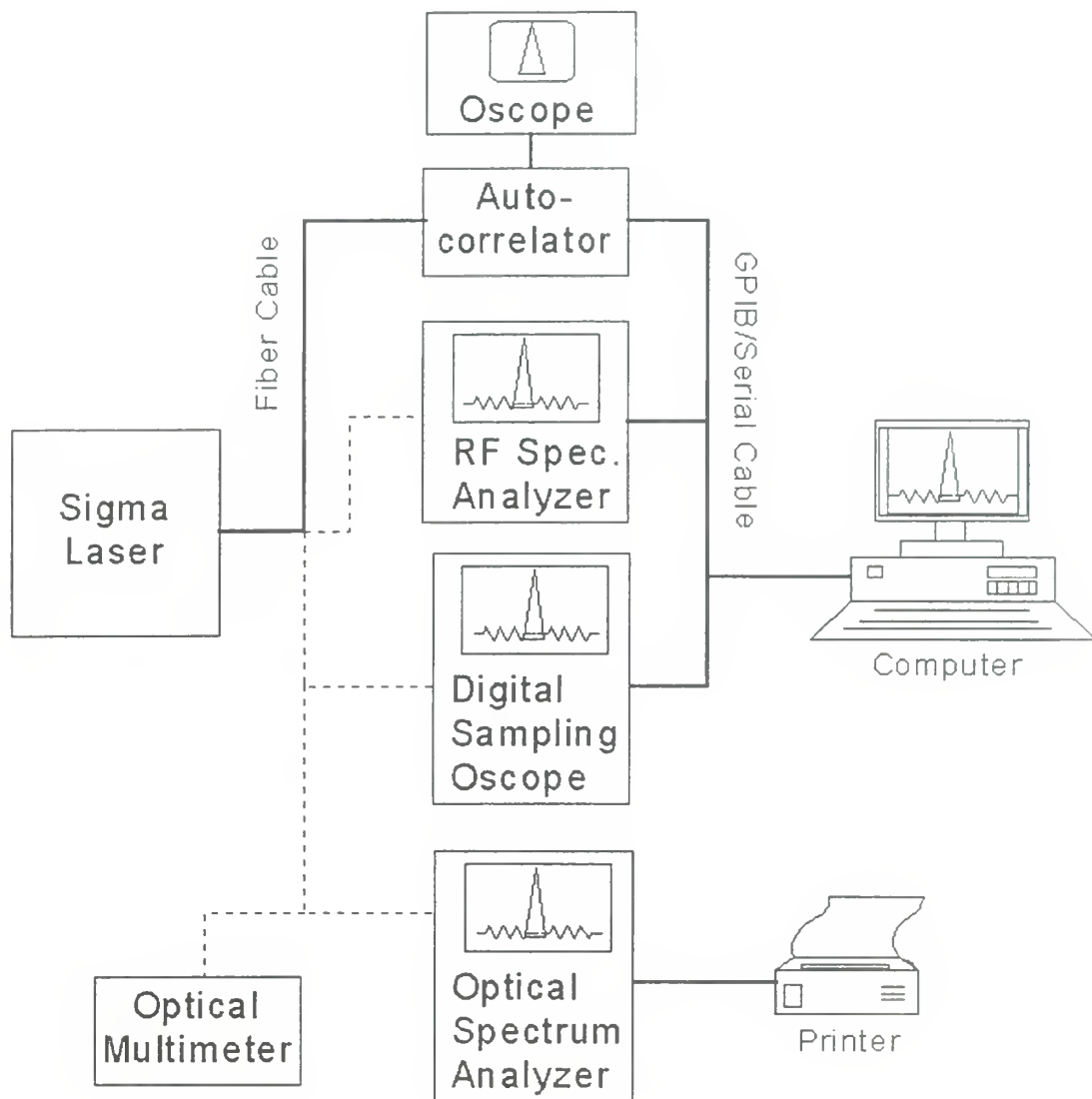


Figure 4.1. Test and measurement equipment layout with connections.

RS-232 serial port, the oscilloscope can transmit both graphics images and numerical text to a file using the Windows Terminal program. The graphics are usually saved to a file and analyzed in detail after the experiment. Figure 1.3 on page 5 is typical graphical data captured from the sampling oscilloscope [Ref. 65].

The optical spectrum analyzer also came with a GPIB interface and can be used by a computer for both graphical and numerical data recording. Since Hewlett-Packard provided the analyzer on a short-term loan, this interface was not pursued. Still,



computer acquisition of the optical spectrum can provide a route for further analysis of data [Ref. 66]

Computer acquisition of data was a major contributor to data recording and analysis for this laser. Overall, more than 100 MB of data were generated and recorded using the computer interfaces listed above. Much of the data is reflected in the discussion and analysis in the rest of the Chapter. Figure 4.2 shows the computer screen displaying both the LABVIEW program with frequency domain data from the RF spectrum analyzer (lower left) and the autocorrelator program (upper right) with a typical laser pulse.

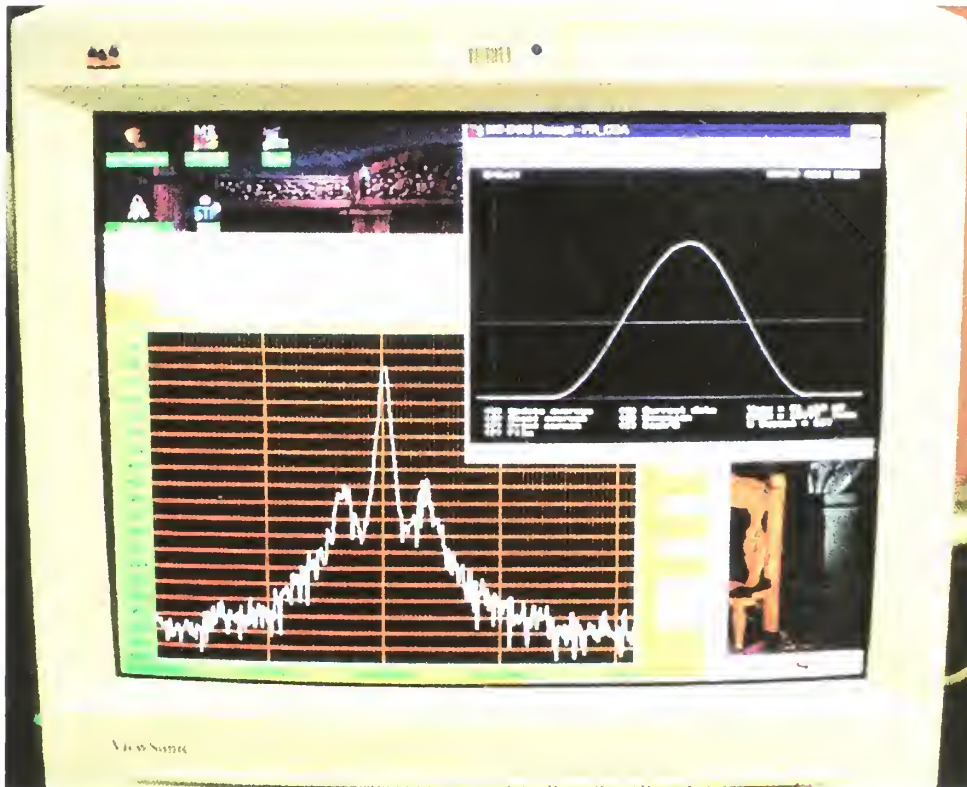


Figure 4.2. Computer screen with RF spectrum analyzer and autocorrelator data.

On the next page, Table 4.2 summarizes the measured and calculated results of 14 mode-locked signals spanning the PRF range of the sigma laser. The results are introduced here as a reference and will be explained in detail throughout the remainder of the Chapter.





Frequency GHz	Pump Power mW	Pulse- width Ps	Low Freq Jitter Fs	High Freq Jitter fs	Ampl Jitter %	Wave- Length nm	Line- Width Nm	Duration- Bandwidth Product	Pulse Shape	Avg Power mW	Peak Power mW	DC Bias Voltage V	RF Drive Power dBm	Comments
7.00010132	200	9.39	141	465	1.37	1561.5	0.46	0.53	Gaussian	2.39	36.36	15.47	41	
7.000200909	200	10.207	137	249	0.97	1563	0.3	0.441/0.315	G/sech^2	2.43	33.65	14	40.5	very good lock
7.00100899	200	8.98	68	2585	49.3	1560.7	0.481	0.532	Gaussian	2.399	38.15	15.56	40.5	poor/ampl varies
8.0066005	200	13.765	285	not meas	1.5	1559.8	0.295	0.5	Gaussian	2.222	20.16	14.51	40.5	
9.0073006	200	14.581	179	not meas	2.05	1560.1	0.24	0.431	Gaussian	2.376	16.93	14.79	40.5	
10.00004	200	7.932	114	not meas	0.686	1559.1	0.432	0.422	Gaussian	2.44	30.76	14.72	40.5	
10.10033977	200	11.14	125	not meas	1.054	1560.3	0.372	0.51	Gaussian	2.41	20.76	14.71	47.19	very good lock
11.0005912	200	12.54	162	not meas	0.72	1560.8	0.265	0.41	Gaussian	2.57	18.41	13.85	40.5	
12.00069982	200	13.298	341	not meas	0.71	1559.4	0.4	0.656	Gaussian	2.56	16.04	14.76	40.5	poor lock
12.09987997	200	13.88	198	not meas	0.68	1560.2	0.323	0.553	Gaussian	2.52	15	15.26	40.4	
13.1001	200	10.848	354	not meas	1.97	1559.5	0.231	0.309/0.282	G/sech^2	2.55	17.92	15.38	40.5	
14.10501501	200	13.59	24	not meas	0.23	1563.5	0.237	0.395/0.361	G/sech^2	2.41	12.59	14.44	45	
15.043381	200	17.673	83.4	not meas	0.39	1562.8	0.105	0.229/0.161	G/exp	2.493	9.34	14.44	45	
16.0002018	200	11.84	34.5	not meas	0.275	1563.1	0.275	0.4	Gaussian	2.433	12.84	15.89	40.5	2 x mod freq

Table 4.2. Summary of results.

## C. POWER MEASUREMENTS

An optical multimeter with a digital readout was used to measure the average laser output. Although power can be measured using the optical spectrum analyzer or RF spectrum analyzer, electronic conversion and cable losses would become a factor in measurement. The laser power is a function of pump input power which is converted from a wavelength of 980 nm to approximately 1560 nm in the erbium-doped fiber amplifier. Most experiments were completed using the pump diodes set at an operational power level of 100 mW for a total of 200 mW input power. The average output power  $P_{avg}$  ranged from 2.22 to 2.55 mW. The average power recorded throughout the measurements at different frequencies is given in Table 4.2.

The peak power is approximated from the average power using the pulse duty cycle  $D$  as

$$D = \Delta t \text{ PRF} . \quad 4.1$$

This equation is normally used for rectangular or triangular pulses but is a good approximation for a laser pulse. The peak pulse power  $P_{pk}$  is calculated using [Ref. 67]

$$P_{pk} = P_{avg} / D . \quad 4.2$$

The calculated peak power ranges from 9 to 38 mW depending on  $\Delta t$ .

## D. OPTICAL SPECTRUM MEASUREMENTS

The optical spectrum analyzer in Figure 4.3 uses an interferometer to scan across a range of wavelengths of interest. The optical power is sampled periodically and displayed electronically on a screen. The sample frequency is the resolution bandwidth. As the analyzer display span is reduced, the resolution bandwidth is automatically reduced to a finer resolution. For the best results, data was recorded at the 2 nm or 5 nm spans.

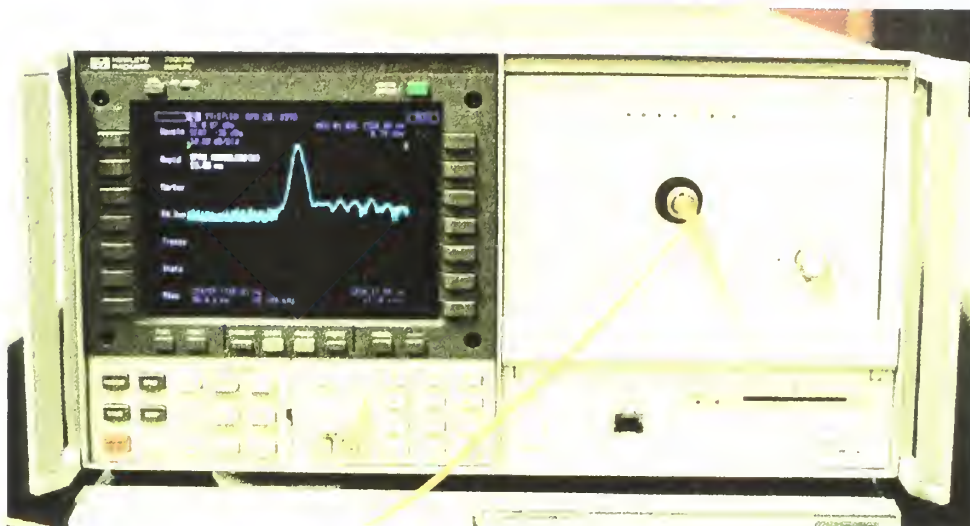


Figure 4.3. Optical spectrum analyzer with mode-locked signal, PRF 10.1 GHz.

Like a RF spectrum analyzer, the peak and  $-3$  dB full-width half-maximum (FWHM) points can be found automatically using the instrument markers. Frequency linewidth is derived from the spectral linewidth  $\Delta\lambda$ , as  $\Delta\nu = c\Delta\lambda/\lambda^2$ .

Figures 4.4a and 4.4b are printouts of the display from the optical spectrum analyzer at spans of 100 nm and 2 nm as noted in the upper left of the figure. The center marker is the wavelength of the signal. The bandwidth markers at the  $-3$  dB points in Figure 4.4b delineate the spectral linewidth  $\Delta\lambda$  of the signal.



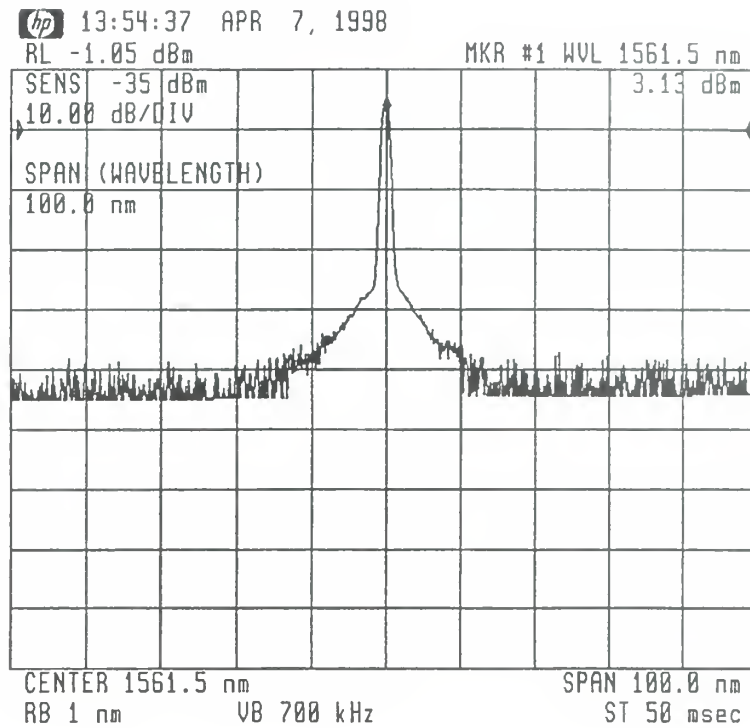


Figure 4.4a. Optical spectrum analyzer, span 100 nm, PRF 7 GHz.

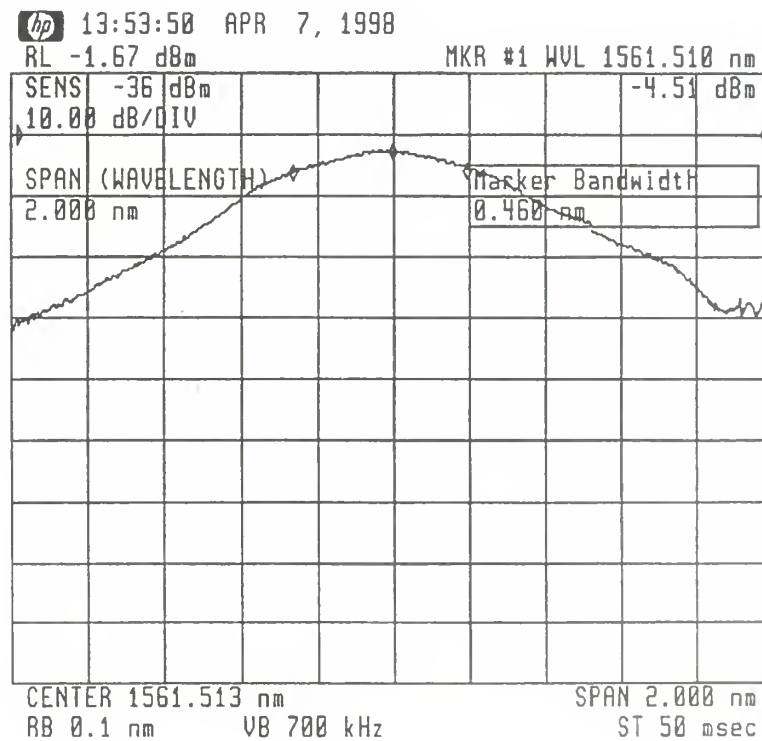


Figure 4.4b. Optical spectrum analyzer, span 2 nm, PRF 7 GHz.



Since this fiber laser is based on an erbium-doped fiber amplifier, amplified spontaneous noise (ASE) is present. The pedestal of noise above the noise floor in Figure 4.4a, from approximately 1545 to 1575 nm, is the ASE noise and also delineates the useable bandwidth of the erbium-doped fiber amplifier [Ref. 68]. This laser lacks an optical filter to force resonance at a specified wavelength, so the signal has centered itself where the most power is available from this amplifier. The optical spectrum analyzer was not available during the construction phase of the laser, so ASE was not measured prior to splicing the amplifier into the cavity.

## **E. PULSEWIDTH MEASUREMENTS**

The laser pulsewidth was measured using the optical autocorrelator. The device works by splitting the laser light into two noncollinear beams using a beam splitter. The beams take separate paths toward a nonlinear lithium iodate ( $\text{LiIO}_3$ ) crystal. The path of one of the beams is broken by a pair of scanning mirrors that rotate at a rate of 10 Hz [Ref. 64]. Figure 4.5 is a top schematic of the internal layout of the Femtochrome autocorrelator. The scanning mirrors effectively allow the beam to pass once per revolution. When both beams are present, they combine in the nonlinear crystal at a small angle of intersection. The photons combining in the nonlinear medium generate a fluorescent second harmonic [Ref. 16].



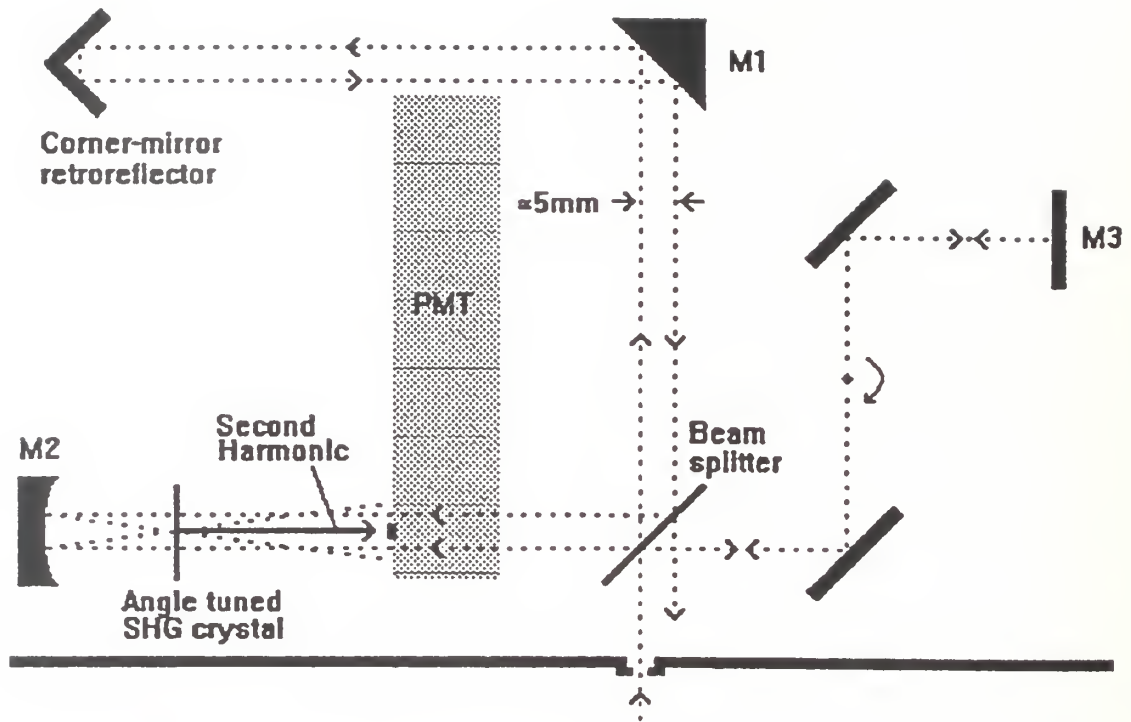


Figure 4.5. Internal layout of Femtochrome autocorrelator. (From [Ref. 64].)

The second harmonic generation (SHG) is the intensity autocorrelation of the pulses in the two beams at that moment in time [Ref. 16]. This light is received by a photomultiplier tube (PMT), is converted to electrical energy, and is then amplified [Ref. 14]. Multiple autocorrelations are displayed over a period of microseconds to form a displayed pulse on an oscilloscope. This data is also converted to digital bits in a computer data acquisition board and sent to a computer for display and further analysis. Figure 4.6a is a picture of the autocorrelator and the connected oscilloscope. Figure 4.6b is a Polaroid picture of the oscilloscope displaying a 10 GHz PRF autocorrelated pulse.

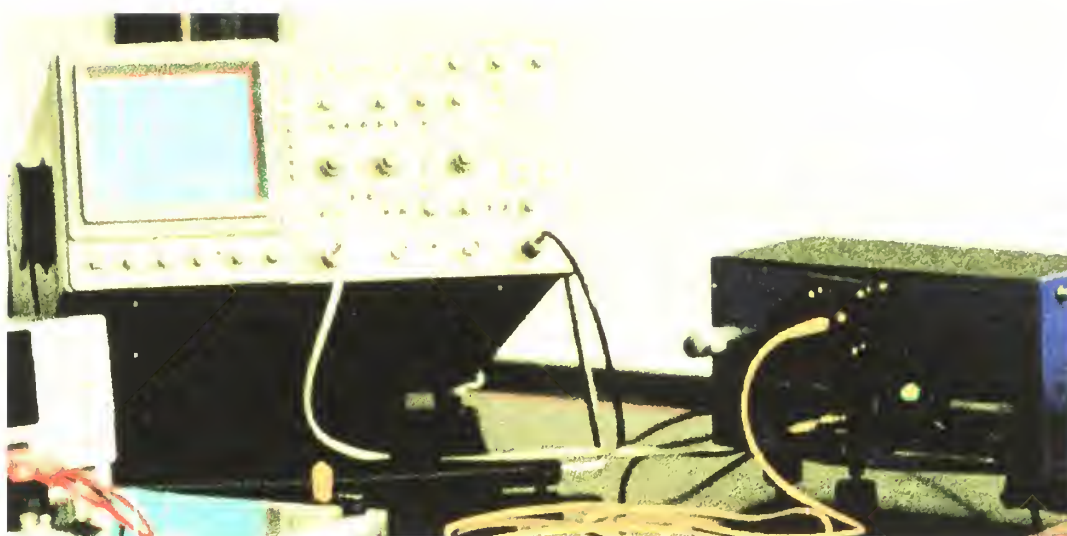


Figure 4.6a. Femtochrome autocorrelator and oscilloscope with displayed pulse.

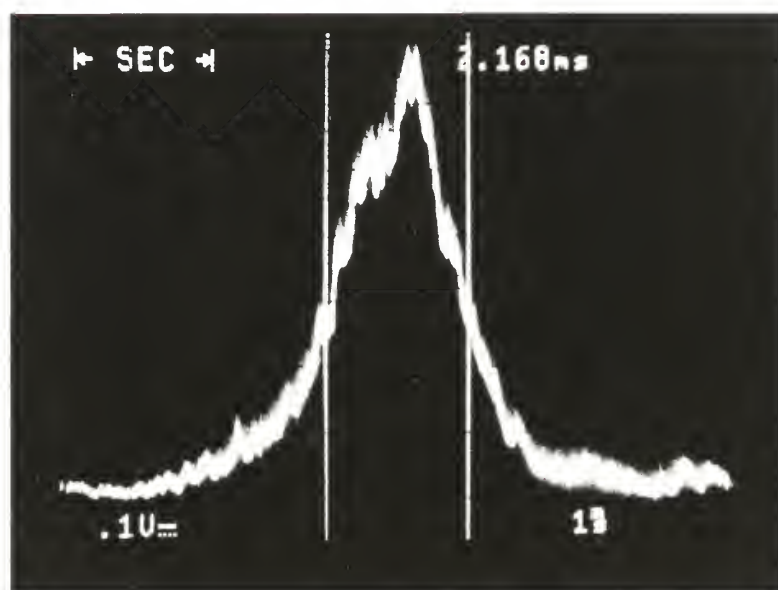


Figure 4.6b. Oscilloscope display of a autocorrelator pulse, 10 GHz PRF.

A conversion factor of 8 ps/ms was used to convert the displayed pulse FWHM measured in milliseconds to the FWHM in picoseconds,  $\Delta T$ . A second factor is used to convert to actual the pulsewidth  $\Delta t$  depending on the shape of the pulse. Gaussian,  $\text{sech}^2$ , Lorentzian, and single-sided exponential are four typical pulse shapes generated by a



mode-locked laser [Refs. 64, 69]. The conversion factor,  $\Delta t/\Delta T$ , is given below in Table 4.3

The pulse shape can be determined in two general ways, by the pulse duration-bandwidth product or by curve fit. The pulse duration-bandwidth product is simply the product of the actual pulsewidth  $\Delta t$  and the frequency linewidth  $\Delta \nu$  to give  $\Delta t \Delta \nu$  [Ref. 16]. The spectral linewidth is measured on the optical spectrum analyzer at the  $-3$  dB points (FWHM) and converted to frequency linewidth using Equation 2.6. Comparison of the duration-bandwidth product using the calculated pulsewidth will determine if the pulse shape is closer to Gaussian,  $\text{sech}^2$ , Lorentzian, or single-sided exponential in shape. The theoretical duration-bandwidth products are also listed in Table 4.3 [Refs. 16, 69].

Pulse Shape	$\Delta t/\Delta T$	$\Delta t \Delta \nu$
Gaussian	0.707	0.4413
$\text{sech}^2$	0.648	0.3148
Lorentzian	0.5	0.2206
Exponential (single-sided)	0.5	0.1103

Table 4.3. Pulse shape, conversion factor, and duration-bandwidth product.

(From [Refs. 16, 69]).

The autocorrelator computer program improves on the oscilloscope display. It averages the pulse sweeps over time to display a clean pulse and calculates the conversions for  $\text{sech}^2$  and Gaussian pulses. The program also provides a curve fit for both pulse types for shape comparison. Figure 4.7 is a typical plot generated by the autocorrelator and computer software. The Gaussian and  $\text{sech}^2$  curve fits are plotted along with the pulse. The pulse rate is 10 GHz. The dark innermost curve is the actual pulse averaged over 233 sweeps. The middle lighter curve, best seen at the bottom outer edges of the pulse, is the Gaussian curve fit. The outermost curve is the  $\text{sech}^2$  curve fit. Almost all pulses are fit to the Gaussian line shape or just inside of it. The conclusion is that these are Gaussian-shaped pulses.



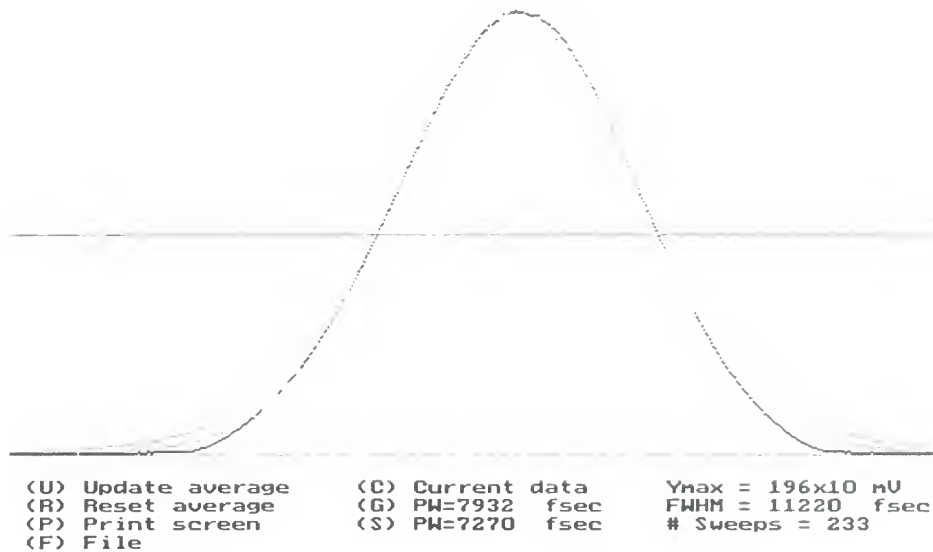


Figure 4.7. Autocorrelator plot of a mode-locked pulse, 10 GHz PRF.

The pulse shape was confirmed using the duration-bandwidth product calculation and comparison to Table 4.3. Ten out of the fourteen measurements were confirmed to be Gaussian shaped pulses using this calculation. Three measurements matched the duration-bandwidth product for  $\text{sech}^2$ ; products for 7.0002 GHz, 13.1 GHz, and 14.1 GHz were 0.315, 0.282, and 0.361, respectively. The 15.04 GHz matched the exponential shape duration-bandwidth product and was calculated to be 0.161. Very narrow linewidths contributed to these deviations.

In the pulsewidth comparison, the single-sided exponential,  $\text{sech}^2$ , and Lorentzian plots all plot outside the pulsewidth of a Gaussian pulse for the same FWHM. The pulses without Gaussian duration-bandwidth products still plot inside the curve fit for a Gaussian shaped pulse. Although a review of the relevant data shows that the data was of reasonable quality and valid, it is believed that these are still Gaussian pulses with narrow linewidths. The reasoning is that the pulse compression mechanisms from dispersion-compensating and dispersion-shifted fibers within the laser cavity still produced Gaussian pulses at most of the modulating frequencies for the same amount of power. A change in pulse shape will require a change in the length of these fibers. No changes to the cavity were made. Figures 4.8a and 4.8b show autocorrelator plots at 7.0002 and 15.04 GHz PRFs.

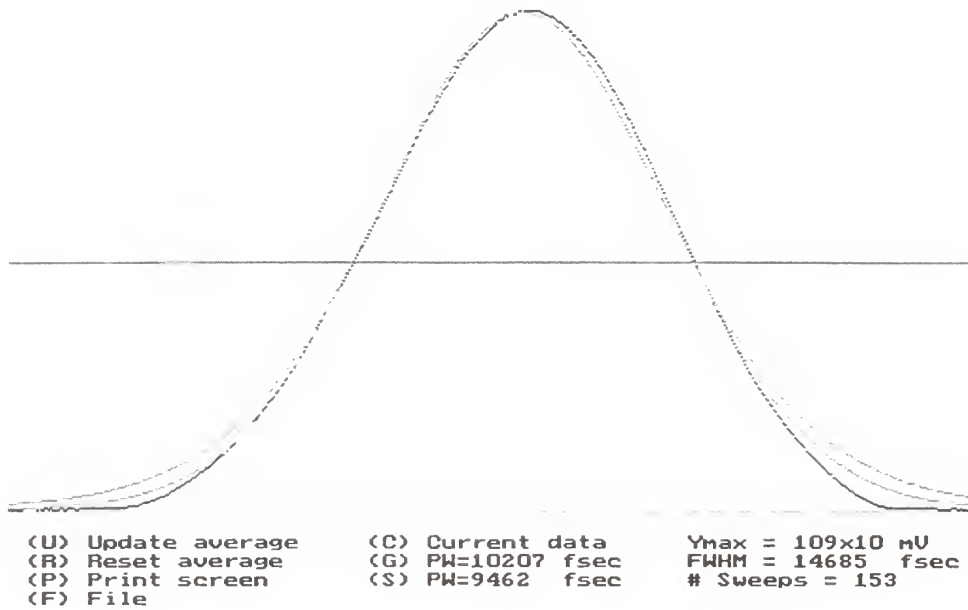


Figure 4.8a. Autocorrelator plot of a mode-locked pulse, 7.0002 GHz PRF.

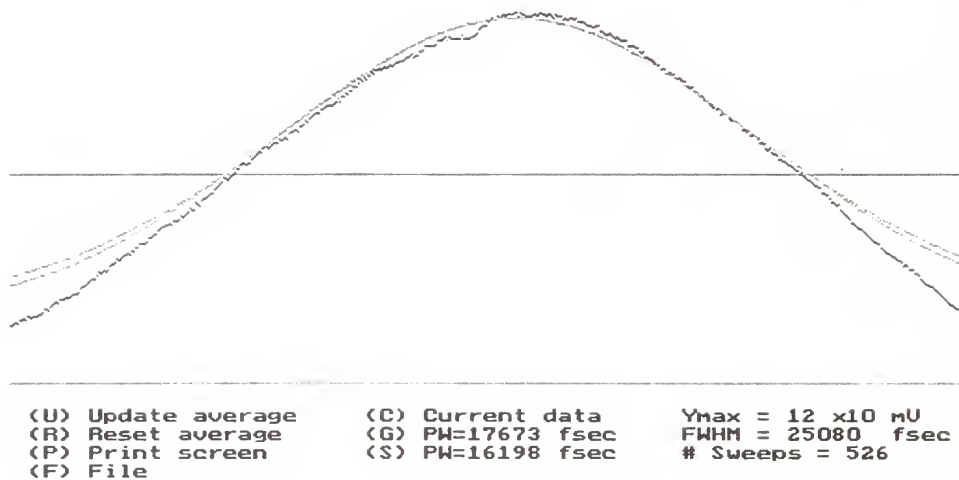


Figure 4.8b. Autocorrelator plot of a mode-locked pulse, 15.04 GHz PRF.

The Gaussian pulsewidths range from 7.39 to 17.67 ps. The difference in pulsewidths can be attributed to the quality of the mode-locked condition at the time of the experiment. For example, at 10 GHz the laser is initially mode-locked with a



pulsewidth of 9.9 ps. Since the condition is unstable at this point the laser was restarted with a few hertz adjustment in modulation frequency. Feedback control was also readjusted to better match the phase difference between the harmonic synthesizer and laser output. The result was a pulsewidth of 7.93 ps. Table 4.2 summarizes measurements for 14 different mode-locked pulse repetition frequencies; pulsewidths are included.

## F. THEORY OF JITTER MEASUREMENT

There are many types of noise present in the output of a mode-locked laser. This section will concentrate on amplitude jitter, high frequency temporal jitter, and low frequency temporal jitter because they have an effect on the optical sampling of microwave signals. Figure 4.9 shows pedestals of noise at the base of a mode-locked laser signal. The measured fundamental pulse repetition frequency is  $f_L$ . The harmonic number is  $M$  and is the integer multiple of the fundamental. The peak amplitude is  $P_A$ . The area of the small pedestal of noise under  $P_B$  is the low frequency temporal jitter noise and can be directly measured whenever present. The area under the larger pedestal of noise under  $P_C$  is a combination of the high frequency temporal jitter noise and the amplitude jitter noise [Ref. 70].

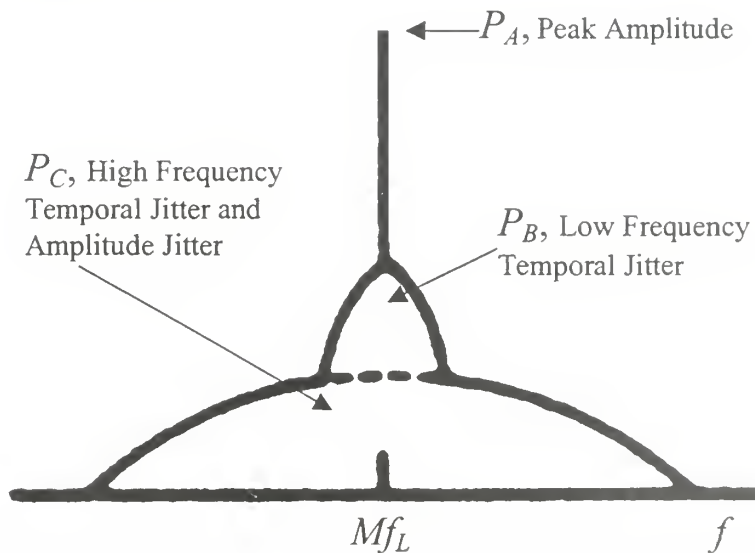


Figure 4.9. Pedestals of jitter noise in a mode-locked laser signal in the frequency domain. (After [Ref. 70].)

Amplitude jitter dominates over high frequency temporal jitter in the  $P_C$  pedestal of the fundamental signal and lower harmonics [Ref. 34]. It is usually measured at the fundamental signal and is specified as a percentage of amplitude. Its presence in the higher  $M$  harmonics is at a maximum a linear function of noise times the harmonic. For example, in the second harmonic, one would expect to find a maximum of twice the amplitude jitter found at the fundamental [Ref. 70].

High frequency temporal jitter noise has a power proportional to  $M^2$ . When present in the higher harmonics, it will dominate the  $P_C$  pedestal [Refs. 34, 70]. If amplitude jitter is measured at a higher harmonic and the value is more than  $M$  times the percentage of the fundamental amplitude jitter, then high frequency temporal jitter is dominant and can be measured at that harmonic [Ref. 70].

The noise power  $P_N$  for all types of jitter is calculated by converting to linear units and integrating the area under the curve of the specific jitter pedestal,  $P_B$  or  $P_C$ . The integration of the noise power is [Ref. 34]

$$P_N = (2 / rbw) \int_{M f_L + f_{low}}^{M f_L + f_{high}} P(f) df . \quad 4.3$$

The frequency span of the pedestal of noise is graphically selected from the spectrum analyzer data. The measured noise power between the frequency points is  $P(f)$ . The high frequency point of the selected noise span of interest is  $f_{high}$  and  $f_{low}$  is the low frequency point. The resolution bandwidth set on the spectrum analyzer is  $rbw$ .

As mentioned previously, the analyzer data were recorded and stored on a computer. The analyzer provided 600 data points covering the frequency span set on the analyzer. The frequency separation  $\Delta f$  between these data points is simply  $span/600$ . Integration was accomplished by using a finite sum to approximate the integral [Ref. 71]. Replacing the integral,  $P_N$  becomes

$$P_N = (2 / rbw) \sum_{M f_L + f_{low}}^{M f_L + f_{high}} P(f) \Delta f . \quad 4.4$$

The amplitude jitter was measured using the noise power  $P_N$  in the  $P_C$  pedestal, normalized by the peak power  $P_A$  of the signal. The actual rms amplitude jitter  $\sigma_{AI}$  measured at the fundamental is [Ref. 34]

$$\sigma_{AI}[f_L + f_{low}, f_L + f_{high}] = \sqrt{P_N / P_A} . \quad 4.5$$

Multiplication of this value by 100 gives the jitter in percentage of pulse amplitude. The rms amplitude jitter  $\sigma_{AM}$  measured at any harmonic  $M$  is

$$\sigma_{AM}[Mf_L + f_{low}, Mf_L + f_{high}] = \sqrt{P_N / P_A} . \quad 4.6$$

This value is compared to  $M\sigma_{AI}$  to determine if amplitude jitter is dominant. If high frequency temporal jitter  $\sigma_{JHF}$  is dominant ( $\sigma_{AM} > M\sigma_{AI}$ ), then  $\sigma_{JHF}$  is related to the measured value  $\sigma_{AM}$  by [Ref. 34]

$$\sigma_{JHF} = (T_L / 2\pi M) \sigma_{AM} = (1 / 2\pi M f_L) \sigma_{AM} . \quad 4.7$$

The pulse repetition interval (PRI) or period of the pulse is  $T_L$ . As a result,  $\sigma_{JHF}$  is usually expressed in seconds. The low frequency temporal jitter is measured using the noise power  $P_N$  in the  $P_B$  pedestal, normalized by the peak power  $P_A$  of the signal. The actual rms low frequency jitter  $\sigma_{JLF}$  is [Ref. 34].

$$\sigma_{JLF}[Mf_L + f_{low}, Mf_L + f_{high}] = (T_L / 2\pi M) \sqrt{P_N / P_A} = (1 / 2\pi M f_L) \sqrt{P_N / P_A} \quad 4.8$$

This jitter is usually measured at the higher harmonics where the bounds of this noise are more easily seen in the spectrum analyzer display [Ref. 70]. If the pedestal is obviously present, it can be measured at the fundamental. Low frequency temporal jitter is also expressed in seconds.



## G. RADIO-FREQUENCY SPECTRUM ANALYZER JITTER NOISE MEASUREMENTS

The sigma laser was mode-locked at pulse frequencies ranging from 7 to 16 GHz. The signal was measured in the frequency domain using a wide bandwidth, 26-GHz photodetector and a RF spectrum analyzer. The photodetector has a conversion factor of 23.46 mV per mW of light energy [Ref. 72]. A DC block was used to protect the spectrum analyzer from a low DC voltage present in the photodetector. The insertion loss from the DC block was measured at 1 dB. Figure 4.10 is a picture of the HP8563E spectrum analyzer with a captured mode-locked signal. The black device to the right of the analyzer is the photodetector with a DC block attached.

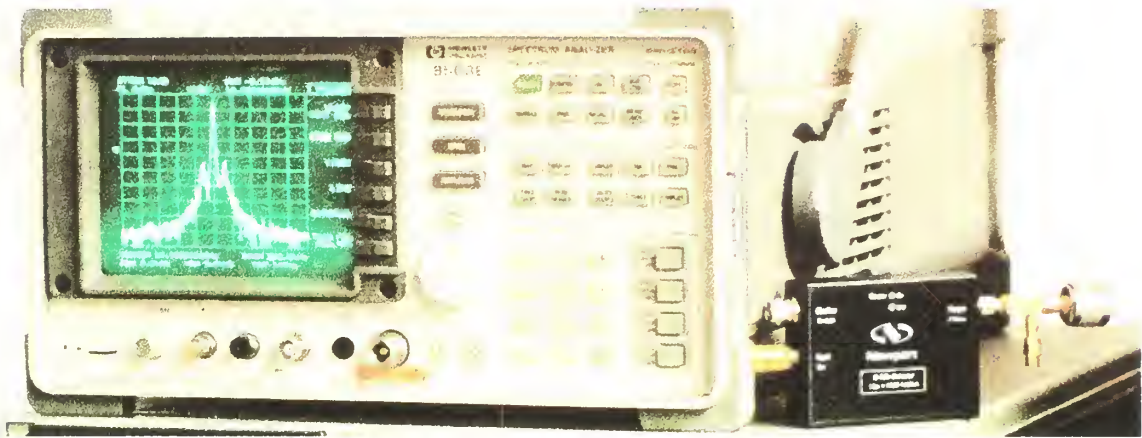


Figure 4.10. Spectrum analyzer with a 10.1 GHz PRF signal, span 400 kHz.

The fundamental and second harmonic of the signal was measured at the minimum spans that displays the different pedestals of noise at the base of the signal. Measurements were taken at spans of 30 to 400 kHz with resolution bandwidths of 0.3 to 3 kHz, respectively. The signal is usually centered on the analyzer display for the wider spans. For the narrow 30 kHz span measurement, the peak of the signal is shifted to one side of the analyzer display to capture the noise at the base of the signal.

The HP8563E spectrum analyzer uses 600 points of data to represent the spectrum set by the front panel of the equipment. This data is extracted from the analyzer's memory using LABVIEW 4.0 software, plotted to the computer display, and saved to the



computer hard disk [Ref. 63]. The saved data were plotted again using MATLAB 5.0 and the noise for each pedestal was determined graphically. Amplitude and temporal jitter were calculated using Equations 4.4 to 4.8 from pages 83 and 84 and a final plot was generated with calculations and other pertinent data.

The jitter noise was calculated using the fundamental and second harmonic for frequencies between 7 and 13 GHz and by using the fundamental for frequencies between 14 and 16 GHz. In either case, the higher harmonics are not available due to the frequency limits of the spectrum analyzer. The calculated results are given in Table 4.2; an example the measurement process is given below.

The laser was mode-locked at 7.0001 GHz and measurements taken at the fundamental and second harmonic. Figure 4.11 shows a span of 200 kHz of the fundamental signal. The two lines located on the trace show the bounds of the amplitude and temporal jitter noise. Since amplitude jitter is dominant,  $\sigma_{AJ}$  is calculated from the area under this curve. The crowns of noise on either side of the signal are included as amplitude noise [Ref. 73]. This inclusion was verified in another experiment in which the laser was poorly mode-locked and the autocorrelator pulse was alternating between two amplitudes at a rate of 1 Hz. When evaluated on the RF spectrum analyzer, this same variation could be seen in these noise crowns as they changed in amplitude at the same rate.



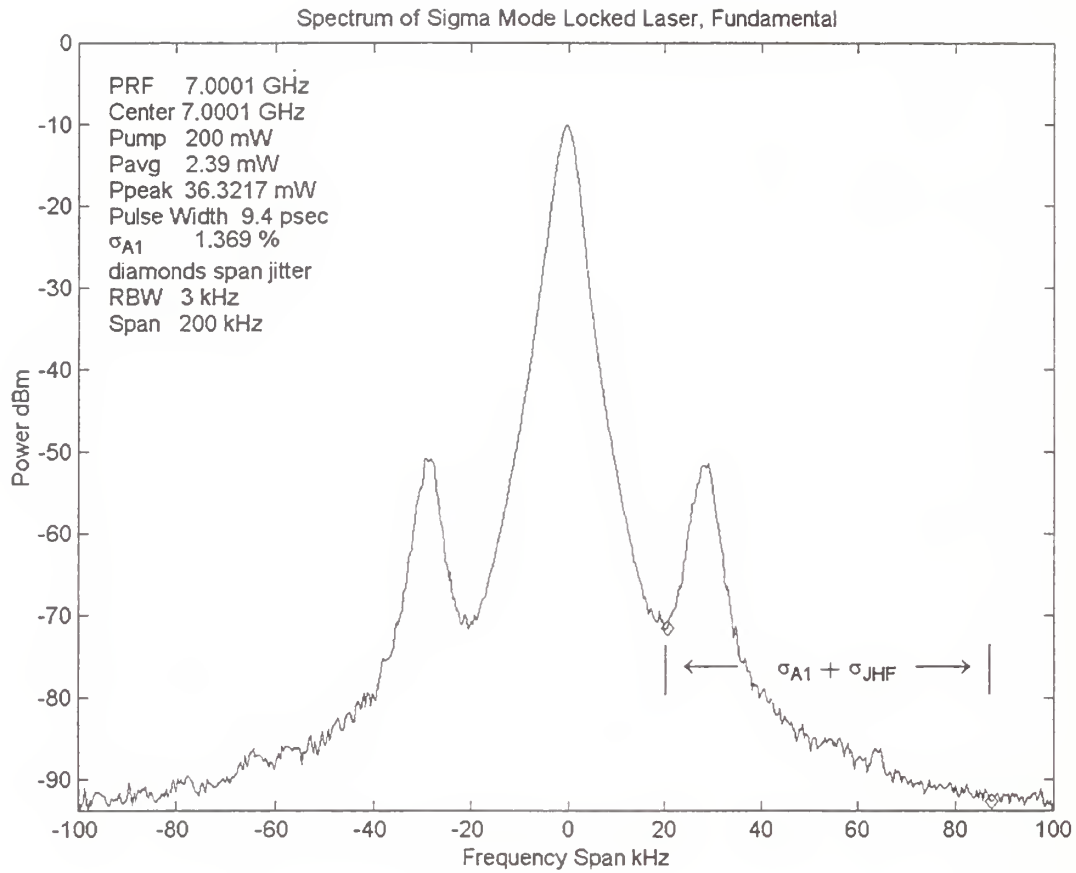


Figure 4.11. Fundamental mode-locked signal, 7 GHz PRF, 200 kHz span.

The second harmonic was evaluated at the same span and  $\sigma_{A2}$ ,  $\sigma_{JHF}$ , and  $\sigma_{JLF}$  were calculated. There are four lines on the plot of the second harmonic in Figure 4.12. The two lines at the lowest point between the peak signal and the noise crown to the right of the peak show the low frequency temporal noise  $\sigma_{JLF}$ . The wide spanning lines, similar to the trace in Figure 4.11, show the combined amplitude and high frequency temporal jitter,  $\sigma_{A2}$  and  $\sigma_{JLF}$ . The high frequency temporal jitter is dominant at this fundamental since  $\sigma_{A2} > 2\sigma_{A1}$ .

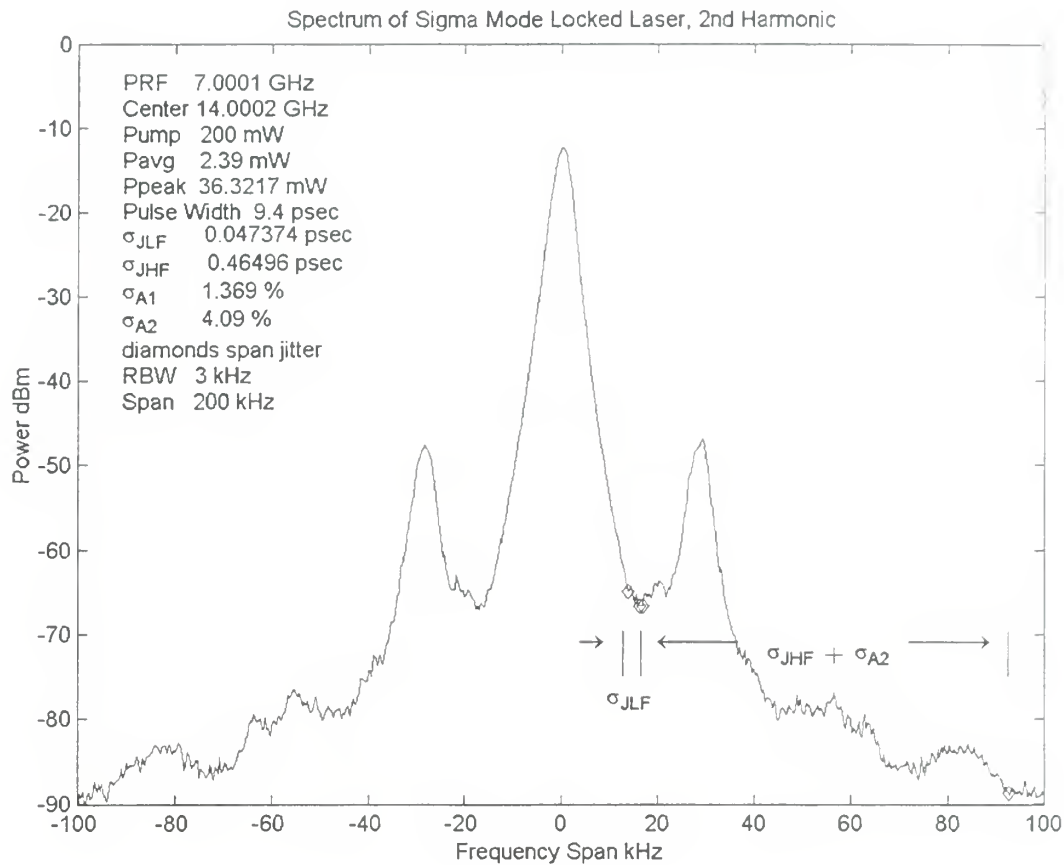


Figure 4.12. Second harmonic mode-locked signal, 7 GHz PRF, 200 kHz span.

When the resolution bandwidth of the spectrum analyzer was narrowed, additional low frequency temporal jitter can be seen [Ref. 70]. The span is narrowed to 30 kHz and the resolution bandwidth was lowered to 300 Hz. Figure 4.13 is the second harmonic at a span of 30 kHz. The low frequency jitter, shown between the two lines, was re-evaluated and found to be higher than in the 200 kHz span above which has a resolution bandwidth of 3 kHz. This measurement is retained as the more accurate  $\sigma_{JLF}$  value.

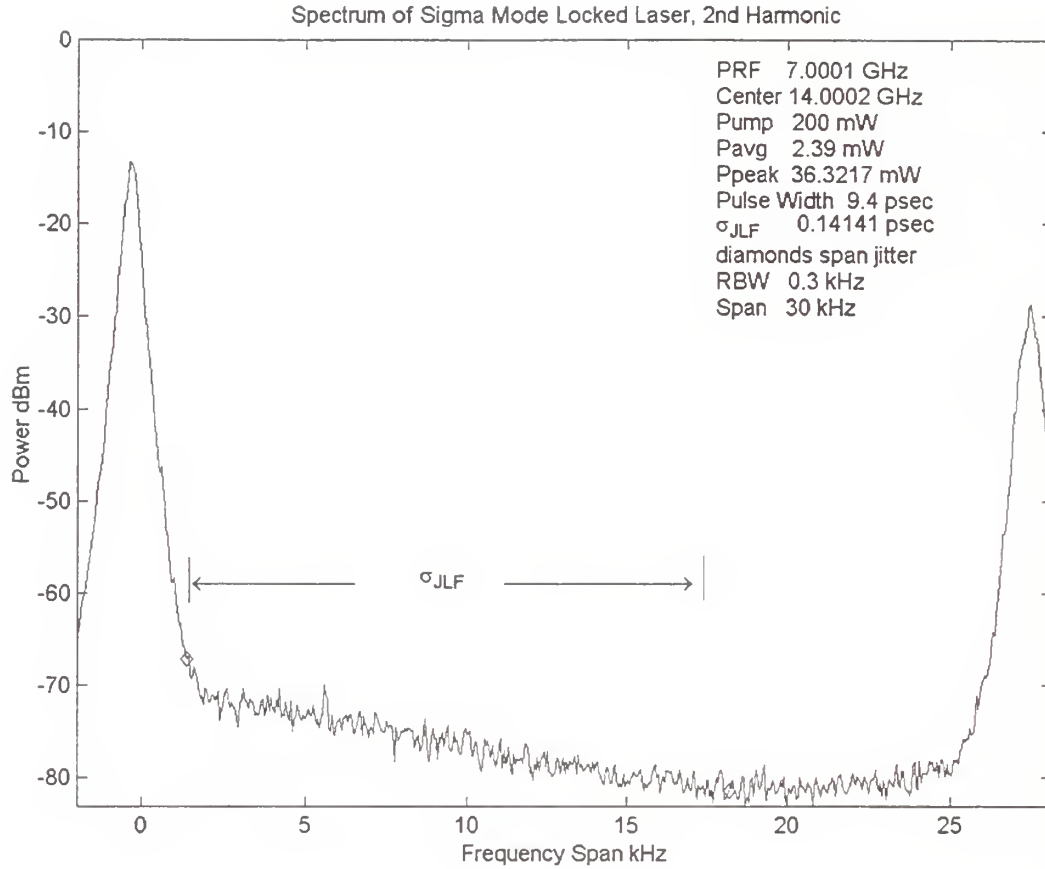


Figure 4.13. Second harmonic mode-locked signal, 7 GHz PRF, 30 kHz span.

High and low frequency temporal jitter can be added together to give a total rms temporal jitter of 606 femtoseconds for the 7.0001 GHz mode-locked signal [Ref. 73]. For purposes of this Thesis, they are left separate since  $\sigma_{JHF}$  is not always available.

## H. SUMMARY OF MEASUREMENTS

Table 4.2 in this Chapter shows the measured and calculated results of 14 mode-locked signals. The pulsewidths and jitter varied widely throughout the experiments. This was due to the quality of the mode-locking condition at the time of the experiment. In two cases labeled *poor lock* in the table, the optical and radio frequency spectrums were extremely noisy. Finding a quality resonant frequency is instrumental in obtaining a

quality mode-locked signal. Three sets of data were taken around 7 GHz with varying results. Of the three, the best locked condition occurred at 7.0002 GHz which yields low jitter noise of 386 fs and a narrow linewidth of 0.3 nm but a slightly longer pulsewidth of 10.2 ps. Mode-locking at 7.0001 GHz produced a high quality signal and a narrower pulse but almost doubles the temporal jitter noise. At 7.001 GHz the optical and frequency spectrums are extremely noisy with a large amount of jitter. This signal, however, has the narrowest pulsewidth.

The resonant frequency also affects the feedback system. Usually the phase difference signal from the microwave mixer can be adjusted to a zero difference using the microwave phase shifter. The integrator circuit is allowed to take over at this point and holds the phase steady. Occasionally a resonant frequency will be found that does not allow a zero difference and a lot of pre-integration offset has to be used to hold the phase difference steady. This causes the feedback circuit to make an excessive amount of adjustments in the voltage on the PZT, makes the laser signal less stable, and creates additional noise in the spectrum.

The signal quality also affects mode-locking. Initial mode-locking is usually accomplished by finding the resonant frequency with the harmonic synthesizer and then turning the feedback system on. The voltage on the PZT can be adjusted on the integrator box or by using the phase shifter to force the cavity length closer to the optimum mode-locking condition. The pulse amplitude usually doubles when feedback is turned on and the system adjusted. An initially weak pulse prior to turning on the feedback makes the mode-locking condition less stable since there is less of a signal to be amplified. The phase difference cannot be optimized properly. The system still holds the phase difference constant and the mode-locked pulse remains weak without an improvement in pulse amplitude.

The 16 GHz PRF signal is different since the PRF is twice the modulation frequency. This was discovered on the RF spectrum analyzer where a small 8 GHz signal was found with  $-45$  dBm of power but a 16 GHz signal occurred with  $-10$  dBm of power. Figure 4.14 shows the two signals plotted together. This is possible since the modulator is DC biased at the top of its voltage/intensity curve allowing for double modulation. Other mode-locked lasers have displayed this behavior of mode-locking at many

multiples of the modulation frequency [Ref. 33]. With more experimentation and modulation at 10 to 15 GHz, this laser may be able to operate at pulse rates from 20 to 30 GHz by taking advantage of this effect.

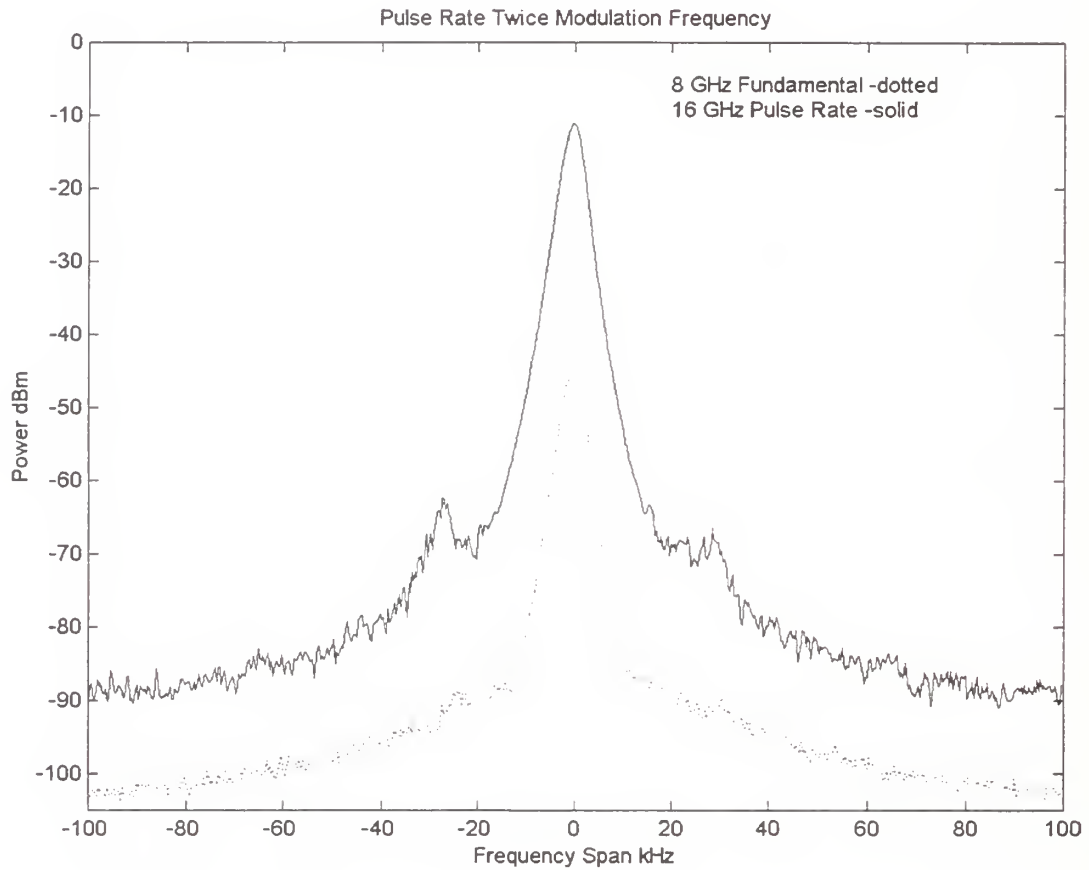


Figure 4.14. Harmonic mode-locking at double the modulation frequency.

Other than doubling the PRF, the bias voltage seems to have little effect on the output power of the laser. Each time the laser is locked at a different frequency, the bias is adjusted to slightly optimize the condition.

## I. OPTICAL POWER EXPERIMENT

An experiment was conducted in which the laser was mode-locked at 10.1 GHz and the pump power reduced incrementally by reducing the drive current for the pump laser diodes. Table 4.4 at the end of this section summarizes the results of all measured parameters during the experiment.

Mode-locking is lost when combined pump power is reduced below 55 mW or below 120 mA of drive current. This is probably due to the lossy nature of the cavity. There is just not enough laser energy to pass through all of the components and maintain a mode-locked condition. As expected, the peak power and average power increase linearly with an increase in pump power, as shown in Figure 4.15.

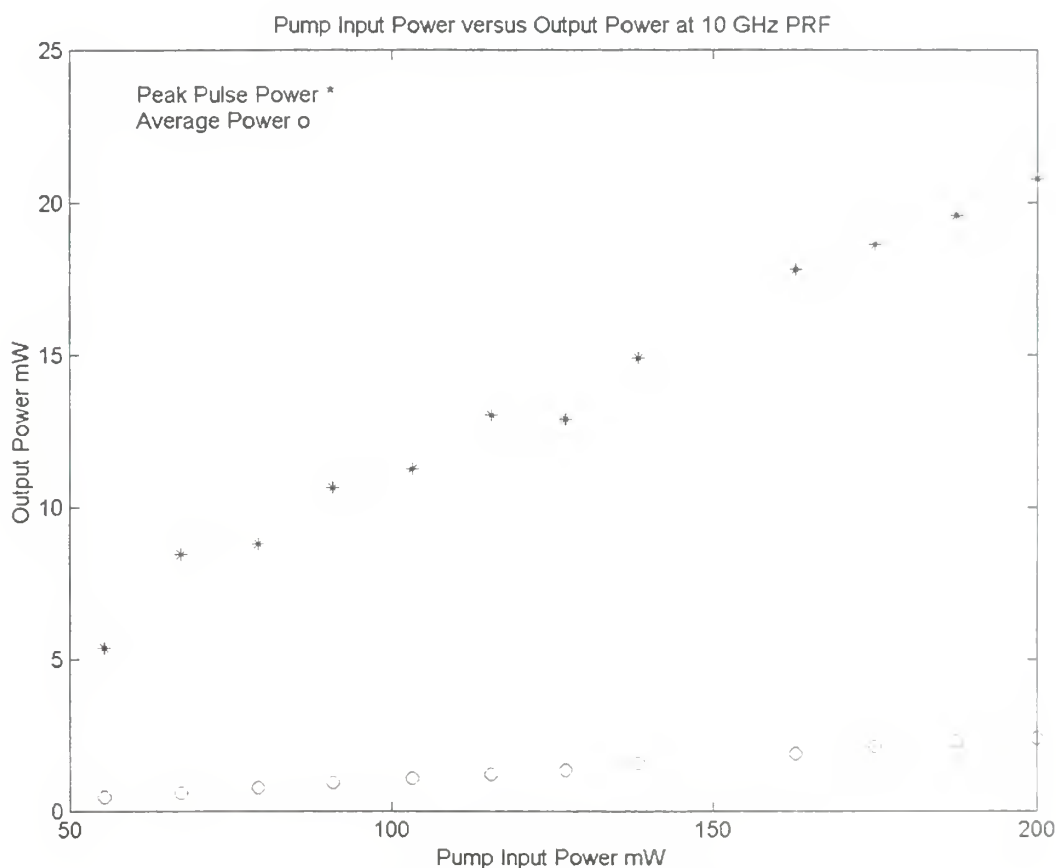


Figure 4.15. Peak and average laser power versus pump power.

The pulsewidth also generally increases with an increase in pump power as shown in Figure 4.16. This is probably due to an overall larger pulse since the pulse amplitude measured on the autocorrelator also increased linearly with pump power. However, a smaller but narrower pulse might be amplified in an external amplifier to increase the amplitude with a limited gain in pulsewidth.

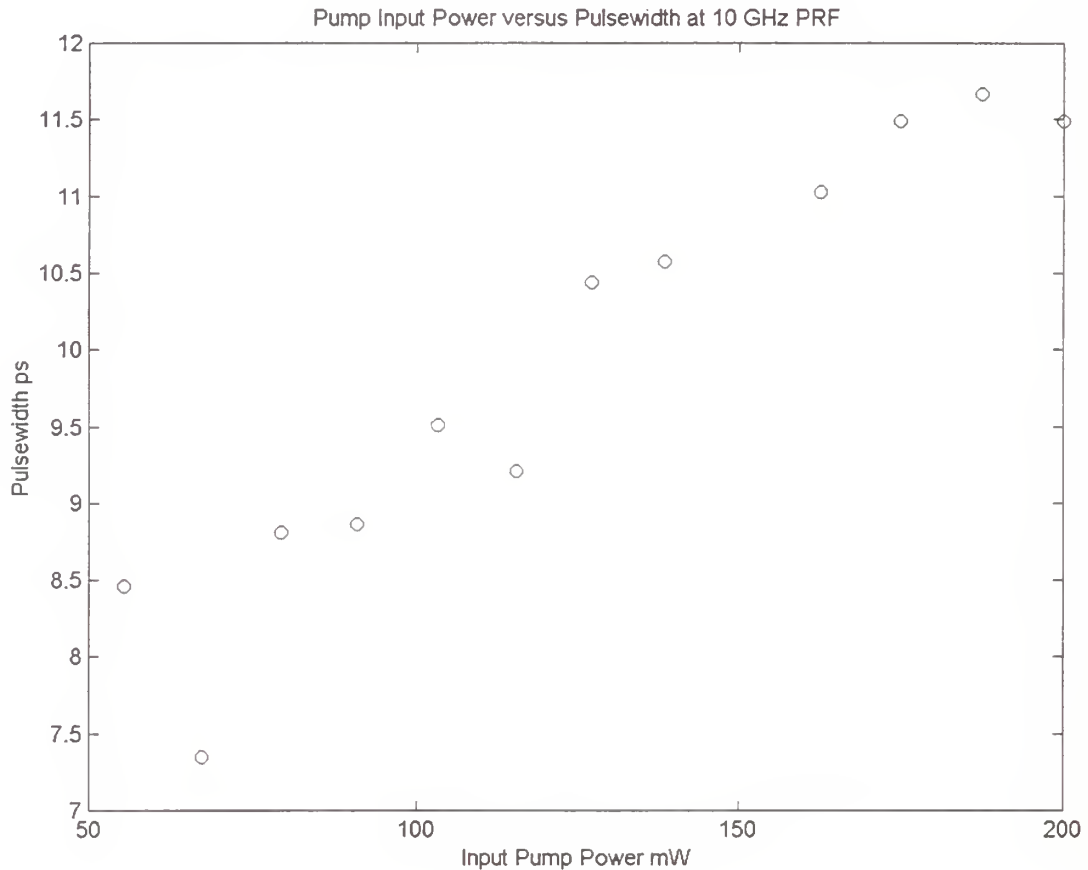


Figure 4.16. Pulsewidth versus pump power.

The most interesting plot is the low frequency temporal jitter versus the pump current. It was found that  $\sigma_{JLF}$  increased as diode drive current is increased (see Figure 4.17). This is significant since the calculation is based on normalized powers. Von der Linde in [Ref. 70] found that  $\sigma_{JLF}$  was due to low frequency fluctuations in the power supply for a mode-locked argon laser. When the power supply was replaced with a more



advance power supply, the jitter was significantly reduced. This may be the case in this laser as well.

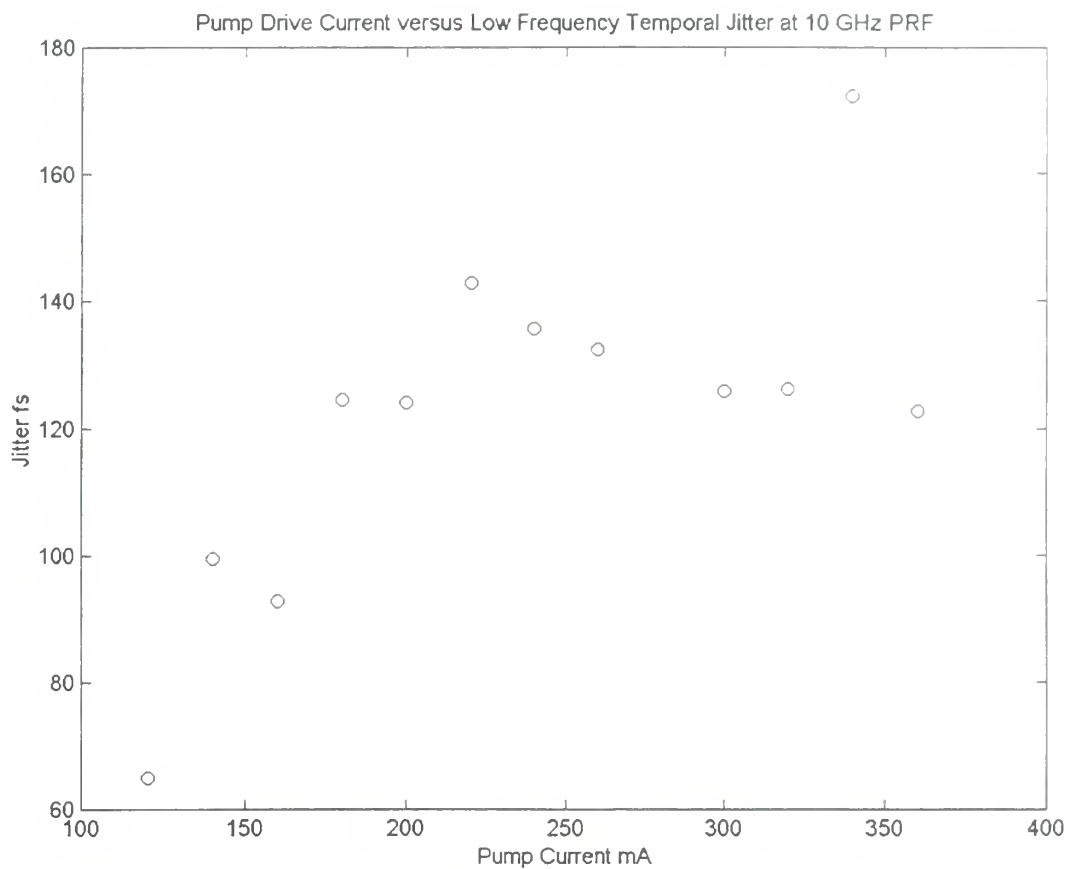


Figure 4.17. Low frequency temporal jitter versus pump current.

Frequency GHz	Pump Power mW	Pulse- width ps	Low Freq jitter fs	High Freq jitter fs	Amplitude jitter %	Wave- Length nm	Line- Width nm	Average Power mW	Peak Power mW	Drive Current mA	DC Bias Voltage V	RF Drive Power dBm
10.10033998	55.3	8.457	64.9	Not meas	1.83	1563.3	0.331	0.461	5.397	120	14.71	47.19
	67.2	7.349	99.4	Not meas	2.89	1561.4	0.337	0.628	8.4605	140		
	79.3	8.807	92.8	Not meas	2.7	1561.6	0.369	0.784	8.8136	160		
	90.9	8.865	124.5	Not meas	3.24	1561.6	0.338	0.952	10.6322	180		
	103.3	9.507	124	Not meas	10.84	1561.9	0.362	1.08	11.247	200		
	115.5	9.207	142.9	Not meas	3.19	1562.2	0.344	1.22	13.024	220		
	127.1	10.44	135.7	Not meas	2.18	1562.4	0.338	1.359	12.897	240		
	138.5	10.577	132.3	Not meas	1.55	1560.4	0.381	1.594	14.9115	260		
	162.7	11.023	125.8	Not meas	1.053	1560.6	0.356	1.902	17.8034	300		
	175	11.49	126.2	Not meas	1.694	1559.8	0.306	2.16	18.6122	320		
	187.6	11.665	172.3	Not meas	1.398	1559.9	0.306	2.308	19.589	340		
	200	11.49	122.7	Not meas	1.22	1560.3	0.372	2.41	20.7664	360		

Table 4.4. Summary results of reduced pump power.

## J. SHORTEST PULSEWIDTHS

In early experiments, the laser was mode-locked at sub-gigahertz frequencies. In modulation ranges from 6 kHz to 950 MHz, the laser can be actively mode-locked but without feedback stabilization due to the operating ranges of the feedback parts. Very narrow pulses are produced and range from 1.88 to 2.84 ps. Without feedback the mode-locking is very unstable and the mode-locked condition would only last for a 30 minutes at the most. Harmonic mode-locking at double the modulation frequency is also observed. On the RF spectrum analyzer, the low PRF signals are very noisy.

These lower frequency pulses are not be very useful in their present form and are not pursued in detail. Still they demonstrate the capability of much narrower pulses. Figure 4.18 is a photograph of a 1.88 ps pulse at a pulse rate of 12.2 MHz on an oscilloscope. Figure 4.19 is the signal captured on a digital sampling oscilloscope. The pulses represented are skewed and broad due to limited response of the oscilloscope as compared to the very narrow pulsewidth. Still, this figure demonstrates a train of mode-locked pulses that can be modulated much like the laser pulses in Figure 1.3 of Chapter I.

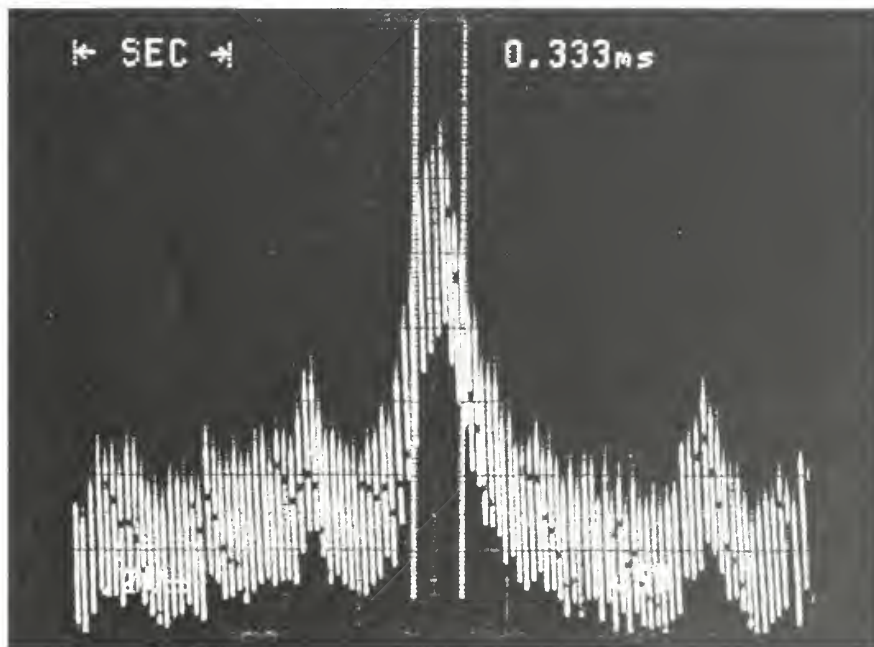


Figure 4.18. Oscilloscope display of a 1.88 ps mode-locked pulse, 12.2 MHz PRF.

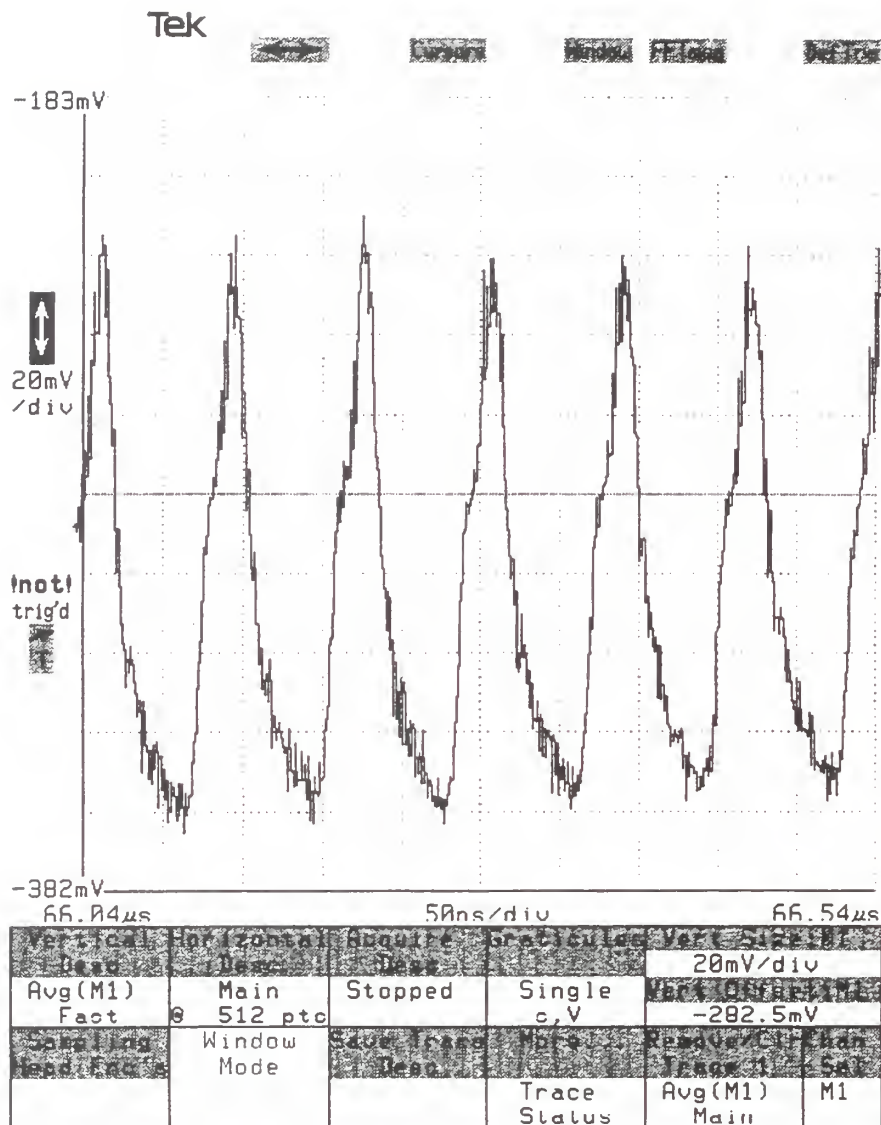


Figure 4.19. Digital sampling oscilloscope display of mode-locked laser pulses, 12.2 MHz PRF.

Currently, pulses of 1 to 2 picoseconds in duration briefly appear on the oscilloscope during attempts to mode-lock the laser at 10 GHz PRF. These pulses only last for a few seconds and cannot be stabilized. With some optimization and modification, this laser can generate 1 to 2 picosecond pulses at the higher PRFs.

This laser demonstrates stable mode-locked pulses with pulsewidths of 7.2 to 17.7 ps at PRFs between 7 and 16 GHz. The stability of the mode-locking condition at these

rates is good and the laser remains locked for six hours or more. Figure 4.20 is the narrowest recorded pulsewidth (7.2 ps) in the GHz spectrum; it is not included in the data above because the rest of the data was not recorded for in-depth analysis. A train of these multi-gigahertz, mode-locked laser pulses can be externally modulated in an optical ADC system [Ref. 6].

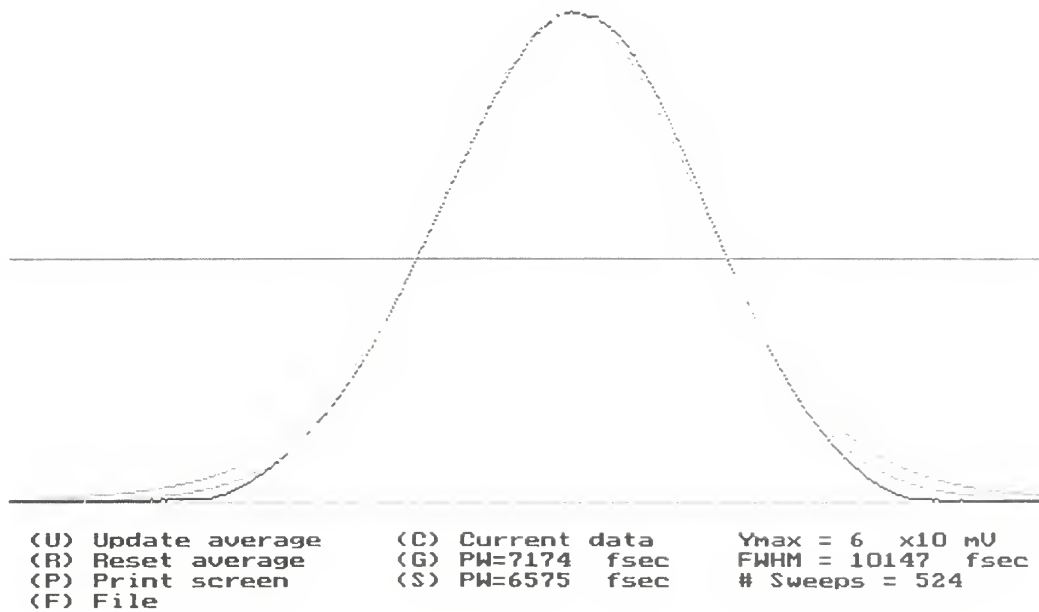


Figure 4.20. Narrowest attained pulsewidth, 10 GHz PRF.

## K. DISPERSION MANAGEMENT AND PULSEWIDTH

Using the pulsewidth and gain bandwidth results, the calculation for group velocity dispersion  $\beta$ , total fiber dispersion  $D_f$ , and gain dispersion  $D_g$  were calculated using Equations 2.13-16 on pages 23-25. The operational wavelength was measured as 1560 nm and the gain bandwidth of the laser was measured as 30 nm, respectively. Using the dispersion for each type of fiber and the different lengths of fiber, the average dispersion of the cavity  $D_{avg}$  was calculated as 2.61 ps/nm/km and is used to calculate a  $\beta$  of  $3.37 \times 10^{-27} \text{ s}^2/\text{m}$ . Using this  $\beta$  and the cavity length of 127 meters, the total fiber dispersion  $D_f$  was calculated to be  $4.281 \times 10^{-25} \text{ s}^2$ .

The steady-state EDFA gain for a large signal such as mode-locked pulse was measured as 5 dB. The gain and gain bandwidth were used to calculate a gain dispersion  $D_g$  of  $2.194 \times 10^{-25} \text{ s}^2$ . As previously mentioned in Equation 2.16, the requirement for soliton formation requires  $D_f/D_g \geq 0.625$ . For this laser this dispersion ratio was calculated to be 1.95, so solitons can form and the pulses can undergo soliton pulse shortening. As a result, the maximum pulse reduction  $R_{max}$  of the actively mode-locking pulsewidth limit is calculated to be a factor of 1.69 using Equation 2.17

The measured spectral linewidth for 7, 10, and 12 GHz pulse rates were used to calculate the theoretical pulsewidth for active mode-locking in Equation 2.12 and are calculated to be 25, 21.7, and 22.87 ps, respectively. The pulsewidths were reduced to 9.39, 7.9, and 13.88 ps for the 7, 10, and 12 GHz pulse rates, respectively. The observed reduction from the actively mode-locked limit ranges from 1.65 to 2.75, which is higher than the calculated value. This is probably due to the dispersion value of the erbium; in reality, it is probably lower than the  $-0.09 \text{ ps/nm/km}$  value uses.

The usefulness of these laser pulses can be determined in their application to optical ADC. The next chapter takes the best results of laser pulse generation and applies them to an amplitude-analyzing optical ADC.

## V. SAMPLING LIMITATIONS OF THE SIGMA LASER

In the previous Chapter, the PRF, pulsewidth, temporal jitter noise, and amplitude jitter noise were measured because they have an effect on the operation and accuracy of an optical sampling system. The PRF is the sampling rate and limits the maximum frequency that can be sampled, especially if using the Nyquist theorem. In addition to the mode-locked laser, the Mach-Zehnder modulator is also a major component within the optical ADC. This device amplitude modulates the laser pulses with the RF signal of interest. The noise in the laser output can have a detrimental and limiting effect in this modulation process. The factors affecting an optical ADC will be discussed in the sections below.

### A. AMPLITUDE JITTER NOISE

Amplitude jitter in the sampling waveform is a problem if its variation is significant enough to exceed an ADC step size or least significant bit. A binary-weighted converter with  $N$  bits of resolution has  $2^N - 1$  quantization levels that can be approximated by  $2^N$ . To avoid exceeding a step size, the amplitude variation  $\Delta A$  must be less than or equal to

$$\Delta A \leq 2A / 2^N \tag{5.1}$$

where  $2A$  is the peak-to-peak voltage amplitude of the sampled signal [Ref. 74]. Since amplitude jitter  $\sigma_A$  is measured as a function of percentage of peak value, Equation 5.1 is rearranged to become a maximum amplitude jitter  $\sigma_{Amax}$  of

$$\sigma_{Amax} = 100\Delta A / A \leq 100 / 2^{N-1}. \tag{5.2}$$

The 100 value is used as a conversion to a percentage. Figure 5.1 is a plot of  $\sigma_{Amax}$  for 6 to 12 bits. Although sampling at 10 bits is the goal of this laser, the 11 and 12 bit values are plotted to see how small this value can get. At 12 bits the minimum tolerable



amplitude jitter is less than 0.05% [Ref. 74]. The minimum measured amplitude jitter in the sigma laser output is 0.23% and is also plotted in Figure 5.1. As seen on the graph, this limits the use of this laser in an optical ADC to 9 bits of resolution.

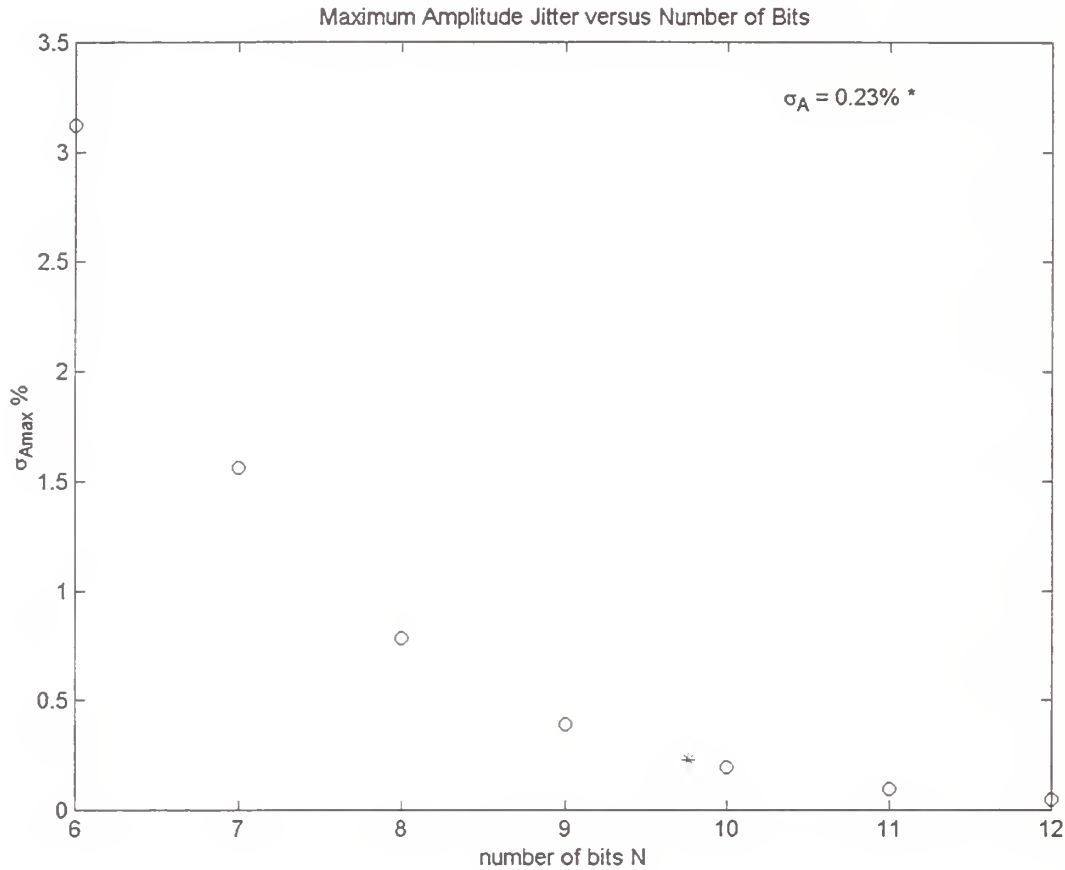


Figure 5.1. Maximum percentage of amplitude jitter versus number of bits.

## B. MAXIMUM TEMPORAL JITTER

The maximum amplitude error given in Equation 5.1 can also be caused by temporal jitter. To prevent amplitude error in an ADC, the maximum temporal jitter is limited to [Refs. 74, 75, 76]

$$\sigma_{t \max} \leq 1 / (2^N \pi f_m). \quad 5.3$$

The best-combined rms temporal jitter  $\sigma_t$  measured in this laser was 386 fs. Because of low amplitude jitter, the temporal jitter measurements at 14.1, 15, and 16 GHz are believed to be lower but the second harmonic spectrum is not available due to the limits of the RF spectrum analyzer. Figure 5.2 is a plot of maximum temporal jitter using Equation 5.3. The curves are plotted using 6 to 10 sampling bits. Using 386 fs for comparison purposes, the maximum frequencies that can be sampled are listed as  $F_{m6}$  through  $F_{m10}$  on the graph.

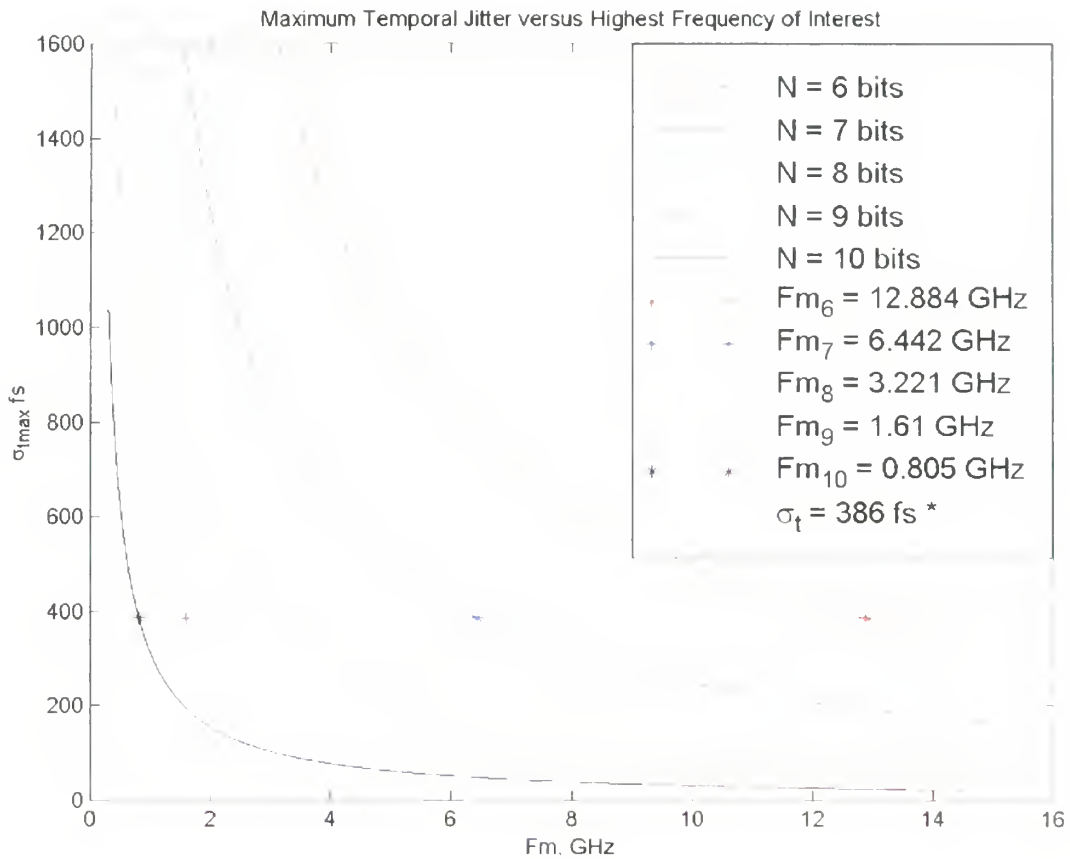


Figure 5.2. Maximum temporal jitter versus highest frequency of interest

The maximum PRF of this laser is measured at 16 GHz. Since Nyquist sampling requires a PRF of at least twice the highest maximum frequency, this laser can be used to Nyquist sample a signal as high as 8 GHz [Ref. 2]. At six bits, the laser is PRF limited to



8 GHz rather than jitter limited to 12.88 GHz. At 10 bits, this laser is timing jitter limited to sampling an 805 MHz signal.

### C. OPTICAL TRANSIT TIME

In an optical sampling system, the Mach-Zehnder modulator is used to modulate the laser pulses with the RF signal to be sampled. The time of interaction between the laser pulse and the RF voltage as the light passes through the electrodes is the electro-optic interaction time. During this period, the electromagnetic energy from the RF signal modulates the passing light energy. As the RF signal increases in frequency, the maximum allowed electro-optic interaction time is decreased since the higher frequency signal is changing more rapidly [Refs. 6, 76].

The original pulse is split into two at the entrance to the modulator. Each half of the light travels through separate arms of the interferometric configuration within the device. In the simplest devices, the RF voltage present on the electrodes alters the phase of the passing light through one arm of the modulator during the entire electro-optic interaction time. When the halves recombine, the phase change amplitude modulates the laser pulse [Ref. 6].

Depending on the type of modulator, the electro-optic interaction time is the sum of the laser pulsewidth and the time it takes the pulse to transit the length of the modulator electrodes. The pulse transit time is also referred to as the optical transit time and can be significantly long compared to the duration of a mode-locked laser pulse [Ref. 76].

There are two types of electro-optic modulators available on the market, the lumped electrode modulator and the traveling waveguide modulator. In the lumped electrode modulator, the RF signal is introduced as a voltage at the center of the electrodes and affects the entire length of the electrodes about equally. In the newer traveling waveguide modulators, the RF signal is transmitted into one end of a waveguide acting as an electrode and the signal travels the same direction as the laser light. The signal and light are velocity matched and travel along together.



In the lumped electrode modulator, the RF signal is rapidly changing with time equally across the entire set of electrodes. As a result, the laser pulse is affected by the time-averaged RF voltage on the electrodes during its duration and during its optical transit time through the electrodes [Ref. 50].

The optical transit time  $T_E$  is a function of the length of the electrodes  $L$ , the speed of light  $c$ , and the material index of refraction  $n$ . For a lumped electrode modulator,  $T_E$  is given by [Ref. 20]

$$T_E = L / v = nL / c . \quad 5.4$$

In an optical ADC, there are multiple modulators with varying lengths of electrodes. The longest set of electrodes will be used for this calculation since shorter lengths will require less time.

In the traveling waveguide modulator, the laser pulse samples only that portion of the RF signal that it is traveling with it instead of the time-averaged signal in the lumped electrode device [Ref. 50]. In this case, the electro-optic interaction time is governed by pulsewidth alone. The optical transit time  $T_E$  is not a factor and is counted as zero.

Due to a number of factors in the design of a traveling waveguide modulator, it has a higher bandwidth [Ref. 50]. For purposes of this Thesis, it was assumed that traveling waveguide modulators are used for an optical ADC. Therefore, the optical transit time  $T_E$  is zero.

## D. MAXIMUM PULSEWIDTH

The electro-optic interaction time  $\Delta T$  is the sum of the pulsewidth  $\Delta t$  and the optical transit time  $T_E$ . Taylor states in [Ref. 6] that there is a maximum electro-optic interaction time based on the highest frequency of interest  $f_m$  and the number of sampling bits  $N$ . The maximum electro-optic interaction time  $\Delta T$  is given by

$$\Delta T = \Delta t + T_E \leq (1 / \pi f_m) \sqrt{3 / 2^{N-1}} . \quad 5.5$$





Using traveling waveguide modulators, the optical transit time  $t_L$  becomes zero, leaving the pulsewidth contribution alone. Hence, the maximum pulsewidth is limited to

$$\Delta t \leq (1/\pi f_m) \sqrt{3/2^{N-1}} \quad 5.6$$

Figure 5.3 is a plot of  $\Delta t$  versus the maximum frequency to be sampled  $f_m$  for values between 6 and 10 sampling bits. The best pulsewidth attained from the NPS laser was 7.2 ps and was used to show the maximum RF frequencies that can be sampled for comparison purposes. These maximums are listed as  $Fm_6$  through  $Fm_{10}$  on the graph.

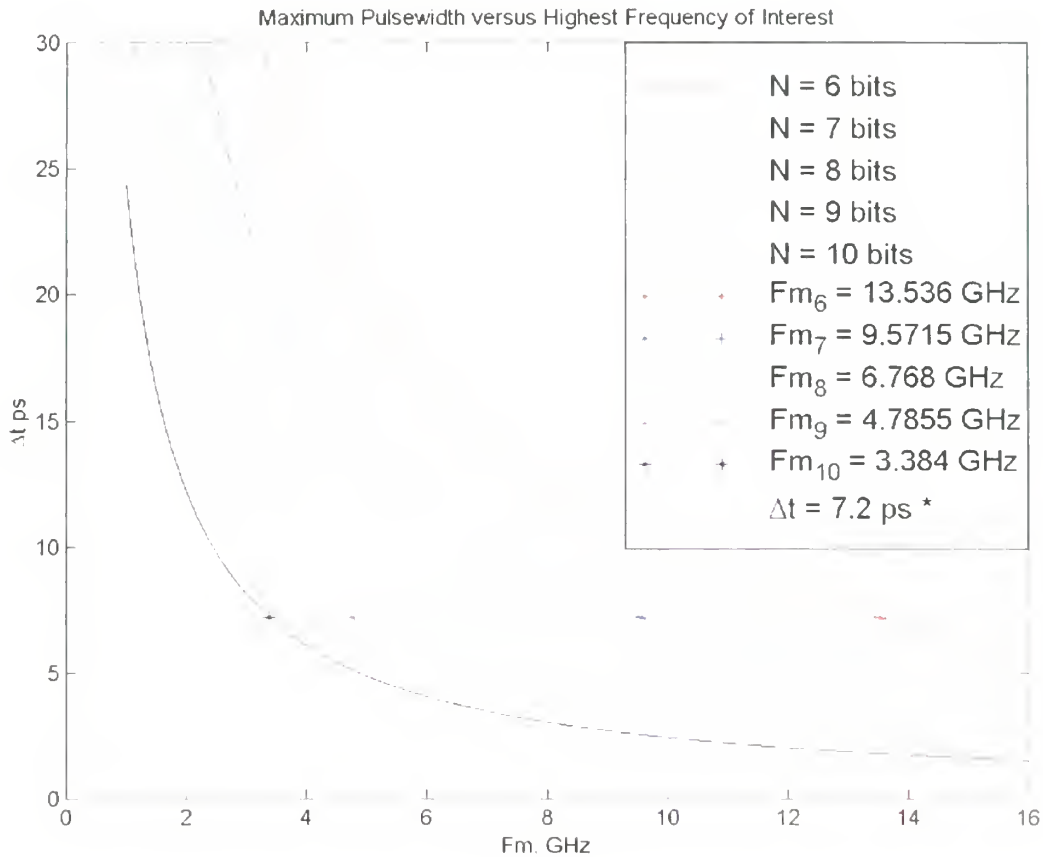


Figure 5.3. Maximum allowed pulsewidth versus highest frequency of interest



Since the NPS sigma laser is PRF limited to Nyquist sampling an 8 GHz signal, sampling at 6 or 7 bits is limited to 8 GHz instead of the frequencies listed on the graph. At 10 bits, the pulsewidth limits sampling to 3.38 GHz. For sampling above the Nyquist rate, a PRF of at least 6.8 GHz would be used to sample the signal at 10 bits.

## **E. CONCLUSION**

The demonstrated output of this laser can be used to sample RF signals in an optical sampling system. Given the analysis above, there are some maximum values to consider in optical sampling with the NPS sigma laser in an amplitude-analyzing ADC. If sampling at 6 bits of resolution, the laser is PRF limited to sampling an 8 GHz signal of interest if using the Nyquist theorem. If sampling at 7, 8, or 9 bits, the laser is temporal jitter limited to sampling 6.44, 3.22, or 1.61 GHz signals respectively. At 10 bits, the laser would be limited to 805 MHz; however, amplitude jitter limits the laser to sampling at a maximum of 9 bits of resolution. In summary, the laser can be used for sampling an 8 GHz signal at 6 bits or a 1.61 GHz signal at 9 bits of resolution. Recommendations to improve the jitter noise and pulsewidth are presented in the next Chapter.



## VI. CONCLUSIONS AND RECOMMENDATIONS

### A. DISPERSION OPTIMIZATION

The NPS sigma laser is capable of and has briefly demonstrated laser pulsewidths of less than two picoseconds. The original sigma laser at NRL currently produces pulsewidths of 744 femtoseconds. The major differences between the NRL and NPS sigma lasers are the input power, optical amplifier type, optical modulator, and optimization of cavity fiber dispersion. Improvements or optimization in these areas is likely to show an improvement in laser performance and increase the useful sampling bandwidth of the laser pulses.

The reduction of the NPS sigma laser pulsewidth might be accomplished by optimizing the cavity dispersion alone and should be the first priority. Other than the work of experimentation, much of the optimization can be done without additional cost. Since this laser uses a different amplifier than the NRL laser, dispersion optimization is much more difficult. The original design used 10 meters of dispersion-compensating (DK) fiber. With this length of fiber, the laser was not very stable in the mode-locked condition. The length of dispersion-compensating fiber was reduced to one meter and the laser works well with the exception that the pulsewidths are longer than desired.

The recommendation is to splice a 10 meter length of DK fiber in place of the existing one meter of fiber and begin pulsewidth measurements. The dispersion-compensating fiber should be reduced by one meter lengths and re-spliced to find the optimized length. A combination of minimum pulsewidth and laser stability should be found in this region. It should be noted that the laser pulses pass through this length of fiber twice during a cavity round trip.

### B. OPTICAL MODULATOR

The current optical modulator in the laser cavity is an E-TEK modulator rated at 10 GHz and has a very large  $V_\pi$  as compared to more modern modulators [Ref. 49]. This is an older 1987 modulator that lacks the quality of today's higher bandwidth devices.

Since this laser can be harmonically mode-locked at twice the modulation frequency, the E-TEK modulator should eventually be replaced with a newer high bandwidth modulator rated at greater than 20 GHz. The newer modulator should also have a much lower  $V_{\pi}$ . This laser is probably capable of a much higher PRF. The higher bandwidth modulator will improve the sampling capability of the laser.

### C. NOISE REDUCTION

There are several areas where efforts can be undertaken to reduce the laser noise. The first is the power supplies for the pump laser diodes. The SDL and Melles Griot laser diode controllers have noise and ripple values of less than 1% [Refs. 77, 78]. The diode lasers are operated at 180 mA so noise fluctuations can be as high as 1.8 mA. Power supplies were a source of low frequency jitter in [Ref. 26] and are possibly a source of noise for this laser.

Efforts should be undertaken to find and reduce this noise source since low frequency jitter is significant in the output of this laser (see Table 4.1 in Chapter IV). In Chapter V, the 386 fs combined temporal jitter limited sampling at 10 bits to a maximum of 805 MHz. If the low frequency component of 137 fs is eliminated from the temporal noise, the maximum frequency that can be sampled would increase by 35% to 1.25 GHz. This is a significant increase and would be one step in the noise reduction process.

The noise reduction can be accomplished in two ways. A filter can be added to the line current between the laser diode and the controller. Given the amount of current flowing (180 mA each) and the cost of replacing the laser diode should something go wrong, this approach might be ill-advised. The opto-electronic companies are starting to sell very low noise controllers and power supplies. For example, ILX Lightwave sells an “Ultra Low Noise Current Source” that boasts less than 850 nA of current noise and ripple [Ref. 79]. This is a big improvement over the existing laser controllers.

The high frequency temporal jitter and amplitude jitter can also be reduced. Experiments in actively mode-locked semiconductor diode lasers emphasized that high frequency temporal jitter and amplitude jitter can be reduced with a reduction in pulsewidth. In the diode mode-locked laser, the presence of high ASE noise allows

additional lower amplitude mode-locking at higher order frequencies (higher order modes) despite the active modulation. The interaction between the additional higher order modes and the fundamental mode-locked signal causes broader pulsewidths and creates additional amplitude and timing fluctuations in the final output [Ref. 26].

Similar to the semiconductor diode laser, the EDFA has an excessive amount of ASE and is a possible cause of both temporal and amplitude jitter. In addition to the higher order modes, the EDFA adds temporal jitter when the pulse undergoes amplification in the presence of high ASE noise. The ASE noise adds random spectral noise to the passing pulses [Ref. 80].

The optical power experiment in Chapter IV shows an increase in low frequency jitter with increasing pump power, which can be attributed to the power supplies. However, ASE noise does dramatically increase when the erbium amplifier is pumped beyond saturation as shown in Chapter III. Techniques to reduce the ASE noise might improve the noise performance of the laser.

#### **D. OPTICAL AMPLIFIER**

The NRL sigma laser uses about five times more power than the NPS sigma laser. The advantage of this is that the higher power can take advantage of the nonlinear effects of the dispersion-compensating and dispersion-shifted fibers to further shorten the laser pulse and create soliton ( $\text{sech}^2$  shaped) pulses [Ref. 12]. The creation of solitons will most likely reduce amplitude and timing jitter in the laser since solitons are much narrower in pulsewidth and are less affected by the ASE noise.

#### **E. SYSTEM MODIFICATION**

It became apparent when creating the operator's manual for this laser that a computer can perform many of the same functions. Initially, a computer and digital acquisition board can replace the integrating amplifier. A program such as LABVIEW can perform the integration and provide the output using another computer port.



The signal generator used for actively mode-locking the system usually has a GPIB port for external control. The AC portion of the error signal from the microwave phase detector increases in amplitude as a pulse begins to form at the beginning of mode-locking. The quality of the mode-locked condition can also be determined from this AC error signal. The LABVIEW program could control the frequency on the signal generator until a pulse is formed and then take over with active feedback and voltage control of the PZT. The system could be programmed to initiate mode-locking on start up, reset the system if the temperature change over time has become too great, or even restart at another frequency if sampling conditions required it. A desktop PC would be the starting point of such a system and would be replaced by an embedded processor for mobile applications.

## **F. MINOR MODIFICATIONS**

Some minor modifications to the current laser configuration might be considered by follow-on users to increase stability and ease of operation. The fiber laser should be enclosed in plexi-glass on its four open sides to prevent changes in cavity length due to air currents and room temperature changes. This should be done after the cavity length optimization is completed. Although the feedback stabilization circuit can handle these changes, enclosing the fiber will reduce cavity length fluctuations and make the laser even more stable.

The integrator circuit can use some modification as well. The post-integrate offset knob is responsible for pre-loading the PZT with a certain amount of voltage. This gives the feedback circuit room to increase or reduce overall voltage on the PZT. The knob can also help in gross tuning the cavity length in an effort to find a resonant frequency. This knob is currently a single 5 k $\Omega$  potentiometer that can pre-load up to -1000 Vdc on the PZT. It should be replaced with a 10 turn potentiometer to improve manual cavity length adjustments and allow a finer pre-load setting.

## G. SUMMARY REMARKS

The results of Chapter IV show that this laser is capable of PRFs between 7 and 16 GHz, pulsewidths as low as 7.2 ps, amplitude jitter of less than 1%, and a temporal jitter of 386 femtoseconds. In addition, this laser can be harmonically mode-locked at twice the modulation frequency to a maximum PRF of 16 GHz. The results of Chapter V show that sampling using an amplitude-analyzing ADC is PRF limited to 8 GHz if using the Nyquist sampling rate. The amplitude jitter limits sampling to 9 bits of resolution and pulsewidth constrains sampling to 6.77 GHz at 8 bits or 4.78 GHz at 9 bits of resolution. However, the laser is currently limited by temporal jitter to sampling a 6.44 GHz signal at 7 bits, 3.22 GHz at 8 bits, or 1.61 GHz at 9 bits of resolution. The amplitude-analyzing ADC should be considered the worst-case example for optical sampling; other sampling techniques will reduce the stringent noise requirements and increase the capability of this laser.

The original goal of this Thesis was to build a laser that can be used in sampling a 5 GHz signal at 10 bits of resolution. Although this goal was not achieved, all is not lost. The Naval Postgraduate School now has a working mode-locked laser in which experimentation and further analysis can be done to shorten the pulsewidth and reduce noise in the output. In addition to construction and operation of the laser, the techniques for measuring pulsewidth and temporal jitter have been outlined in greater detail than the originators of the process. Finally, this laser can also be used in sampling applications within its the current limits. The sampling bandwidth of this laser has already exceeded that of commercially available ADCs.

This Thesis successfully describes the theory of mode-locked lasers, construction of a mode-locked laser for GHz performance, and accurate measurement of the laser output including the noise. The output performance is used to calculate the limits of optical sampling in an amplitude-analyzing ADC and recommendations for improvements are made. The Naval Postgraduate School now has a working mode-locked laser in which to pursue optical sampling for Joint Electronic Warfare purposes.

The signal generator used for actively mode-locking the system usually has a GPIB port for external control. The AC portion of the error signal from the microwave phase detector increases in amplitude as a pulse begins to form at the beginning of mode-locking. The quality of the mode-locked condition can also be determined from this AC error signal. The LABVIEW program could control the frequency on the signal generator until a pulse is formed and then take over with active feedback and voltage control of the PZT. The system could be programmed to initiate mode-locking on start up, reset the system if the temperature change over time has become too great, or even restart at another frequency if sampling conditions required it. A desktop PC would be the starting point of such a system and would be replaced by an embedded processor for mobile applications.

## **F. MINOR MODIFICATIONS**

Some minor modifications to the current laser configuration might be considered by follow-on users to increase stability and ease of operation. The fiber laser should be enclosed in plexi-glass on its four open sides to prevent changes in cavity length due to air currents and room temperature changes. This should be done after the cavity length optimization is completed. Although the feedback stabilization circuit can handle these changes, enclosing the fiber will reduce cavity length fluctuations and make the laser even more stable.

The integrator circuit can use some modification as well. The post-integrate offset knob is responsible for pre-loading the PZT with a certain amount of voltage. This gives the feedback circuit room to increase or reduce overall voltage on the PZT. The knob can also help in gross tuning the cavity length in an effort to find a resonant frequency. This knob is currently a single 5 k $\Omega$  potentiometer that can pre-load up to  $-1000$  Vdc on the PZT. It should be replaced with a 10 turn potentiometer to improve manual cavity length adjustments and allow a finer pre-load setting.

## G. SUMMARY REMARKS

The results of Chapter IV show that this laser is capable of PRFs between 7 and 16 GHz, pulsewidths as low as 7.2 ps, amplitude jitter of less than 1%, and a temporal jitter of 386 femtoseconds. In addition, this laser can be harmonically mode-locked at twice the modulation frequency to a maximum PRF of 16 GHz. The results of Chapter V show that sampling using an amplitude-analyzing ADC is PRF limited to 8 GHz if using the Nyquist sampling rate. The amplitude jitter limits sampling to 9 bits of resolution and pulsewidth constrains sampling to 6.77 GHz at 8 bits or 4.78 GHz at 9 bits of resolution. However, the laser is currently limited by temporal jitter to sampling a 6.44 GHz signal at 7 bits, 3.22 GHz at 8 bits, or 1.61 GHz at 9 bits of resolution. The amplitude-analyzing ADC should be considered the worst-case example for optical sampling; other sampling techniques will reduce the stringent noise requirements and increase the capability of this laser.

The original goal of this Thesis was to build a laser that can be used in sampling a 5 GHz signal at 10 bits of resolution. Although this goal was not achieved, all is not lost. The Naval Postgraduate School now has a working mode-locked laser in which experimentation and further analysis can be done to shorten the pulsewidth and reduce noise in the output. In addition to construction and operation of the laser, the techniques for measuring pulsewidth and temporal jitter have been outlined in greater detail than the originators of the process. Finally, this laser can also be used in sampling applications within its the current limits. The sampling bandwidth of this laser has already exceeded that of commercially available ADCs.

This Thesis successfully describes the theory of mode-locked lasers, construction of a mode-locked laser for GHz performance, and accurate measurement of the laser output including the noise. The output performance is used to calculate the limits of optical sampling in an amplitude-analyzing ADC and recommendations for improvements are made. The Naval Postgraduate School now has a working mode-locked laser in which to pursue optical sampling for Joint Electronic Warfare purposes.



## APPENDIX A. PARTS AND EQUIPMENT

### A. POLARIZATION MAINTAINING LOOP

- Signal Generator  
HP8350 B Sweep Oscillator or  
HP83731B Synthesized Signal Generator Short Term Demonstration Loan  
Hewlett Packard (650) 694-2439  
Replace with HP83711B or higher.
- Mach Zehnder Modulator  
Microwave Wideband Electro-Optic Modulator  
#MEOM-1550-MZ-10, on loan from NRL  
E-TEK Inc., this company no longer makes modulators, replace with a higher  
frequency Uniphase (UTP) or Lucent Technologies brand.
- Microwave Amplifier  
#AMF-5B-080180-80-25P, 8-18 GHz  
MITEQ (516) 436-7400 x339
- Power Supply, High Current Rating, for Microwave Amplifiers  
Model 3650S Regulating DC Power Supply, 5 A  
Power Designs Inc.  
(Quantity: 2)
- Power Supply for Modulator Bias Voltage  
Model 5005S Regulating DC Power Supply  
Power Designs Inc.
- Polarization Maintaining Fiber Coupler 20/80  
E-TEK #PMFC2 1 20 00 7 1 0 1  
Valley Scientific Instrument (408) 296-0383
- Singlemode Fiber Coupler 20/80  
E-TEK #SWBC 2120 (non PM)  
Valley Scientific Instrument (408) 296-0383
- Polarization Maintaining Isolator  
#PMFI52D111, Single Polarization, Dual Stage, 1550nm  
OPLINK (408) 433-0606, San Jose  
Order with specification of isolation on fast axis, slow axis passage.

- Polarization Beam Splitter  
JDS Fitel #PB100-3U-15-NC  
JDS Fitel (613) 727-1303  
Imported through Realm Communications (408) 295-7589
- Microwave Power Divider  
#1515, 0-18 GHz  
Weinschel Corp., (800) 542-4457

## **B. ERBIUM-DOPED FIBER AMPLIFIER**

- Erbium-Doped Fiber  
#F-EDF (Fibercore #DF1500A)  
Newport (800) 225-6440  
(Quantity: 32 meters)
- Wavelength Division Multiplexer  
#20 1A9815, 1x2, Grade A, 980/1550 nm  
Princeton Optics (609) 393-2424  
(Quantity: 2)
- Laser Diode  
#QLM9S470-910-980NM EDFA, Butterfly Package, 100 mW, 980 nm  
Lasertron (617) 280-3300  
(Quantity: 2)
- Laser Diode Mount  
LDM 4980 Series, # LDM4984, Butterfly Mount  
ILX Lightwave (406) 586-1244  
(Quantity: 2)
- Laser Diode Controller  
SDL-800, and cables  
Spectra Diode Labs (408) 943-9411  
(Quantity: 2)
- Laser Diode Thermoelectric Temperature Controller  
# LDT-5412, and cables  
ILX Lightwave (406) 586-1244  
(Quantity: 2)



## **C. PROPAGATION AND BIREFRINGENCE COMPENSATION BRANCH**

- Polarization Controllers  
#PLC-003 PolaRITE In-line  
General Photonics (909) 590-5473  
(Quantity: 2)
- Faraday Mirror  
#MFI-IR2  
Optics for Research (201) 228- 4480
- PZT Ceramic Cylinder, 2.25" long, 2.25" diameter, 0.135" thickness  
Lead Zirconate Titanate #C-5500 Thin-walled Cylinder  
Channel Industries (805) 967-0171
- Dispersion-shifted Fiber  
Corning SMF/DS CPC6 Singlemode Fiber  
Alcatel Telecommunications Cable, 100 m sample, (540) 265-0618  
Lucent Technologies, 1000 m sample, (510) 556-1438  
(Quantity: 80 meters)
- Dispersion-compensating Fiber  
Lucent DK-SM Single Mode Fiber  
Lucent (510) 556-1438  
Imported through Realm Communications, (408) 295-7589  
(Quantity: 1 meter)

## **D. FEEDBACK LENGTH STABILIZATION CIRCUIT**

- Phase Shifter (Tuning Stub)  
#2054-6102-00  
M/A-COM Inc., (508) 442-4373
- Microwave Limiting Amplifier  
#DWT-18636, 6-18 GHz  
DBS Microwave, (916) 939-7545  
(Quantity: 2)
- Phase Detector/Mixer  
#M80618 LS  
Marki Microwave (408) 379-2200  
Vendor: Realm Communications (408) 295-7589

- Infrared Detector for Stabilization Circuit  
#D-30ir-ST, 15 GHz  
Newport (800) 222-6440
- Operational Amplifier Integrated Chips  
MC34082  
Motorola Inc., samples, (602) 897-3820  
(Quantity: 5)
- Power Supply, Operational Amplifier Circuit  
Model 1300 DC Power Supply  
Global Specialties
- High Voltage Piezoelectric Amplifier  
PI Physik # E-461.OE1 HVPZT, one kilovolt  
Imported through Realm Communications (408) 295-7589

## **E. TEST EQUIPMENT**

- Autocorrelator  
FR103MN Rapid Scanning with Fiber Interface (FC Connector) and Computer Interface  
Femtochrome Research Inc., (510) 644-1869
- RF Spectrum Analyzer  
HP8566B Spectrum Analyzer or  
HP8563E Spectrum Analyzer Short Term Demonstration Loan  
Hewlett Packard (650) 694-2439  
Replace with HP8563E or higher.
- Infrared Detector for RF Analysis Purposes  
#D-15ir-ST, 29 GHz  
Newport (800) 222-6440
- Oscilloscope  
Any High Frequency Laboratory Oscilloscope  
(Quantity: 2)
- Digital Multimeter  
Fluke 8440A capable of one kilovolt for PZT monitoring  
Any digital multimeter for monitoring modulator bias voltage  
(Quantity: 2)

- Optical Spectrum Analyzer  
HP71450B Optical Spectrum Analyzer Short Term Demonstration Loan  
Hewlett Packard (650) 694-2439  
Replace with HP71450B or higher.
- DC Block  
Omni-Spectra #2047-6011-00  
T.T.I. (612) 933-8555

## **F. OTHER EQUIPMENT**

- Fiber Splicing Machine  
Sumitomo 11X Splicing Machine, SM fiber splicing only  
Sumitomo (919) 541-8100  
Fujikura FSM-20PM Splicing Machine, PM fiber splicing, NRL, Washington DC  
Vytran FFS-1000 Automated Filament Fusion Splicing Machine, ER Fiber Demo.  
Vytran (908)-2880  
Replace Sumitomo machine with Fujikura FSM-20PM splicing machine or better.

Note: Quantity of one assumed unless otherwise specified.



## APPENDIX B. CONFIGURATION AND OPERATION OF THE SIGMA LASER

### A. SIGMA LASER CONNECTIONS AND CONFIGURATION

There are three main systems to configure for the sigma laser: the feedback length stabilization circuit, the modulation circuit, and the control of the pump diodes. The measuring equipment, such as the autocorrelator and RF spectrum analyzer, require some setup as well. The Figures at the end of this section can be used as an aid in finding some connections; most connections will be obvious. Figure B.1 is an actual layout of the upper and lower levels of the laser. The lower level contains the fiber optic components and the upper level contains the microwave and other electronic components. Figure B.2 depicts the platform and connections for the laser diode mounts. This smaller platform actually rests on top of the laser.

#### 1. Feedback Length Stabilization Configuration

The feedback length stabilization circuit maintains active mode-locking and accounts for changes in room temperature.

##### *a. Integrating Amplifier Configuration*

The integrating amplifier can be powered by a Global Specialties Model 1300 Power Supply.

- Connect a red banana plug (BP) cable to the positive (+) terminal of channel A of the power supply.
- Connect a short black BP cable between the negative (–) terminal and the power supply common ground.
- Connect a long black BP cable to the common ground.
- Connect the two cables to digital multimeter and set +15 Vdc.
- Turn the power supply off and connect the red cable to the red +15V terminal on the integrating amplifier.

- Connect a yellow BP cable to the (–) terminal of channel B of the power supply.
- Connect a short black BP cable between the (+) terminal and ground.
- Connect the two cables to digital multimeter and set –15 Vdc.
- Turn off the power supply and connect the yellow cable to the yellow –15V terminal and the black cable to the “Ground” terminal on the integrating amplifier. Leave the power supply off.

An oscilloscope is used to monitor the microwave mixer error signal in channel two (CH2) and the integrated signal out in channel one (CH1).

- Connect a BNC-to-BP female adapter to CH2 of the oscilloscope.
- Connect a green BP cable from the green “Signal In” terminal on the integrating amplifier to the red terminal of the adapter on CH2.
- Connect a black BP cable from the ground terminal on the integrating amplifier to the black terminal of the adapter on CH2.
- Insert a BNC-to-BP male adapter into the back of the green and black cables on CH2 of the oscilloscope. Maintain polarity by aligning the two GND tabs on the sides of the BNC-to-BP adapters.
- Connect a BNC cable to the BNC-to-BP male adapter on CH2 and connect the other end to the Marki Microwave Mixer in the circuit on top of the laser using a SMA-female-to-BNC male adapter. The mixer is directly connected between two DBS Microwave limiting amplifiers.
- Connect a BNC-to-BP female adapter to CH1 of the oscilloscope.
- Connect a blue BP cable from the blue “Signal Out” terminal on the integrating amplifier to the red terminal of the adapter on CH1.
- Connect a short black BP cable from the black terminal of the adapter on CH1 to any ground terminal jack (hole in the top) of the adapters on CH2 of the oscilloscope.
- Insert a BNC-to-BP male adapter into the back of the blue and black cables on CH1 of the oscilloscope. Maintain polarity by aligning the two GND tabs on the sides of the BNC-to-BP adapters.
- Connect a BNC cable to the BNC-to-BP male adapter on CH1 and connect the other end to the “Signal In 0-5V” BNC terminal on top of the laser. This terminal is

located on the same circuit board as the silver PI Physik Instruments HVPZT amplifier.

- Tektronix 2336 Oscilloscope settings for integrator and mixer monitoring are:

Switch/Button/Knob	Setting
CH1 V/Div	1 V
CH1 AC-GND-DC	DC, set 0 V beam position at bottom of scope
CH2 V/Div	0.1 or 0.2 V
CH2 AC-GND-DC	AC, set 0 V beam position at center of scope
Sec/Div	0.05 microseconds
Vertical Mode	chop
Horiz. Mode	A
Trigger	neg. slope, auto
Coupling	AC
Source	CH2

***b. Microwave Limiting Amplifiers and High Voltage Piezoelectric Amplifier Configuration***

The DBS Microwave Limiting and PI Physik Instruments High Voltage Piezoelectric (PZT and HVPZT) amplifiers should be powered by a Power Designs Inc. Model 3650S Regulating DC Power Supply or equivalent due to high current requirements.

- Insert a BNC-to-BP male adapter into the “DC+” and “DC–” terminals on the power supply. Maintain polarity by aligning the ground tab with DC–.
- Connect a small black BP cable between the ground “G” terminal and the ground terminal jack (hole in the top) of the adapter.
- Connect a BNC cable to the adapter on the power supply and connect the other end to a digital multimeter.
- Settings for the Model 3650S Power Supply are:



Switch/Button/Knob	Setting
Current	max
Meter Function	V
AC	up for power on

- Set +12 Vdc using the multimeter and coarse and fine knobs on the power supply.
- Turn the power supply off and connect the BNC cable to the “DBS Amps and PI Physik HVPZT +12Vdc” BNC jack on the circuit board on top of the laser.

#### *c. Microwave Amplifier Setup*

The MITEQ Microwave amplifier should also be powered by a Power Designs Inc. Model 3650S Regulating DC Power Supply or equivalent due to a high current requirement. Setup is identical to that of the DBS Microwave and PI Physik Instruments HVPZT amplifiers above except:

- A voltage of +15 Vdc should be set using the multimeter.
- After setting +15 V, turn the power supply off and connect the BNC cable to the “MITEQ RF amp +15Vdc” BNC jack on the circuit board on top of the laser.

#### *d. Feedback Detector Setup*

The detector should already be connected to the DBS microwave amplifier using SMA connectors.

- Insert the ST connector of the shortest yellow fiber cable of the laser output into the Newport D-30ir Photodetector.

#### *e. Piezoelectric Cylinder Setup*

The piezoelectric cylinder is driven by high voltage from the PI Physik Instruments HVPZT amplifier and is monitored by a digital multimeter. A Fluke 8440A Digital Multimeter or equivalent should be used because it can accept and measure up to one kilovolt. **Warning**, the HVPZT amplifier produces high voltage up to –1000 Vdc.

- Ensure all power supplies are off before making any connections.
- Connect a BNC male to male adapter to the output cable of the HVPZT amplifier.
- Connect a BNC-T to the BNC male adapter.
- Connect a BNC cable from the BNC-T to the BNC jack next to the ceramic PZT in the laser.

**Warning,** be careful not touch any fiber on or around the PZT or the device itself. The PZT easily builds up electrostatic electricity and will most likely give you a mild shock. The fiber is easily damaged.

- Insert a BNC-to-BP male adapter into the multimeter “Hi” and “Low” terminals of the digital multimeter. Maintain polarity by aligning the ground tab with the low terminal.
- Connect a BNC cable from the BNC-T and to the adapter on the multimeter.
- Fluke 8440A Digital Multimeter settings are:

Switch/Button/Knob	Setting
Power	on
Input	front
VDC	pressed so that VDC listed in digital display
AUTO	pressed, AUTO listed in digital display

## 2. Mach-Zehnder Modulator Configuration

The optical modulator requires a DC bias voltage and a constant-wave RF signal for operation. The modulator is used for active mode-locking of the sigma laser.

### *a. Modulator Bias Voltage Setup*

The modulator is DC biased by a Power Designs Inc. Model 5005S Regulating DC Power Supply or equivalent and is monitored using any digital multimeter. The E-TEK modulator is gold in color and is located in the laser directly underneath MITEQ microwave amplifier.

- Insert a BNC-to-BP male adapter into the DC+ and DC– terminals on the power supply. Maintain polarity by aligning the ground tab with DC–. The ground terminal G is not used.
- Connect a BNC-T to the adapter.
- Connect a BNC cable between the BNC-T and the digital multimeter.
- Connect a BNC-male-to-SMC female adapter to the SMC male connection on the modulator.
- Settings for the Model 5005S Power Supply are:

Switch/Button/Knob	Setting
Range	0-50 mA
Current	10 mA
Meter Function	V
AC	on

- Set +14.45 Vdc on the multimeter using coarse and fine knobs on the power supply.
- Turn the power supply off and connect the BNC cable between the power supply and the modulator.

The +14.45 Vdc setting works well for normal operation. Different bias voltages can be used based on the experiment. If attempting harmonic mode-locking for a PRF of twice the modulation frequency, then 15.9 Vdc should be used as a starting point.

#### ***b. Modulator Microwave Modulation Signal Setup***

The laser light is modulated by a constant-wave (CW) signal from a HP8350B Sweep Oscillator (signal generator) or equivalent. A Weinschel Model 1550 Power Divider equally divides the microwave signal. The signal from one port of the power divider is used for modulation; the signal from the other port is used for feedback length stabilization. The MITEQ amplifier amplifies the modulation signal. The MITEQ amplifier should already be connected to the modulator by a SMA waveguide.

- Connect a BNC-to-SMA male adapter to the power divider if not already present.
- Connect a 6' RG-9U (green) cable to the output on the back of the signal generator.

- Connect an N-type male-to-BNC female adapter to the green cable and connect to the power divider.
- Settings for the HP8350B will be covered during laser operation.

### 3. Pump Diode Configuration

#### *a. Laser Diode Mounts*

The two “butterfly” packaged laser diodes within the ILX LDM-4980 laser diode mounts do not require configuration and should not be tampered with.

**Warning**, laser diodes are extremely sensitive to electrostatic shock. If the diodes must be removed, the cables should be removed and an electrostatic wrist strap must be connected to the mount and worn [Ref. 39]. Each diode mount is internally configured for use with the SDL 800 Laser Controller and ILX LDT-5412 Temperature Controller. Use of any other equipment requires verification of laser pin out and cable connections as per the manufacturers’ instructions.

#### *b. Pump Diode Temperature Controller Setup*

Two ILX LDT-5412 Temperature Controllers are used for laser diode cooling [Ref. 81].

- Connect the 9 pin female cable coming out of the back of the temperature controller to the 9 pin male connector on the ILX LDM 4980 diode mount.
- Connect a temperature controller to each of the two mounts.
- Rear settings for the temperature controllers are:

Switch/Button/Knob	Setting
Set Resistance	int
Thermistor Current	100 mA

### *c. Pump Diode Laser Controller Setup*

Two SDL 800 Laser Diode Controllers are used for laser diode current control [Ref. 77].

- Connect the round 7 pin male cable to the front “Laser Head.”
- Connect the 9 pin male connector on the cable to the 9 pin female connector on the ILX LDM 4980 diode mount. The 9 pin female connector on the cable will remain unconnected.
- Connect a diode controller to each laser diode mount.
- Settings for back of the diode controllers are:

Switch/Button/Knob	Setting
Remote Interlock Plug	inserted
TE Cooler	external

## **4. Measurement Equipment Setup**

### *a. Femtochrome FR103MN Autocorrelator Setup*

The autocorrelator and associated oscilloscope are used to monitor pulse formation and to aid in mode-locking the laser. The machine is configured for computer acquisition as well as pulse presentation on an oscilloscope. The autocorrelator software should already be installed in the “C:\Femto” directory on the computer [Ref. 64].

- Connect a BNC cable from “SIG.” on back of autocorrelator to CH1 of oscilloscope.
- Connect a BNC cable from “TRIG.” on back of autocorrelator to CH4 of oscilloscope.
- Connect a 9 pin serial cable from back of autocorrelator to the 24 pin serial port (com2) on the computer using a 9-to-24 pin adapter.
- **Warning**, remove the beam splitter plastic slipcover and second harmonic generation (SHG) crystal cover with desiccant (pink rocks) from inside of the autocorrelator. Autocorrelator should be turned off when removing the cover.

- The unmarked black knobs on the side are for internal mirror alignment and should be left in their current settings. Refer to operator's manual for adjustment.

The autocorrelator is tuned to the FC fiber cable connector presently attached to the machine. Use of another connector will require calibration and is discouraged unless necessary.

- Settings for the autocorrelator are:

Switch/Button/Knob	Setting
Slide Switch (on rear of unit)	1ps
Gain	full clockwise to start
Delay	pointed at delay on/off button (unmarked)
Front Micrometer (SGH Crystal)	0.401" (+1/2 tic mark)
Side Micrometer (90 deg. Mirrors)	0.1168" (+1/2 tic mark)

An oscilloscope attached to the autocorrelator is required for initial operation of the sigma laser. Most laboratory oscilloscopes will do except for digital sampling oscilloscopes.

- Settings for a Tektronix 2247A Oscilloscope for autocorrelator pulse output are:

Switch/Button/Knob	Setting
Vertical Mode	CH1
CH1 V/Div	0.1 to 0.5 V, 0.1V initially
CH1 Coupling	DC, set 0 V beam position at bottom of scope
CH4 V/Div	0.1 V
Sec/Div	1 to 2 ms, 2 ms initially
Horiz. Mode	A
Trigger	pos. slope, A select, norm,
Source	CH4
Coupling	noise rej.
Measurements (Cursors)	time, seconds for measuring pulsewidth

### ***b. RF Spectrum Analyzer***

The RF spectrum analyzer is a common laboratory device so its operation will not be discussed here. However detector use, GPIB connections, and Labview will be covered.

(1) Detector Use. Signal input is accomplished through a Newport D-15ir detector through a DC block. The detector is battery powered by two “3 V 2/3A-size” batteries available at any electronics store. If the “low” light flashes the batteries need to be replaced. Alternatively, if the device is left on while not in use, the batteries will discharge [Ref. 72]. **Warning**, many RF spectrum analyzers are sensitive to DC voltage from an input signal and can be damaged. This detector generates about 10 mV of DC voltage in its output signal. A DC block should be used to prevent damage to the spectrum analyzer.

- Connect a SMA male-to-N-type female adapter to the input of the Spectrum Analyzer.
- Connect 50  $\Omega$  terminator to the DC side of a DC block such as an Omni-Spectra part #2047-6011-00.
- Connect the male SMA connector on the DC block to the female SMA connector on the detector.
- Connect detector and DC block to the SMA terminal on the input to the spectrum analyzer.

When taking measurements, turn the detector on prior to inserting the laser output into the detector ST connector. This produces the best-detected signal for measurement.

(2) General Purpose Interface Bus Connections. The spectrum analyzer can be controlled and RF frequency and amplitude data obtained by a computer using the general-purpose interface bus (GPIB). The computer must have a GPIB card installed.

- Connect a GPIB cable between the back of the analyzer and the computer.



(3) Labview Software. The laboratory computer is loaded with Labview 4.0 software. Jeff Knight, a NPS laboratory engineer, created a Labview program to extract amplitude and frequency data from an RF spectrum analyzer, display the spectrum on the computer screen, and save the data to a text file. There are two programs in the “E:\Vi\Moose.llb” Labview library. The program “Moose.vi” is used for the HP8566B analyzer and the program “MooseII.vi” is used for a HP8563E analyzer. The program is written for a GPIB address of 16, so the start up spectrum analyzer address may have to be changed. The HP8566B generates 1000 points of data and the HP8563E generates 600 points. In each case, the data can be save to a text file. This program requires that data be saved to “C:\Data\{filename}”. This program was written to save frequency data of less than 2 GHz; any frequency higher than that must be separately recorded and regenerated in Matlab. To hand record the frequency data, center the signal on the analyzer display using the “peak search” and “center marker” buttons. Record the center frequency and the analyzer frequency span. These two values can be used to regenerate the frequency data in MATLAB or any other mathematical program. The data in the text file should double checked before moving on to other measurements. It is best to center the signal of interest on the analyzer and then record the frequency span and the center frequency. The program display does not automatically update the x-axis on the screen. These can be manually entered on the bottom of the Labview graph to show the signal.

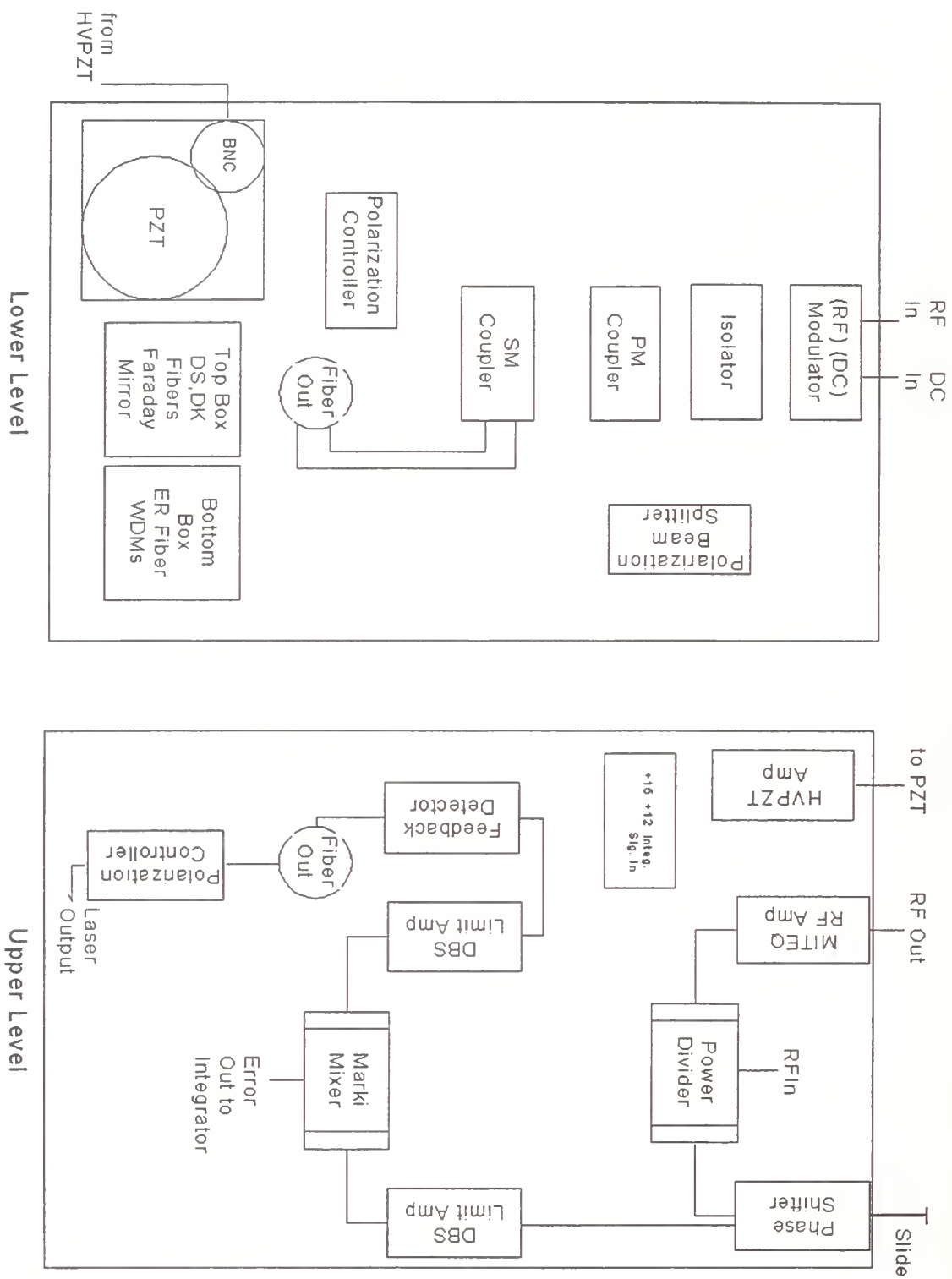
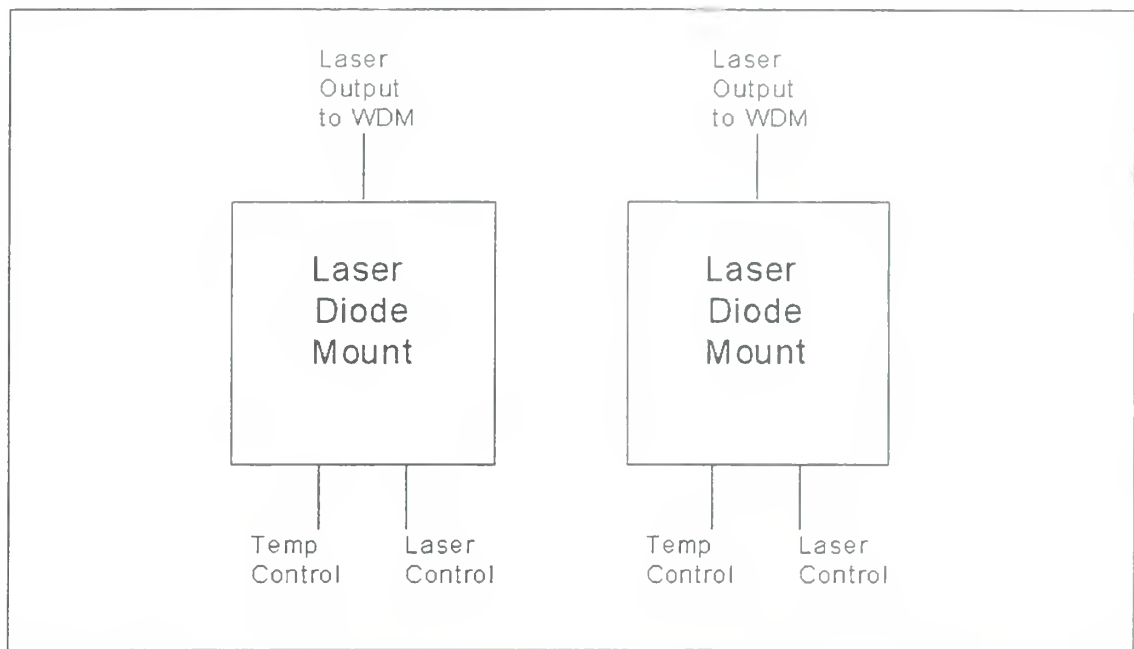


Figure B.1. Layout and connections of NPS sigma laser.



**Laser Diode Mount Platform**

Figure B.2. Layout and connections for NPS sigma laser pump diodes.

## B. SIGMA LASER OPERATION

There are seven basic steps to operation of the sigma laser. In order, they include the pump diode temperature control, pump diode current control, polarization control, modulation, setup of the autocorrelator, mode-locking, and feedback control. The laser output pigtails should be connected to the autocorrelator and the feedback detector. The longest pigtail should be connected to the autocorrelator through an ST/ST fiber connector. A second cable connects the laser output to the device using a FC connector. If the autocorrelator cover is to be removed during laser operation, or the laser output pigtail is moved to another device, then the Kentek “Near IR and CO<sub>2</sub>” # SES-BW laser safety spectacles must be worn for safety purposes. **Warning**, the sigma laser is a pulsed laser with invisible output at 1560 nm. It can damage the eye.

### 1. Pump Diode Temperature Controller Operation

**Warning**, without proper cooling, the laser diodes will overheat and fail permanently. The green light indicating temperature controller output is in a position where it is difficult to see. This light should be triple checked before turning the SDL 800 laser diode controller pump current on.

- Front settings for the temperature controllers are as follows:

Switch/Button/Knob	Setting
Power	on
Limit	1.5
Set R	10.00 K $\Omega$ using large control knob.

After turning the power on, if the “Open Therm” remains on, double-check the cable connections. If it still remains on, turn the unit off and seek assistance.

- Switch the “Display Mode” to “Actual R” and read the resistance on the LED display.
- Press “Output” to start cooling, the LED should change to 10.00 K $\Omega$ . The green output light under the large knob should come on.
- Verify that the “Display Mode” is set to “Actual Current,” the LED display reads 10.00 K $\Omega$ , and the output light is on.

The temperature controllers tend to drift during operation and may be adjusted back to 10.00 k $\Omega$  while in operation. During the start of cooling, the “Limit” indicator may flash briefly; however, if it stays on, turn the output off and seek assistance.

## 2. Pump Diode Laser Controller Operation

**Warning,** turning on the laser output with “Average Current” other than zero will probably ruin the laser diode. The highlighted LEDs next to the selection options are easily misread as to which option is selected. Furthermore, the selection buttons are sticky and may click down to another selection inadvertently. The “laser on” button often sticks and the device will let the user turn the current up to the desired level while in setup mode without any other warning. If this occurs, turn the current down and then turn the laser on. The user should double check that the highlighted LED is next to “Average Current” and that 0 mA is set prior to pumping current through the laser diode.

- The SDL 800 laser controller operational settings are:

Switch/Button/Knob	Setting
Power	On using key switch; the device turns on in the setup mode.
Current Limit	191 mA using current limit knob
Average Current	0 mA using bias level knob. Select this control option using the buttons outside of the indicating arrows, the appropriate LED will be lighted.
Setpoint Temp.	unused
Det. Cal.”	unused

- Verify that the laser diode controller “Average Current” is 0 mA.

**Warning,** laser light not contained in fiber or equipment can be an eye hazard.

- Verify that the laser output pigtailed are connected to the feedback detector and the autocorrelator.
- Push the button next to “Laser” to switch from “Setup” to “On.”

The setup LED will flash for about 5 seconds and then the device will turn the laser diodes on. If the controller turns on the “Error” light instead of the “On” light, turn the controller off by the key, double check all cable connections and try again. If the error light comes on again, turn the controller off and seek assistance.

- Verify that the temperature controller green output lights are lit and the “Actual R” on both controllers is 10 k $\Omega$ .
- Slowly turn the bias control knob until the display reads 15 mA and then turn the current up at a reasonable rate until 180 mA is attained.

At 180 mA, each diode pumps 100 mW of 980 nm laser light into the erbium-doped fiber in the laser. **Warning**, operating the laser diodes at greater than 210 mA of drive current will shorten the life of the diode. Operating the diode greater than 265 mA will damage the diode permanently [Ref. 39]. The error light will flash if drive current is within 10 mA of the current limit [Ref. 77]. If this occurs, double check that the current limit is set at 191 mA. If the error light comes on while turning the current up, seek assistance. This is a sign that the laser diode has failed. The resistance displayed on the temperature controllers will drop slightly by a few tenths of a k $\Omega$  while turning the current up on the diodes. If the resistance does not return to the set point within a few seconds or the resistance continues to drop, turn the laser controller current down to zero and seek assistance.

### 3. Polarization Controller Operation

The polarization controller fine-tunes the laser light polarization for alignment with the polarization-maintaining fiber on the beam splitter.

- The polarization controller (PC) on the lower platform is adjusted as follows:
- After donning the laser safety spectacles, remove the FC connector from the autocorrelator and connect it to the ILX Optical Multimeter.

**Warning**, the fiber passing through the PC is fragile and easily broken at the insertion and exit points.

- Monitor the power from the laser while slowly rotating the PC. Rotate the PC until the power is maximized.

Once set, the PC should not require any adjustments unless the cavity fiber is manipulated or changed.

#### 4. Modulation

##### *a. DC Bias Voltage*

A modulator bias voltage of +14.45 Vdc works well for normal operation. Different bias voltages can be used based for experimentation. If attempting to harmonically mode-lock the laser to attain a PRF of twice the modulation, then +15.9 Vdc should be used as a starting point. A digital multimeter should be used to monitor the DC power supply voltage.

**Warning**, a bias voltage of higher than 20 Vdc may ruin the E-TEK modulator; do not exceed this voltage or the sigma laser will be remain inoperable until a new modulator is spliced into the laser cavity. This splicing requires a PM fiber splicing machine; NPS currently does not own a PM splicer.

- Turn on the attached digital multimeter and the Model 5005S DC power supply. Verify +14.45 Vdc.

##### *b. Signal Generator*

**Warning**, a maximum RF voltage rating is unavailable from the manufacturer, a maximum of 7 volts should be observed. The attached microwave amplifier will not produce more than 400 mV. Ideally, the HP8350B Sweep Oscillator should be turned on without transmitting a signal for a few hours prior to operation. This reduces frequency drift in this type of signal generator. The modulation frequency of 10.1 GHz is a good starting point but values between 7 and 15 GHz have successfully been used.

- HP8350B Sweep Oscillator settings are:



Switch/Button/Knob	Setting
Line Power	on
Frequency	depress CW
Keypad	type in “10.1 GHz”
Sweep Trigger	int
Frequency/Time	off
Sweep	time
Power	depress Power Level
Keypad	type in “15.5 dBm”
ALC Mode	int
RF	on
CW Filter	on

The unlevelled light should be extinguished at this point. If not, try turning the generator off and then on. The signal generator is power limited at higher frequencies. The light might also be extinguished by reducing the power level. If this does not work, seek assistance from the microwave lab.

#### *a. MITEQ Microwave Amplifier Operation*

- Turn on the MITEQ amplifier by turning on the Model 3650S power supply that was previously set for +15Vdc.

The Model 3650S power supply set for +12 Vdc and Model 1300 amplifier for the integrating amplifier should remain off.

### **5. Autocorrelator Operation**

The laser is mode-locked while watching for pulse formation on the oscilloscope next to the autocorrelator. The laboratory overhead lights directly above the autocorrelator must be turned off because they interfere with the highly sensitive photomultiplier tube inside the device even with the lid on.

- The attached oscilloscope settings are:

Switch/Button/Knob	Setting
Power	on
CH1 V/Div	0.1 V initially
Sec/Div	2 ms initially

- Turn the autocorrelator on using the unmarked switch; the green light directly above it will come on.
- Rotate the laser output polarization controller (PC) on top of the laser until a pedestal of noise appears on the left side of the scope. Maximize the pedestal using the PC.

The FC connector cable attached to the autocorrelator occasionally interferes with the polarization control. If the PC appears ineffective, carefully rotate the yellow output cable until the maximum pedestal of noise appears. Further maximize the pedestal using the PC.

- Change the oscilloscope Sec/Div to 1 ms.

## 6. Integrating Amplifier Pre-Operational Setup

- Leave the Model 1300 power supply off.
- Settings for the integrating amplifier are as follows:

Switch/Button/Knob	Setting
Proportional AC Gain	12 o'clock
Post-Integrate Offset	12 o'clock
Time Constant	100 ms
Pre-Integrate Offset	4.5 turns clockwise from the full-stop counter-clockwise position

The Pre-Integrate Offset knob is a 10-turn variable resistor. To set the Pre-Integrate Offset, rotate the knob counter clockwise continually until it reaches the full-stop position. Turn the knob clockwise 4.5 turns. This is the initial starting point for integrating the signal.

- Turn on the oscilloscope connected to the mixer and integrating amplifier output. This oscilloscope will be used to setup the feedback length stabilization.

- Turn on the feedback detector on top of the laser.
- Turn on the digital multimeter monitoring the PZT voltage.

## 7. Mode-locking

### *a. Mode-Locking Technique*

The technique to initiate mode-locking is relatively simple and consists of finding a frequency that matches a multiple of the cavity rate.

- Slowly adjust the frequency knob above the CW button on the signal generator while watching for pulse formation on the oscilloscope next to the autocorrelator. As the mode-locked pulse grows in amplitude, it will be necessary to increase CH1 V/Div on the oscilloscope to 0.2 and 0.5 V/Div.
- When a pulse begins to form, slowly change the frequency up and down until the pulse is maximized.
- Press the vernier button next to the frequency knob to initiate fine tuning of the modulation frequency in the MHz range.
- Slowly adjust the knob in the low frequency mode up and down until the pulse is maximized.

The laser is now actively mode-locked but unstable due to slight variations in room temperature.

### *b. Feedback*

Configuring the feedback to maintain mode-locking is more difficult due to the number of adjustments that have to be coordinated. The technique listed below works well with the equipment on hand but requires some patience and practice.

- Continually hold the reset button on the integrating amplifier while turning on the feedback system power supplies, the Model 3650S power supply set for +12 Vdc and Model 1300 amplifier set for  $\pm 15$  Vdc.

- Keep the reset button depressed.
- Lightly adjust the Post-Integrate Offset knob on the integrating amplifier until the digital multimeter that reads the voltage on the PZT reaches approximately  $-200$  Vdc.
- If the mode-locked pulse disappears, adjust the frequency knob until it re-appears and is maximized while holding the reset button in. The pulse will often disappear or drastically increase in amplitude at this point.
- Adjust the trombone slide on the MA/COM phase shifter while watching the CH2 signal on the oscilloscope. Use the slide to center the signal at zero or slightly below zero volts. The amplitude of this signal will often increase when the mode-locked condition improves and the pulse amplitude increases.

Note: if the slide will not center the signal near zero but stays high or low, the system cannot be easily set up for this frequency. Turn off the feedback power supplies and find a pulse at another frequency, possibly 500 MHz or more in either direction.

- Release the reset button and watch the integrated signal on CH1. If it significantly climbs in voltage, press and hold the reset button and turn the Pre-Integrate Offset knob half a turn in the counter-clockwise direction. If it significantly drops in voltage, press and hold the reset button and turn the Pre-Integrate Offset knob half a turn in the clockwise direction.

This is an iterative process, holding reset, adjusting pre-integration up or down, releasing and adjusting again. This technique will take some practice. Occasionally the frequency and shifter slide will have to be readjusted as well.

- When the CH1 signal is stable, let the feedback system operate for a while watching the digital multimeter that monitors the PZT voltage. The PZT voltage should drift up and down a few volts at a time.
- If the voltage is climbing slowly and doesn't reverse direction or the voltage fluctuates but climbs on average over a minute or so, turn the pre-integrate offset a quarter turn counter-clockwise. The reset button should not be depressed. If the voltage is dropping slowly and does not reverse direction or the voltage fluctuates but drops on average over a minute or so, turn the pre-integrate offset a quarter turn or less clockwise. This is also an iterative process that takes practice.

- Final phase adjustment and pulse shaping is accomplished using the Proportional AC Gain knob.
- If the PZT voltage is still climbing slowly, adjust the knob counter-clockwise up to half a turn. If it is dropping, adjust clockwise.
- If the laser pulse has a rough shape, it may be smoothed to a Gaussian appearance by adjusting the Proportional AC Gain.

When mode-locking is stable, the PZT voltage will drift up and down a hundred volts or more over a period of hours. This laser can maintain a mode-locked condition for up to six hours or more. When the laser loses lock, the PZT voltage will peak to almost –1000 volts or drop to near zero. If mode-locking is lost, re-initiate by turn off the feedback power supplies, let the PZT voltage drop to zero, and start over by finding a pulse while adjusting the frequency.

## **8. Autocorrelator Software**

The laser pulsewidth can be measured using an oscilloscope. This measurement is in milliseconds and a series of calculations must be made using the formulas in the operator's manual. The best analysis is accomplished by using the Femtochrome software on the computer.

- Double click on the MS-DOS icon or open an MS-DOS window from the Windows 95 start menu. The program executable is "C:\Femto\FR\_CDA." Alternatively, there are batch (bat) files in the default MS-DOS "C:\Windows" and the "C:\Femto" directories.
- Type the word "femto" and the program will start.
- During program initialization, type "2" for COM2 and type "0" for rapid scan.
- When instructed, press the reset button on the back of the autocorrelator next to the wall power connection.

The delay knob on the autocorrelator is useful for centering the pulse on the computer screen.

- Press the black button next to the delay knob and turn the delay knob so the pulse is centered about the third time division from the left on the oscilloscope screen. This

will nearly center the pulse on the computer. The delay can be further adjusted as necessary.

The software program is not set up to print directly to printer due to a mismatch in MS-DOS programming and the advanced printers used in the lab. The program will print the plot to a graphics file or will print the numerical data to text file. Any graphics program can display and print the graphics file and any math program can plot the numerical data [Ref. 64].

## 9. Turning Off the Sigma Laser

The order for securing the sigma laser is important. Most importantly the temperature controllers must remain on until the drive current through the diodes is reduced to zero.

- Hold the integrator reset button while turning off the feedback power supplies.
- Turn off the bias voltage and +15 Vdc power supplies.
- On the signal generator, turn off the RF button; the yellow light will be out.
- Turn off the signal generator.
- Turn the current down to zero on both laser diode controllers and switch the laser controller to setup.
- Turn off the laser diode controllers using the keys.
- Turn off the output to the temperature controllers; the resistance should change. If the resistance drops significantly to 9 k $\Omega$ s or less, turn the output back on and let the diodes cool for a while.
- Turn the temperature controllers, autocorrelator, oscilloscopes, and multimeters off.
- Turn the feedback detector off using the button on top. **Warning**, the microwave amplifiers nearby will be hot. Check that the “Power On” light is extinguished. If the detector is left on, the batteries will need to be replaced next time the laser is to be operated.





## LIST OF REFERENCES

- [1] Phillip Pace, "Introduction to High-Performance Signal Converters for Information Operations Performance, Analysis, and Design," EC4700 Course Notes, pp. 43-251, Naval Postgraduate School, Monterey, CA, 1997.
- [2] William D. Stanley, *Electronic Communications Systems*, Reston Publishing Co. (Preston Hall), pp. 262-269, 1982.
- [3] Phillip Pace and David Styer, "High-Resolution Encoding Process for an Integrated Optical Analog to Digital Converter," *Optical Engineering*, vol. 33, no. 8, pp. 2638-2644, 1994.
- [4] Micro Networks Corporation, *Data Conversion Frequency Control Specialty Products Shortform Catalog*, pp. 3, Worcester, MA, 1997.
- [5] Paul Gray, "High-Speed CMOS A/D Converters," Short Course Slides, University of California, Berkeley, pp. 13, Berkeley, CA, 1995.
- [6] Henry F. Taylor, "An Optical Analog to Digital Converter – Design and Analysis," *IEEE Journal of Quantum Electronics*, vol. 15, no. 4, pp. 210-216, 1979.
- [7] K. V. Reddy, Ultrafast Optical Clock, Specification Sheet, PriTel, Inc., Naperville, IL, 1998.
- [8] J. P., "Supplementary Notes on Optical Modulators," EC4210 Course Notes, Naval Postgraduate School, Monterey, CA, pp.1-2, 1998.
- [9] UTP Electro-optics Products Division, *Catalog of Integrated Optical Circuits*, Bloomfield, CT, pp. 13, 1997.
- [10] S. A. Hamilton, D. R. Yankelevich, A. Knoesen, R. A. Hill, R. T. Weverka, and B. C. Bjorklund, "Ultrawide Bandwidth, Large Dynamic Range Fiber Electro-optic Modulator," *Proceedings of Eighth Annual DARPA Symposium on Photonic Systems for Antenna Applications*, 1998.
- [11] Phillip E. Pace and John P. Powers, "Photonic Sampling of RF and Microwave Signals," *Technical Report*, Naval Postgraduate School, Monterey, CA, 1986.
- [12] Thomas F. Carruthers and Irl. N. Duling III, "10-GHz, 1.3-ps erbium fiber laser employing soliton pulse shortening," *Optics Letters*, vol. 21, no.23, pp. 1927-1929, 1996.
- [13] Anthony E. Siegman, *Lasers*, University Science Books, Palo Alto, CA, 1986.

- [14] John Powers, "An Introduction to Electro-Optic Systems," EC3210 Course Notes, Naval Postgraduate School, Monterey, California, pp.166, 1997.
- [15] Jeff Hecht, *The Laser Guidebook*, McGraw-Hill Inc. New York, 1986.
- [16] Jean-Claude Diels, Wolfgang Rudolph, *Ultrashort Laser Pulse Phenomena*, Academic Press Inc. San Diego, CA, pp. 209-391, 1996.
- [17] Thomas F. Carruthers, "Solitons in Ultrafast Fiber Lasers," Briefing, *Conference on Lasers and Electro-Optics*, 1996.
- [18] Ference Krausz, Martin E. Fermann, Thomas Brabec, Peter F. Curley, Martin Hofer, Manfred H. Ober, Christian Spielmann, Ernst Wintner, and A. J. Schmidt, "Femtosecond Solid-State Lasers," *IEEE Journal of Quantum Electronics*, vol. 28, no. 10, pp. 2097-2122, 1992.
- [19] Thomas F. Carruthers, Phone Conversations Regarding Published Papers, May 1998.
- [20] John Powers, *An Introduction to Fiber Optic Systems*, 2<sup>nd</sup> edition, McGraw-Hill WBC (formerly Richard D. Irwin, Inc.), Chicago, IL, 1997.
- [21] William T. Silfvast, *Laser Fundamentals*, Cambridge University Press, NY, pp. 368-381, 1996.
- [22] William Stallings, *Data and Computer Communications*, Prentice Hall, Upper Saddle River, NJ, pp. 84, 1997.
- [23] W. Sibbett, "Some Advances in Self Mode-Locked Lasers," *Mode-Locked and Solid State Lasers, Amplifiers, and Applications*, SPIE, vol. 2041, pp. 3-6, 1993.
- [24] Lightwave Electronics Corp., "Introduction to Diode-Pumped Solid-State Lasers," Mountain View, CA, 1993.
- [25] Roger G. M. P. Koumans and Ramond van Roijen, "Theory for Passive Mode-Locking in Semiconductor Laser Structures Including the Effects of Self-Phase Modulation, Dispersion, and Pulse Collisions," *IEEE Journal of Quantum Electronics*, vol. 32, no. 3, pp. 478-492, 1996.
- [26] Inho Kim and Kam Yin Lau, "Frequency and Timing Stability of Mode-Locked Semiconductor Lasers – Passive and Active Mode Locking up to Millimeter Wave Frequencies," *IEEE Journal of Quantum Electronics*, vol. 29, no. 4, pp. 1081-1090, 1993.
- [27] OKI R&D Group, "Terahertz Optical Short Pulse Generation from Monolithic Mode-Locked Laser Diodes," Internet Home Page, (<http://www.oki.co.jp/OKI/RDG/English/kikaku/vol.2/kawai/main.html>), OKI Electronic Industry Co., Ltd, 1996.

- [28] E. Yoshida and M. Nakazawa, "80-200 GHz Erbium Doped Fibre Laser Using Rational Harmonic Mode-Locking Techniques," *Electronics Letters*, vol. 32, no. 15, pp. 1370-1372, 1996.
- [29] I. N. Duling III, C. -J. Chen, P. K. A. Wai, and C. R. Menyuk, "Operation of a Nonlinear-loop-mirror in a Laser Cavity," *IEEE Journal of Quantum Electronics*, vol. 30, no. 1, pp. 194-199, 1994.
- [30] Thomas F. Carruthers and I. N. Dulling III, "A High-Repetition Rate Ultrafast Fiber Laser for Fiber-Optic Communications Systems," *Technical Report*, Naval Research Laboratory, Washington D.C., 1996.
- [31] B. P. Singh, K. Ieda, R. Nomura, M. Mori, T. Goto, "Performance Characterization of Amplitude Modulated Harmonically Mode-Locked  $\text{Er}^{3+}$  Doped Fiber Ring Laser," *IEEE Instrumentation and Measurement Technology Conference*, Brussels, pp. 144-149, 1996.
- [32] E. Yoshida, Y. Kimura, and M. Nakazawa, "20 GHz, 1.8 ps pulse generation from a regeneratively modelocked erbium-doped fibre laser and its femtosecond pulse compression," *Electronics Letters*, vol. 31, no. 5, pp. 377-378, 1995.
- [33] R. Fontana, G. Grasso, N. Manfredini, M. Romagnoli, and B. Daino, "Generation of Sequences of Ultrashort Pulses in Erbium Doped Fibre Single Ring Lasers," *Electronics Letters*, vol. 28, no.14, pp. 1291-1293, 1992.
- [34] Ursula Keller, Kathryn D. Li, Mark Rodwell, and David M. Bloom, "Noise Characterization of Femtosecond Fiber Raman Soliton Lasers," *IEEE Journal of Quantum Electronics*, vol. 25, no. 3, pp. 280-288, 1989.
- [35] H. Ammann, W. Hodel, H. P. Weber, C. Holtmann, and H. Melchior, "Passive mode-locking of 1.3  $\mu\text{m}$  semiconductor laser amplifier in loop mirror configuration," *Electronics Letters*, vol. 31, no. 15, pp. 1257-1258, 1995.
- [36] Optics and Instrumentation Department, "Optics Glossary," Internet Web Site, (<http://www.om.tu-harburg.de/re/glossary.htm> ), Technical University Hamburg Harburg, Denmark, 1997.
- [37] Wave Optics, *Specialty Fiber Optic Products Catalog*, Mountain View, CA, 1997.
- [38] Optics for Research, *Fiber-Optic Products*, Caldwell, NJ, 1997.
- [39] Lasertron, *1996/97 Product Guide*, Burlington, MA, pp. 29-71, 1996.
- [40] Corning, Inc., SMF/DS CPC6 Singlemode Dispersion-Shifted Optical Fiber, Specification Sheet, Corning, NY, 1995.

- [41] Lucent Technologies, DK-SM Dispersion-compensating Fiber, *Specification Sheet*, Denmark, 1997.
- [42] Newport, Inc., Product Catalog, Irvine, CA, pp. 4-2, 1997.
- [43] D.S. Gasper, P.F. Wysocki, W.A. Reed, and A.M. Vengsarkar, "Evaluation of Chromatic Dispersion in Erbium-Doped Fibers," *IEEE Lasers and Electro-Optics Society (LEOS) Conference Proceedings*, pp. 167-168, 1993.
- [44] Preston Buck, Corning Fiber Technical Representative, Phone Conversation Regarding Corning Fiber, August, 1997.
- [45] Sumitomo Electric, Ltd., *Instruction Manual for Optical Fiber Fusion Slicing Kit Type 11X*, Research Triangle Park, NC, 1985.
- [46] JDS Fitel, Polarization Beam Splitter, Specification Sheet, Nepean, Ontario, Can., 1997.
- [47] OPLINK Communications, Inc., Polarization Maintaining Fiber Isolator, Specification Sheet, San Jose, CA, 1997.
- [48] E-TEK Dynamics, Inc., Product Catalog, San Jose, CA, 1997.
- [49] E-TEK Dynamics, Inc., *Operating Instructions Microwave Wideband Electro-Optic Modulator Instructions*, San Jose, CA, 1993.
- [50] Rod C. Alferness, "Waveguide Electrooptic Modulators," *IEEE Transactions on Microwave Theory and Techniques*, vol. 30, no. 8, pp.1121-1137, 1982.
- [51] Integrated Optical Components Ltd., *Introduction to Modulators*, Essex, UK, 1996.
- [52] MITEQ Inc., Amplifier Model AMF-5B-080180-80-25P, Specification Sheet, Hauppauge, NY, 1995.
- [53] Hewlett Packard Co., *HP8370 Series Synthesized Sources*, Palo Alto, CA, 1995.
- [54] D. Foursa, P. Emplit, R. Leners, and L. Meuleman, "18 GHz from a  $\sigma$ -cavity er-fibre laser with dispersion management and rational harmonic active-mode-locking," *Electronics Letters*, vol. 33, no. 6, 1997.
- [55] Eric J. Lerner, "Fiber Amplifiers Expand Network Capacities," *Laser Focus World*, PennWell Publishing Co., vol.5, no. 9, pp. 85-95, 1997.
- [56] Stephen Grubb, "Fiber Amps and Lasers Get Down to Earth," *IEEE Circuits and Devices Magazine*, vol.11, iss. 2, pp. 37-41.

- [57] Jay R. Simpson, "1.55  $\mu\text{m}$  Erbium-Doped Fiber Amplifier," *IEEE Lasers and Electro-Optics Society 1995 Annual Meeting Conference Proceedings*, vol. 2, pp. 65-66, 1995.
- [58] X. Shan, D. Cleland, and A. Ellis, "Stabilizing Er fiber soliton laser with pulse phase locking," *Electronics Letters*, vol. 28, no. 2, pp. 182-183, 1992.
- [59] William D. Stanley, *Linear Operational Amplifier Circuits*, 3<sup>rd</sup> edition, Prentice Hall, Englewood Cliffs, NJ, pp. 73-262, 1994.
- [60] Sherif Michael, "Advanced Electronics Engineering," EC3200 Course Notes, Naval Postgraduate School, Monterey, CA, pp. 8, 1997.
- [61] Channel Industries, Inc., "Piezoelectric Ceramics," Product Guide, Santa Barbara, CA, 1984.
- [62] John Powers, "EC3550 Laboratory Experiments", EC3550 Course Notes, Naval Postgraduate School, Monterey, CA, 1995.
- [63] John Watkins, "Integrated Naval Post Graduate School Government Broadcast System Test Bed," Master's Thesis, Naval Postgraduate School, Monterey, CA, 1997.
- [64] Z. A. Yasa, *FR-103MN Autocorrelator Instruction Manual*, Femtochrome Research, Inc, 1997.
- [65] Roger Ensrud, "Transferring Hardcopies Over the RS323 Port Using the Microsoft Windows Terminal Application," Instruction Sheet, Tektronix Corporation, 1997.
- [66] Hewlett Packard, *HP71450B/1B/2B Optical Spectrum Analyzers Instruction Manual*, Santa Rosa, CA, 1995.
- [67] Naval Air Systems Command, Naval Air Warfare Center, *Electronic Warfare and Radar Systems Engineering Handbook*, Pt. Mugu, CA, 1997.
- [68] C. R. Giles, "Optical Amplifiers: New Challenges in Lightwave," *IEEE Lasers and Electro-Optics Society Annual Meeting LEOS Conference Proceedings*, NY, pp. 382, 1993.
- [69] Kenneth L. Sala, Geraldine A. Kenney-Wallace, and Gregory E. Hall. "CW Autocorrelation Measurements of Picosecond Laser Pulses," *IEEE Journal of Quantum Electronics*, vol. 16, no. 9, pp. 210-216, 1980.
- [70] D. von der Linde, "Characterization of the Noise in Continuously Operating Mode-Locked Lasers," *Applied Physics B*, vol. 39, pp. 201-217, 1986.



- [71] Ross L. Finney and George B. Thomas Jr., *Calculus*, 2<sup>nd</sup> edition, Addison-Wesley Publishing Co, Reading, MA, pp. 282, 1994.
- [72] Newport Corp., *Photodetector Model D-15ir-ST Users Manual*, Irvine, CA, pp. 8, 1996.
- [73] M. Hofer, M. H. Ober, F. Haberl, and M. E. Fermann, "Characterization of Ultrashort Pulse Formation in Passively Mode-Locked Fiber Lasers," *IEEE Journal of Quantum Electronics*, vol. 28, no. 3, pp. 720-728, 1992.
- [74] Rudy van de Plassche, *Integrated Analog-to-Digital Converters and Digital-to-Analog Converters*, Kluwer Academic Publishers, Boston, MA, pp. 6-9, 1994.
- [75] Michael J. Demler, *High-Speed Analog-to-Digital Conversion*, Academic Press, Inc., San Diego, CA, pp. 71-73, 1991.
- [76] Richard A. Becker, Charles E. Woodward, Fredrick J. Leonberger, and Richard C. Williamson, "Wide-Band Electrooptic Guided-Wave Analog-to-Digital Converters," *Proceedings of the IEEE*, vol. 72, no. 7, pp.802-818, 1984.
- [77] Spectra Diode Labs, *SDL 800 Laser Diode Driver User's Manual*, San Jose, CA, 1986.
- [78] Melles Griot, *Operator's Manual 06 DLD 03 Diode Laser Controller*, Boulder, CO, 1993.
- [79] ILX Lightwave, *Product Catalog*, Bozeman, MT, pp. 46, 1998.
- [80] Karsten Rottwitt, Anders Bjarklev, Jorn Hedegaard Povlsen, Ole Lumholt, and Thomas P. Rasmussent, "Fundamental Design of Distributed Erbium-Doped Fiber Amplifier for Long-Distance Transmission," *IEEE Journal of Lightwave Technology*, vol. 10, no. 11, 1992.
- [81] ILX Lightwave, *LDT-5412 Instruction Manual for Thermoelectric Temperature Controller*, Bozeman, MT, 1997.

## INITIAL DISTRIBUTION LIST

1. Defense Technical Information Center..... 2  
8725 John J. Kingman Rd., STE 0944  
Ft. Belvoir, VA 22060-6218
  
2. Dudley Knox Library, Code 52..... 2  
Naval Postgraduate School  
411 Dyer Rd.  
Monterey, CA 93943-5002
  
3. Chairman, Code EC..... 1  
Department of Electrical and Computer Engineering  
Naval Postgraduate School  
Monterey, CA 93943-5121
  
4. Associate Professor Phillip E. Pace, Code EC/Pc..... 1  
Department of Electrical and Computer Engineering  
Naval Postgraduate School  
Monterey, CA 93943-5121
  
5. Professor John P. Powers, Code EC/Po..... 1  
Department of Electrical and Computer Engineering  
Naval Postgraduate School  
Monterey, CA 93943-5121
  
6. Director, Center for Reconnaissance Research, Code EC/Po..... 5  
Department of Electrical and Computer Engineering  
Naval Postgraduate School  
Monterey, CA 93943-5121
  
7. Commanding Officer..... 1  
Naval Research Laboratory  
(Attn: Dr. Irl Duling III, Code 5670)  
Optical Sciences Division  
4555 Overlook Ave, SW  
Washington D.C. 203075
  
8. Commanding Officer..... 1  
Naval Research Laboratory  
(Attn: Dr. Tom Carruthers, Code 5670)  
Optical Sciences Division  
4555 Overlook Ave, SW  
Washington D.C. 203075



9. Commanding Officer..... 1  
Naval Research Laboratory  
(Attn: Dr. Mike Dennis, Code 5670)  
Optical Sciences Division  
4555 Overlook Ave, SW  
Washington D.C. 203075
10. Commanding Officer..... 1  
Naval Research Laboratory  
(Attn: Dr. William Burns, Code 5671)  
Optical Sciences Division  
4555 Overlook Ave, SW  
Washington D.C. 203075
11. Headquarters, Naval Security Group..... 1  
(Attn: Code N9)  
9800 Savage Road  
Fort George G. Meade, MD 20755-6000
12. Naval Information Warfare Activity..... 1  
(Attn: Code 40)  
9800 Savage Road  
Fort George G. Meade, MD 20755-6000
13. LT James M. Butler..... 2  
141 Brownell Circle  
Monterey, CA 93940
14. K.V. Reddy..... 1  
PriTel, Inc.  
Naperville, IL 60567-4025
15. Gene Kaiser..... 1  
ALCATEL Telecommunications Cable  
7669 Roanoke, VA 24019



12 483NPG 3250  
TH  
10/99 22527-200 HJLLE









DUDLEY KNOX LIBRARY



3 2768 00368262 6